

Measurement of  $e^+ e^- \rightarrow \pi^+ \pi^-$   
cross section by CMD-3 and its  
implications to hadronic  
contribution to muon (g-2)

Ivan Logashenko (BINP) on behalf of CMD-3 collaboration

Объединенный  
семинар ОФВЭ и  
ОТФ ПИЯФ

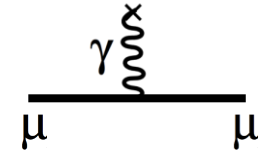
15 февраля 2024

# Rather long introduction

# The basics

**Gyromagnetic ratio  $g$**  connects magnetic moment  $\mu$  and spin  $s$

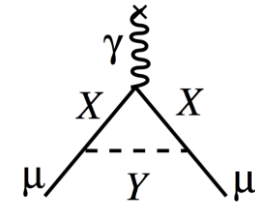
$$\vec{\mu}_s = g \frac{e}{2m} \vec{S}$$



For point-like particle  $g = 2$

**Anomalous magnetic moment  $a$**  arises in higher-orders

$$a = (g - 2)/2$$



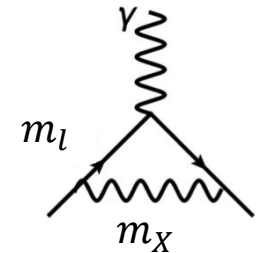
$$a_e \approx a_\mu \approx \frac{\alpha}{2\pi} \approx 10^{-3} \quad (\text{QED dominated})$$

**Idea of experiment:** by comparing measured value of  $a$  with the theory prediction we probe extra contributions beyond theory expectations

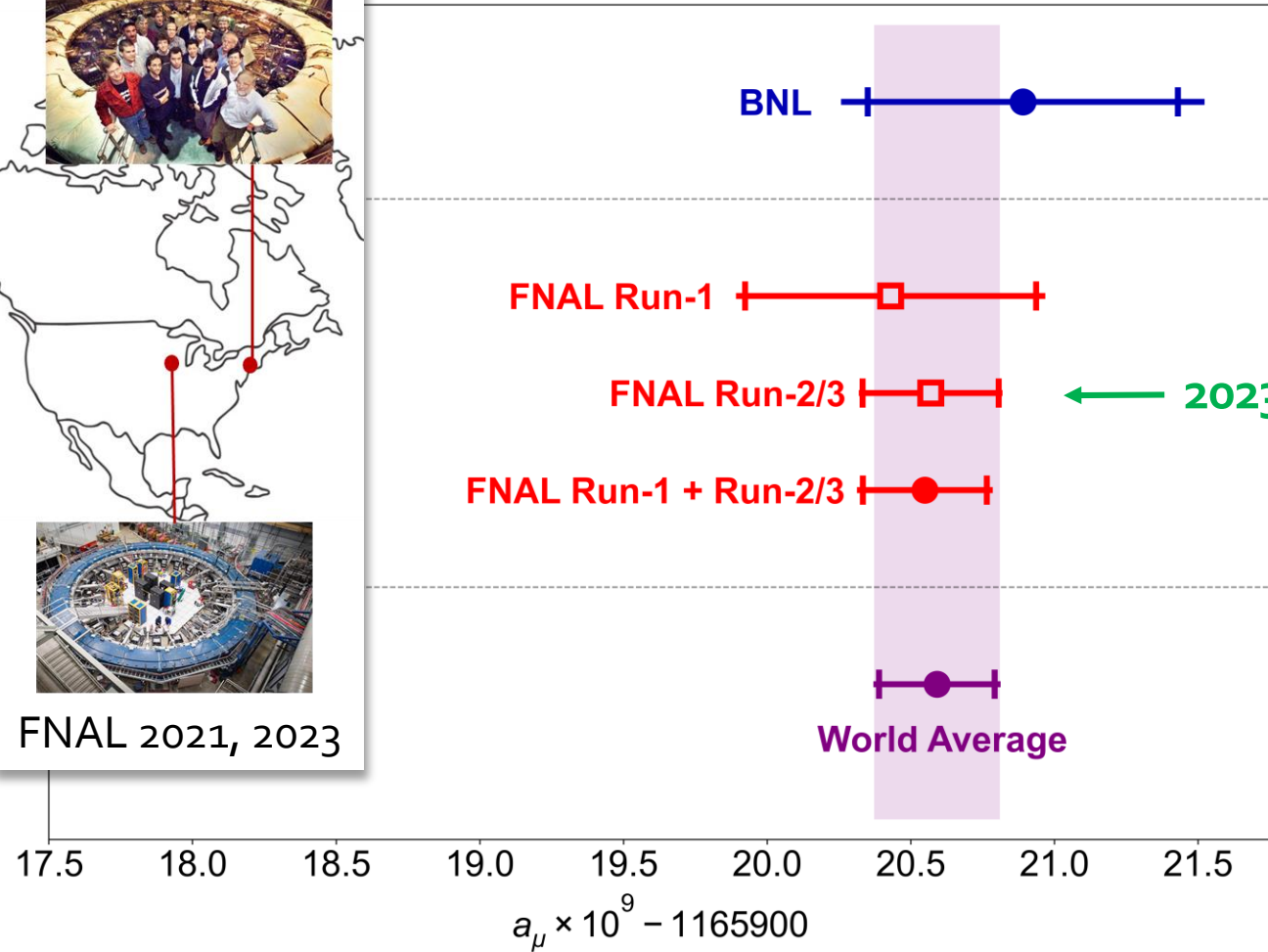
$$a_\mu(\text{strong})/a_\mu(\text{QED}) \approx 6 \times 10^{-5} \quad a_\mu(\text{weak})/a_\mu(\text{QED}) \approx 10^{-6}$$

**Why muon?** For massive fields there is natural scaling, which enhances contribution to  $a_\mu$  by  $(m_\mu/m_e)^2 \sim 43000$  compared to  $a_e$

$$\Delta a \sim \left( \frac{m_l}{m_X} \right)^2$$



# Muon G-2 2023 result



$$a_\mu(\text{Exp}) = 0.00116592059(22) \quad [190 \text{ ppb}]$$

# Muon G-2 collaboration



## USA

- Boston
- Cornell
- Illinois
- James Madison
- Kentucky
- Massachusetts
- Michigan
- Michigan State
- Mississippi
- North Central
- Northern Illinois
- Regis
- Virginia
- Washington

## USA National Labs

- Argonne
- Brookhaven
- Fermilab

181 collaborators  
33 Institutions  
7 countries



## China

- Shanghai Jiao Tong



## Germany

- Dresden
- Mainz



## Italy

- Frascati
- Molise
- Naples
- Pisa
- Roma Tor Vergata
- Trieste
- Udine



## Korea

- CAPP/IBS
- KAIST



## Russia

- Budker/Novosibirsk
- JINR Dubna



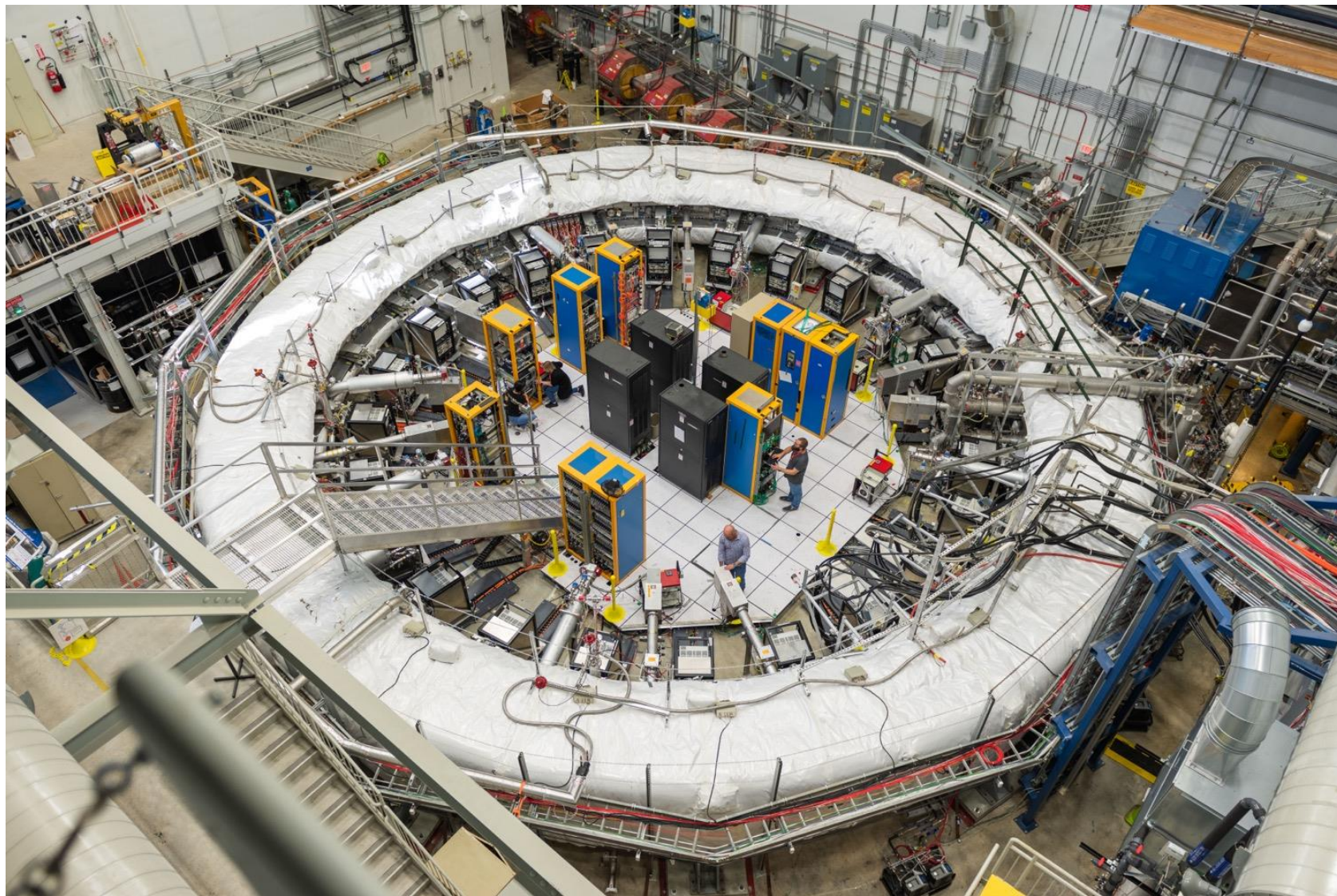
## United Kingdom

- Lancaster/Cockcroft
- Liverpool
- Manchester
- University College London



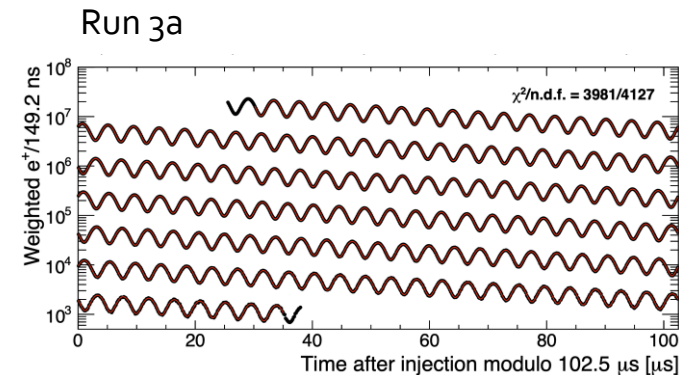
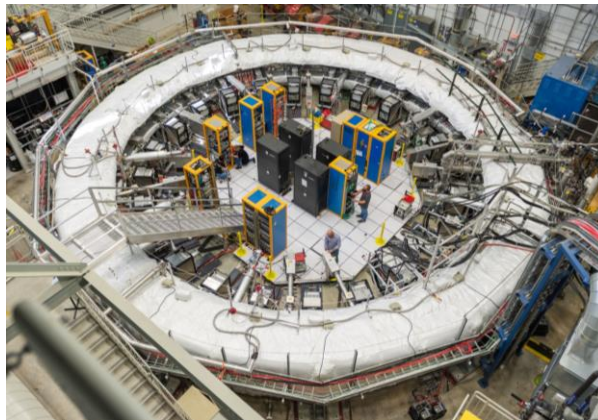
Muon g-2 Collaboration Meeting @ Elba, May 2019

# Muon G-2 Ring @FNAL



# Generations of $a_\mu$ measurements

FNAL Run 2-3  
(USA)



$$g_\mu(\text{эксп}) = 0.001\,165\,920\,55(24) \quad \text{FNAL2023}$$

$$g_\mu(\text{теория}) = 0.001\,165\,918\,10(43) \quad \text{WP2020}$$

QED

Strong

Weak

Contributions of known interactions

# Principles of CERN-III type measurement

1. Spin precesses relative to momentum with frequency  $\omega_a$  proportional directly to  $a_\mu$

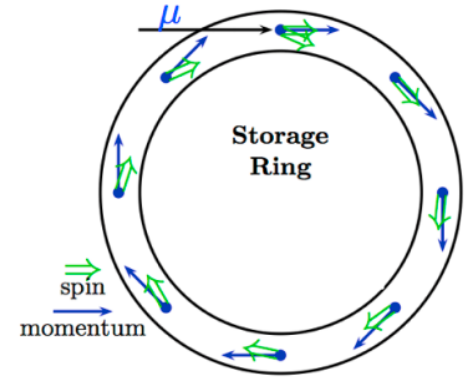
$$\omega_a = \omega_S - \omega_C = a_\mu eB/mc$$

$$a_\mu = \frac{mc}{e} \frac{\omega_a}{B}$$

2. Effect of electric field is canceled out for muons of "magic" momentum

$$\vec{\omega}_a = -\frac{e}{m} \left[ a_\mu \vec{B} - \left( a_\mu - \frac{1}{\gamma^2 - 1} \right) \frac{\vec{\beta} \times \vec{E}}{c} \right]$$

zero for  $\gamma_\mu = 29.3$



Muons are stored in a storage ring  
 $\omega_a$  and  $B$  are measured

Need focusing!

Muons with  $p = 3.09 \text{ GeV}/c$  are used

Focusing with electrostatic quadrupoles



# Obtaining $a_\mu$

Corrections due to beam dynamics

$$\frac{\omega_a}{\omega_p} = \frac{\omega_a^m}{\omega_p^m} \frac{1 + C_e + C_p + C_{pa} + C_{dd} + C_{ml}}{1 + B_k + B_q}$$

Measured Values

Corrections due to transient magnetic fields

$$a_\mu = \left( \frac{\omega_a}{\omega_p} \right) \times \frac{\mu'_p(T_r)}{\mu_e(H)} \frac{\mu_e(H)}{\mu_e} \frac{m_\mu}{m_e} \frac{g_e}{2}$$

Metrological constants known to ~25 ppb

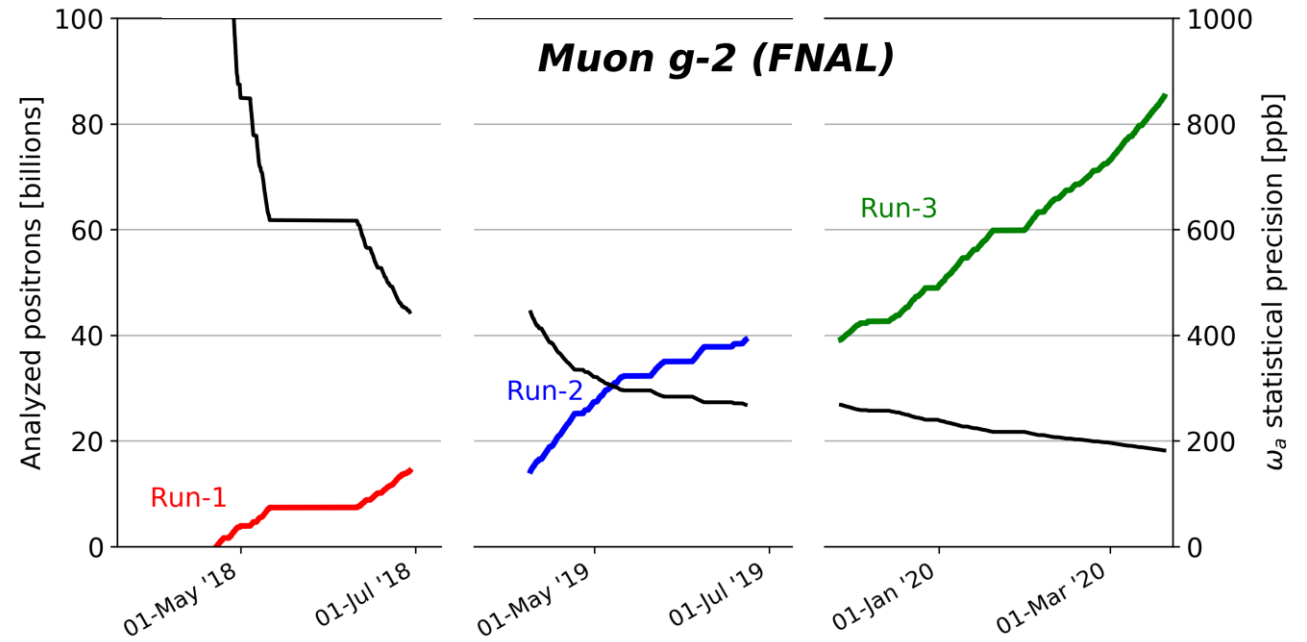
Total correction is about 622 ppb

# Run-1 vs Run-2/3

# Statistics

Weighted  $e^+$  in our final fit after quality control

$E > 1 \text{ GeV}$   
 $t > 30 \text{ us}$



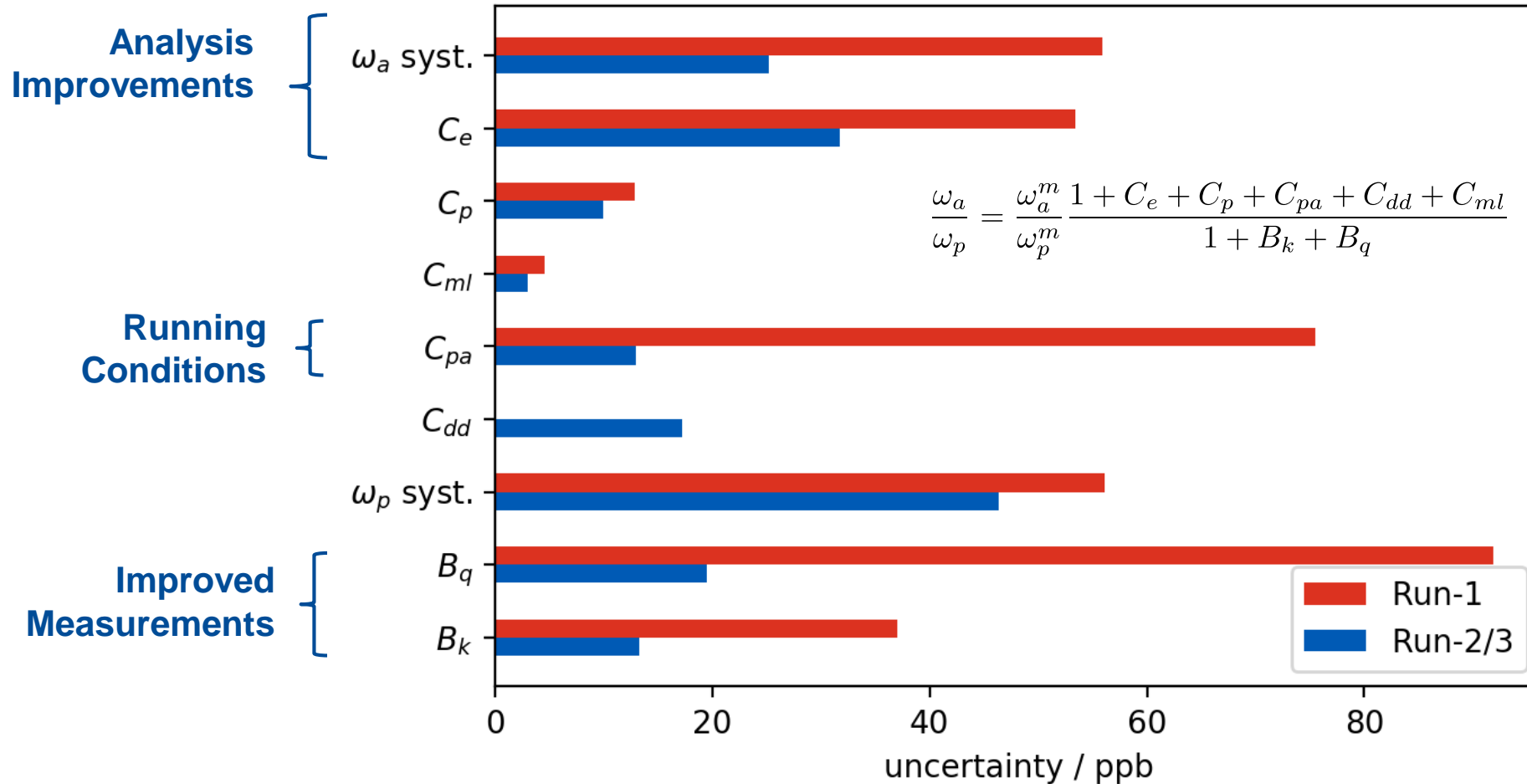
- **Factor 4.7** more data in Run-2/3 than Run-1

Dataset	Statistical Error [ppb]
Run-1	434
Run-2/3	201
Run-1 + Run-2/3	185

Improvement by factor 2.2

Run-1 vs  
Run-2/3

Systematics



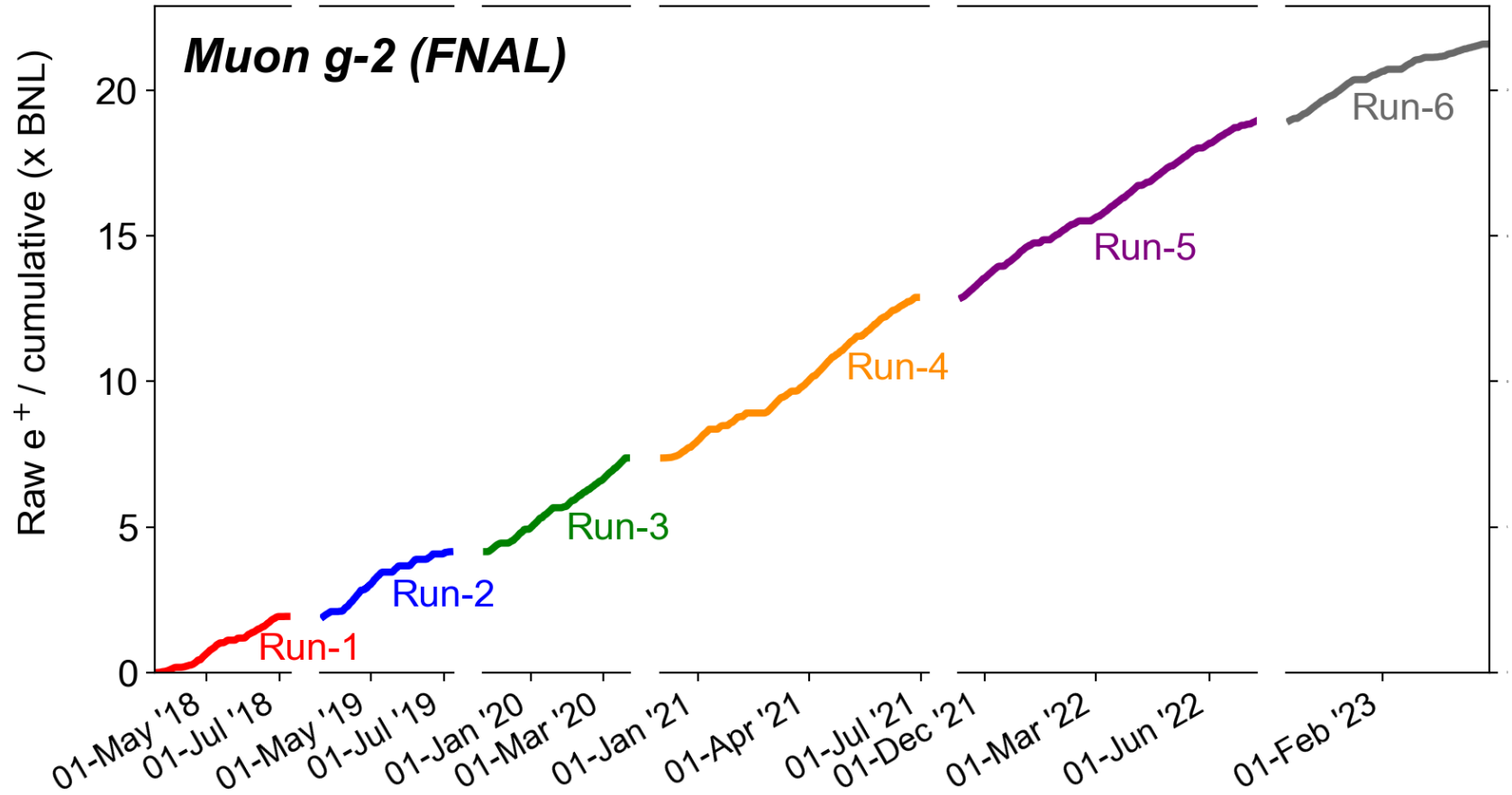
Overall improvement by factor 2.2

# Final error table

Quantity	Correction [ppb]	Uncertainty [ppb]
$\omega_a^m$ (statistical)	–	201
$\omega_a^m$ (systematic)	–	25
$C_e$	451	32
$C_p$	170	10
$C_{pa}$	-27	13
$C_{dd}$	-15	17
$C_{ml}$	0	3
$f_{\text{calib}} \langle \omega'_p(\vec{r}) \times M(\vec{r}) \rangle$	–	46
$B_k$	-21	13
$B_q$	-21	20
$\mu'_p(34.7^\circ)/\mu_e$	–	11
$m_\mu/m_e$	–	22
$g_e/2$	–	0
Total systematic	–	70
Total external parameters	–	25
Totals	622	215

The Run-2/3 result is statistically dominated  
**70 ppb systematic uncertainty surpasses the proposal goal of 100 ppb!**

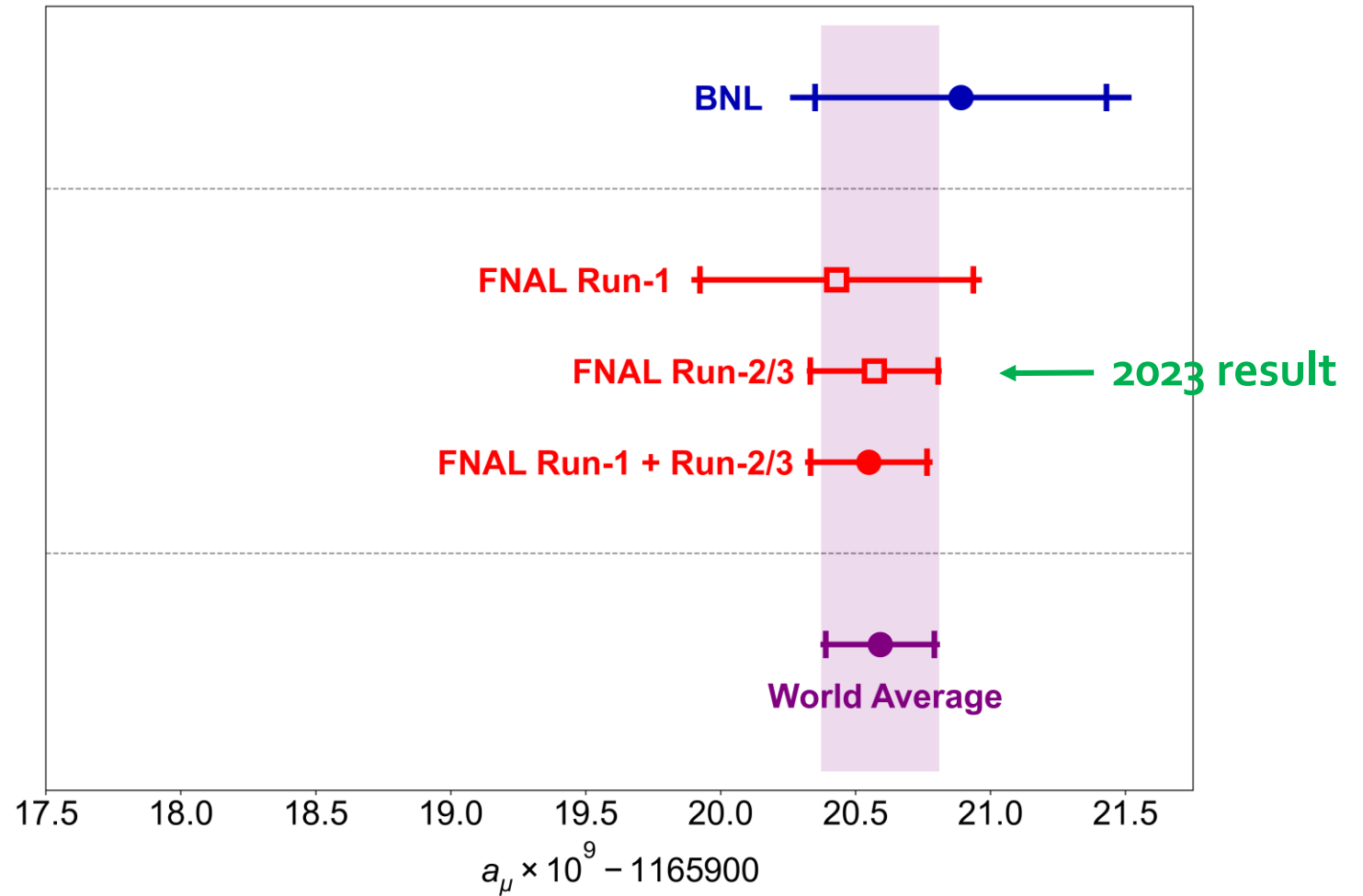
# Total collected statistics



21.9 BNL datasets have been collected in FNAL (proposal – 21 BNL)

Run 4/5/6 statistics is x3 Run-1/2/3

# Muon G-2 2023 result



What about theory?

# Experiment vs SM prediction

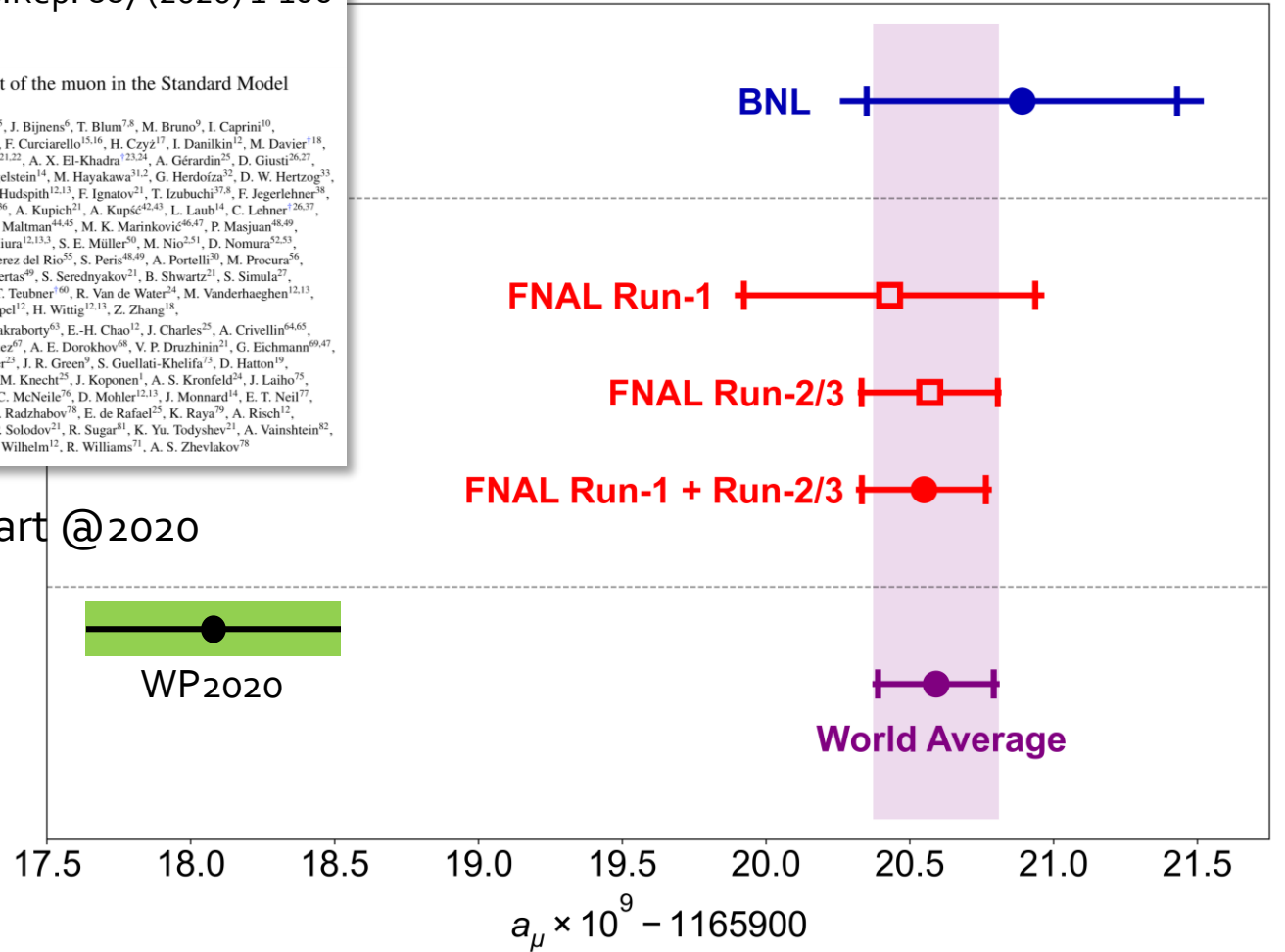
## Muon G-2 Theory Initiative Consortium of >100 theorists and experimental physicists "White paper", Phys.Rep. 887 (2020) 1-166

### The anomalous magnetic moment of the muon in the Standard Model

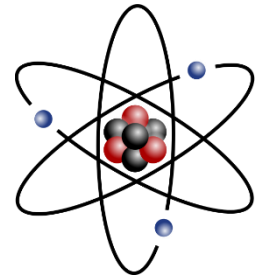
T. Aoyama<sup>1,2,3</sup>, N. Asmussen<sup>4</sup>, M. Benayoun<sup>5</sup>, J. Bijnens<sup>6</sup>, T. Blum<sup>7,8</sup>, M. Bruno<sup>9</sup>, I. Caprini<sup>10</sup>, C. M. Carloni Calame<sup>11</sup>, M. Cè<sup>9,12,13</sup>, G. Colangelo<sup>14</sup>, F. Curciarello<sup>15,16</sup>, H. Czyz<sup>17</sup>, I. Danilkin<sup>12</sup>, M. Davier<sup>18</sup>, C. T. H. Davies<sup>19</sup>, M. Della Morte<sup>20</sup>, S. I. Eidelman<sup>21,22</sup>, A. X. El-Khadra<sup>23,24</sup>, A. Gérardin<sup>25</sup>, D. Giusti<sup>26,27</sup>, M. Golterman<sup>28</sup>, Steven Gottlieb<sup>29</sup>, V. Gülpers<sup>30</sup>, F. Hagelstein<sup>14</sup>, M. Hayakawa<sup>31,2</sup>, G. Herdoíza<sup>32</sup>, D. W. Hertzog<sup>33</sup>, A. Hoecker<sup>34</sup>, M. Hoferichter<sup>14,35</sup>, B.-L. Hoid<sup>36</sup>, R. J. Hudspeth<sup>12,13</sup>, F. Ignatov<sup>21</sup>, T. Izubuchi<sup>37,8</sup>, F. Jegerlehner<sup>38</sup>, L. Jin<sup>7,8</sup>, A. Keshavarzi<sup>39</sup>, T. Kinoshita<sup>40,41</sup>, B. Kubis<sup>36</sup>, A. Kupich<sup>21</sup>, A. Kupś<sup>42,43</sup>, L. Laub<sup>14</sup>, C. Lehner<sup>26,37</sup>, L. Lellouch<sup>25</sup>, I. Logashenko<sup>21</sup>, B. Malaescu<sup>5</sup>, K. Maltman<sup>44,45</sup>, M. K. Marinkovic<sup>46,47</sup>, P. Masjuan<sup>48,49</sup>, A. S. Meyer<sup>27</sup>, H. B. Meyer<sup>12,13</sup>, T. Mibe<sup>11</sup>, K. Miura<sup>12,13,3</sup>, S. E. Müller<sup>50</sup>, M. Nio<sup>51</sup>, D. Nomura<sup>52,53</sup>, A. Nyffeler<sup>12</sup>, V. Pascalutsa<sup>12</sup>, M. Passera<sup>54</sup>, E. Perez del Rio<sup>55</sup>, S. Peris<sup>48,49</sup>, A. Portelli<sup>30</sup>, M. Procura<sup>56</sup>, C. F. Redmer<sup>12</sup>, B. L. Roberts<sup>57</sup>, P. Sánchez-Puertas<sup>49</sup>, S. Serednyakov<sup>21</sup>, B. Shwartz<sup>21</sup>, S. Simula<sup>27</sup>, D. Stöckinger<sup>58</sup>, H. Stöckinger-Kim<sup>58</sup>, P. Stoffer<sup>59</sup>, T. Teubner<sup>60</sup>, R. Van de Water<sup>21</sup>, M. Vanderhaeghe<sup>12,13</sup>, G. Venanzoni<sup>61</sup>, G. von Hippel<sup>12</sup>, H. Wittig<sup>12,13</sup>, Z. Zhang<sup>18</sup>, M. N. Achasov<sup>21</sup>, A. Bashir<sup>62</sup>, N. Cardoso<sup>47</sup>, B. Chakraborty<sup>63</sup>, E.-H. Chao<sup>12</sup>, J. Charles<sup>25</sup>, A. Crivellin<sup>64,65</sup>, O. Deineka<sup>12</sup>, A. Denig<sup>12,13</sup>, C. DeTar<sup>66</sup>, C. A. Dominguez<sup>67</sup>, A. E. Dorokhov<sup>68</sup>, V. P. Druzhinin<sup>21</sup>, G. Eichmann<sup>69,47</sup>, M. Fael<sup>70</sup>, C. S. Fischer<sup>71</sup>, E. Gámiz<sup>72</sup>, Z. Gelzer<sup>25</sup>, J. R. Green<sup>9</sup>, S. Guellati-Khelifa<sup>73</sup>, D. Hattori<sup>19</sup>, N. Hermansson-Truedsson<sup>14</sup>, S. Holz<sup>36</sup>, B. Hörz<sup>74</sup>, M. Knecht<sup>25</sup>, J. Koponen<sup>1</sup>, A. S. Kronfeld<sup>24</sup>, J. Laiho<sup>75</sup>, S. Leupold<sup>42</sup>, P. B. Mackenzie<sup>24</sup>, W. J. Marciano<sup>37</sup>, C. McNeile<sup>76</sup>, D. Mohler<sup>12,13</sup>, K. Monnard<sup>14</sup>, E. T. Neil<sup>77</sup>, A. V. Nesterenko<sup>68</sup>, K. Ottnad<sup>12</sup>, V. Pauk<sup>12</sup>, A. E. Radzhabov<sup>78</sup>, E. de Rafael<sup>25</sup>, K. Raya<sup>79</sup>, A. Risch<sup>12</sup>, A. Rodríguez-Sánchez<sup>8</sup>, P. Roig<sup>80</sup>, T. San José<sup>12,13</sup>, E. P. Solodov<sup>21</sup>, R. Sugar<sup>81</sup>, K. Yu. Todyshev<sup>21</sup>, A. Vainshtein<sup>82</sup>, A. Vaquero Avilés-Casco<sup>66</sup>, E. Wei<sup>71</sup>, J. Wilhelm<sup>12</sup>, R. Williams<sup>71</sup>, A. S. Zhevlakov<sup>78</sup>

$$a_\mu(\text{Exp}) = 0.00116592059(22) \quad [190 \text{ ppb}]$$

State-of-art @2020

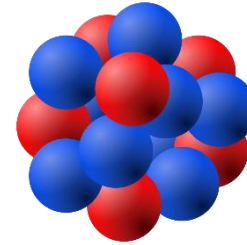


# Standard Model prediction for $a_\mu$



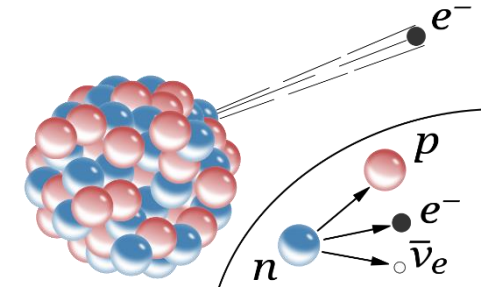
Electromagnetic interactions

0.001 165 847 19 (0.1)



Strong interactions

0.000 000 069 37 (43)



Weak interactions

0.000 000 001 54 (1)

$$a_\mu = 0.001\ 165\ 918\ 10\ (43)$$

The uncertainty is dominated by contribution of strong interactions



# Hadronic contribution to muon (g-2)

Leading order (LO)

$$(6\,931 \pm 40) \times 10^{-11}$$

$$a_{\mu}^{\text{had}}$$

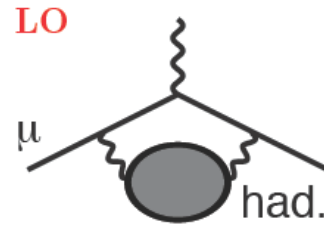
$$= a_{\mu}^{\text{had,VP LO}}$$

+

$$a_{\mu}^{\text{had,VP NLO}}$$

+

$$a_{\mu}^{\text{had,Light-by-Light}}$$



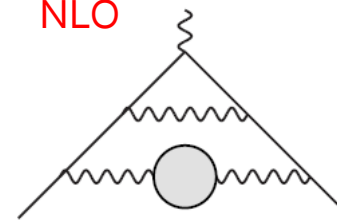
345 ppb (0.6%)

Dominant!

Next to leading order (NLO+NNLO)

$$(-85.9 \pm 0.7) \times 10^{-11}$$

NLO

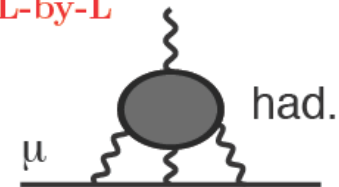


10 ppb

Light-by-light (LBL)

$$(92 \pm 18) \times 10^{-11}$$

L-by-L



155 ppb

# HVP: what do we need to measure

Dispersion relation:

$$\begin{aligned}
 & \text{Diagram: Triangle with wavy line on top, wavy line on bottom, and a shaded circle in the middle.} \\
 & a_\mu^{\text{had}}(LO) = \int_0^\infty \frac{ds}{s} \frac{1}{\pi} \text{Im}\Pi'(s) \times \text{Diagram: Triangle with wavy line on top, wavy line on bottom, and a shaded circle in the middle.} \\
 & \propto \frac{1}{q^2 - s} \\
 & \frac{\alpha}{\pi} K_\mu(s)
 \end{aligned}$$

Optical theorem:

$$\begin{aligned}
 & 2 \text{Im} \left[ \text{Diagram: Triangle with wavy line on top, wavy line on bottom, and a shaded circle in the middle.} \right] = \left| \text{Diagram: Triangle with wavy line on top, wavy line on bottom, and a shaded circle in the middle.} \right|^2 \\
 & \text{Im} \Pi'(s) = \frac{s}{4\pi\alpha} \sigma^0(e^+e^- \rightarrow \gamma \rightarrow \text{hadrons} + \dots)
 \end{aligned}$$

Lets put everything together:

$$a_\mu^{\text{had}}(LO) = \frac{\alpha^2}{3\pi^2} \int_{4m_\pi^2}^\infty \frac{ds}{s} R(s) K_\mu(s)$$

This is what we need to measure

$$R(s) = \frac{\sigma^0(e^+e^- \rightarrow \gamma \rightarrow \text{hadrons})}{4\pi\alpha^2/3s}$$

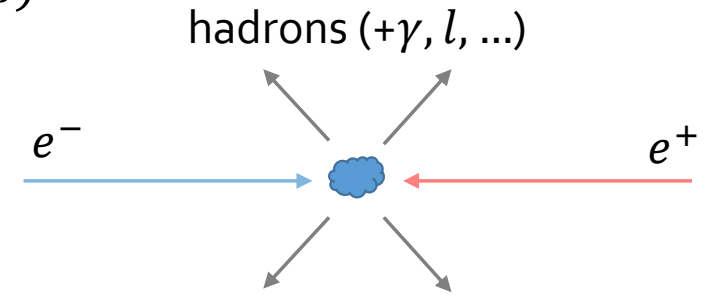
$$\sigma^0(e^+e^- \rightarrow \mu^+\mu^-)$$

$$s = (\text{c.m. energy})^2$$

# Energy scan approach

Direct measurement of  $\sigma(e^+e^- \rightarrow \text{hadrons})$   
(energy scan approach):

- performed at electron-positron collider
- collect data at different beam energy
- at each energy point: select final states with hadrons, subtract background and normalize to luminosity



Number of signal events

Number of background events

$$\sigma = \frac{N_{obs} - N_{bg}}{\varepsilon \cdot \int \mathcal{L} dt}$$

Detection efficiency:

- kinematical limits of detector (fiducial volume) – detector never has  $4\pi$  coverage
- detector response

Luminosity integral

- measured by selection of monitoring events with known cross section

# Exclusive vs inclusive measurement

Detection efficiency is (usually) calculated using MC simulation

- In order to calculate  $\varepsilon$ , we need to know the energy and angular distributions of final particles (including all correlations)

For high energies, where multiplicity is large enough, there are effective models of hadronization, which describe data reasonably well

At low energy the detection efficiency varies significantly between different final states and different paths of hadronization (intermediate states)

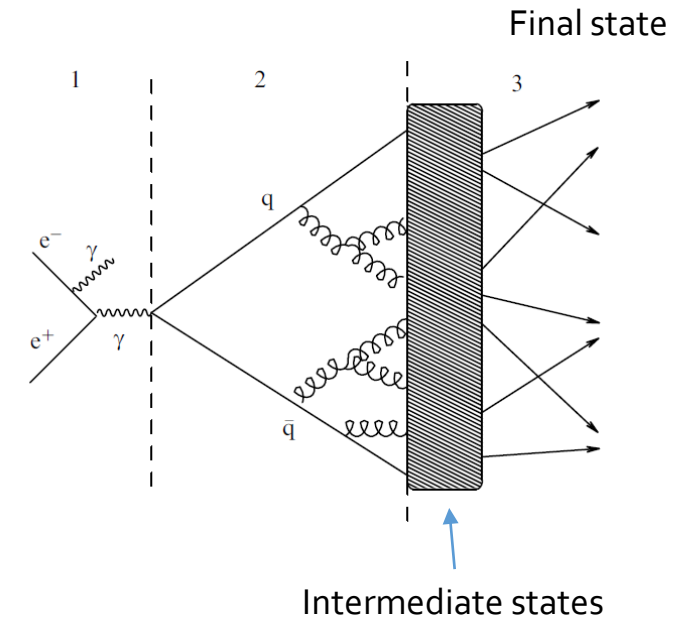
At low energies we have to measure cross section for each possible final state separately and then calculate sum to get R (**exclusive approach**)

At high energy we can measure total cross section directly (**inclusive approach**)

The practical boundary between two approaches in  $\sqrt{s} = 2 \text{ GeV}$ .

The  $a_{\mu}^{had}(LO)$  calculation is mostly based on exclusive measurements.

$$\sigma = \frac{N_{obs} - N_{bg}}{\varepsilon \cdot \int \mathcal{L} dt}$$



# Contribution of exclusive hadronic cross sections to $a_\mu$

In exclusive approach, we calculate  $a_\mu$  integral for each final state and sum them:

$$a_\mu^{had}(LO) = \sum_{X=\pi^0\gamma, \pi^+\pi^-, \dots} a_\mu^X(LO) = \sum_X \frac{1}{4\pi^3} \int \sigma^0(e^+e^- \rightarrow X) K_\mu(s) ds$$

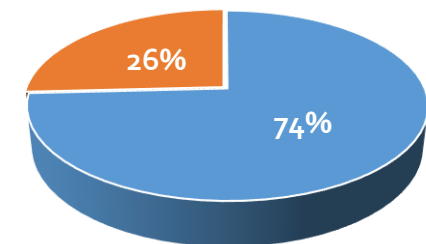
Channel	$a_\mu^{had,LO} [10^{-10}]$
$\pi^0\gamma$	$4.41 \pm 0.06 \pm 0.04 \pm 0.07$
$\eta\gamma$	$0.65 \pm 0.02 \pm 0.01 \pm 0.01$
$\pi^+\pi^-$	$507.85 \pm 0.83 \pm 3.23 \pm 0.55$
$\pi^+\pi^-\pi^0$	$46.21 \pm 0.40 \pm 1.10 \pm 0.86$
$2\pi^+2\pi^-$	$13.68 \pm 0.03 \pm 0.27 \pm 0.14$
$\pi^+\pi^-2\pi^0$	$18.03 \pm 0.06 \pm 0.48 \pm 0.26$
$2\pi^+2\pi^-\pi^0$ ( $\eta$ excl.)	$0.69 \pm 0.04 \pm 0.06 \pm 0.03$
$\pi^+\pi^-3\pi^0$ ( $\eta$ excl.)	$0.49 \pm 0.03 \pm 0.09 \pm 0.00$
$3\pi^+3\pi^-$	$0.11 \pm 0.00 \pm 0.01 \pm 0.00$
$2\pi^+2\pi^-2\pi^0$ ( $\eta$ excl.)	$0.71 \pm 0.06 \pm 0.07 \pm 0.14$
$\pi^+\pi^-4\pi^0$ ( $\eta$ excl., isospin)	$0.08 \pm 0.01 \pm 0.08 \pm 0.00$
$\eta\pi^+\pi^-$	$1.19 \pm 0.02 \pm 0.04 \pm 0.02$
$\eta\omega$	$0.35 \pm 0.01 \pm 0.02 \pm 0.01$
$\eta\pi^+\pi^-\pi^0$ (non- $\omega, \phi$ )	$0.34 \pm 0.03 \pm 0.03 \pm 0.04$
$\eta2\pi^+2\pi^-$	$0.02 \pm 0.01 \pm 0.00 \pm 0.00$
$\omega\eta\pi^0$	$0.06 \pm 0.01 \pm 0.01 \pm 0.00$
$\omega\pi^0$ ( $\omega \rightarrow \pi^0\gamma$ )	$0.94 \pm 0.01 \pm 0.03 \pm 0.00$
$\omega2\pi$ ( $\omega \rightarrow \pi^0\gamma$ )	$0.07 \pm 0.00 \pm 0.00 \pm 0.00$
$\omega$ (non- $3\pi, \pi\gamma, \eta\gamma$ )	$0.04 \pm 0.00 \pm 0.00 \pm 0.00$
$K^+K^-$	$23.08 \pm 0.20 \pm 0.33 \pm 0.21$
$K_S K_L$	$12.82 \pm 0.06 \pm 0.18 \pm 0.15$

From DHMZ'19

The larger the contribution, the better relative precision is required

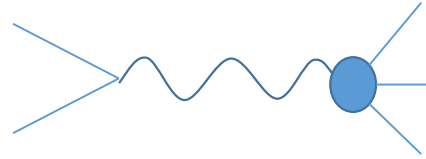
$e^+e^- \rightarrow \pi^+\pi^-$  is by far the most challenging and has got the most attention (74% of total hadronic contribution!)

All the rest



$\pi^+\pi^-$

# Radiative corrections



We want to measure  $e^+e^- \rightarrow H$ , but these events are accompanied by similar events where photons are emitted by any of the particles.

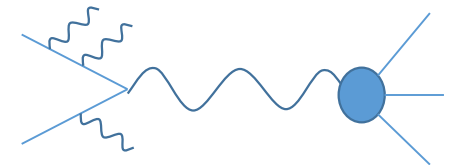
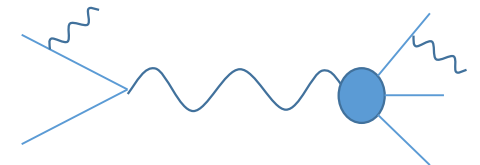
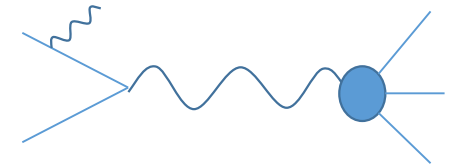
Radiation of high-energy  $\gamma$  is suppressed by  $\alpha$ , but radiation of soft photons is enhanced.

Radiation changes both the cross-section and the kinematics of the final state:

$$\sigma = \frac{N_{obs} - N_{bg}}{\varepsilon(\delta) \cdot (1 + \delta) \cdot \int \mathcal{L} dt}$$

And we have to calculate radiative corrections to the cross section of monitoring process as well

## Radiative processes



ISR

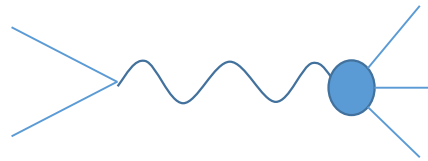
FSR

*Initial*

*Final*

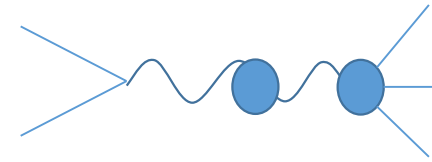
*state radiation*

# Vacuum polarization



$$\sigma^0(e^+e^- \rightarrow \gamma \rightarrow X)$$

In  $a_\mu$  calculation



$$\sigma(e^+e^- \rightarrow \gamma^* \rightarrow X)$$

In experiment

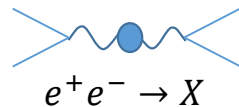
In the calculation of  $a_\mu$ , we assume the lowest order photon propagator  $1/q^2$ . But the real propagator includes higher order effects (loop corrections):  $1/(q^2 - \Pi(q^2))$ . Therefore the measured cross section have to be corrected:

$$\sigma^0(e^+e^- \rightarrow X) = \sigma(e^+e^- \rightarrow X) \times \frac{|\alpha(s)|^2}{\alpha^2}$$

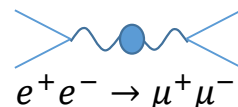
The running fine structure constant is also calculated via dispersion relation based on  $R(s)$ :

$$\Delta\alpha_{had}(s) = -\frac{\alpha s}{3\pi} \int_0^\infty \frac{R(s')}{s'(s-s'-i0)} ds'$$

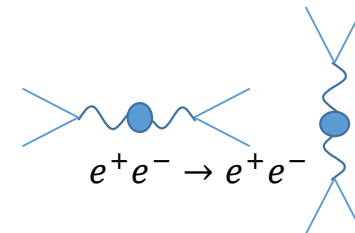
Nice way to avoid this correction is to use  $e^+e^- \rightarrow \mu^+\mu^-$  for luminosity measurement



$$e^+e^- \rightarrow X$$



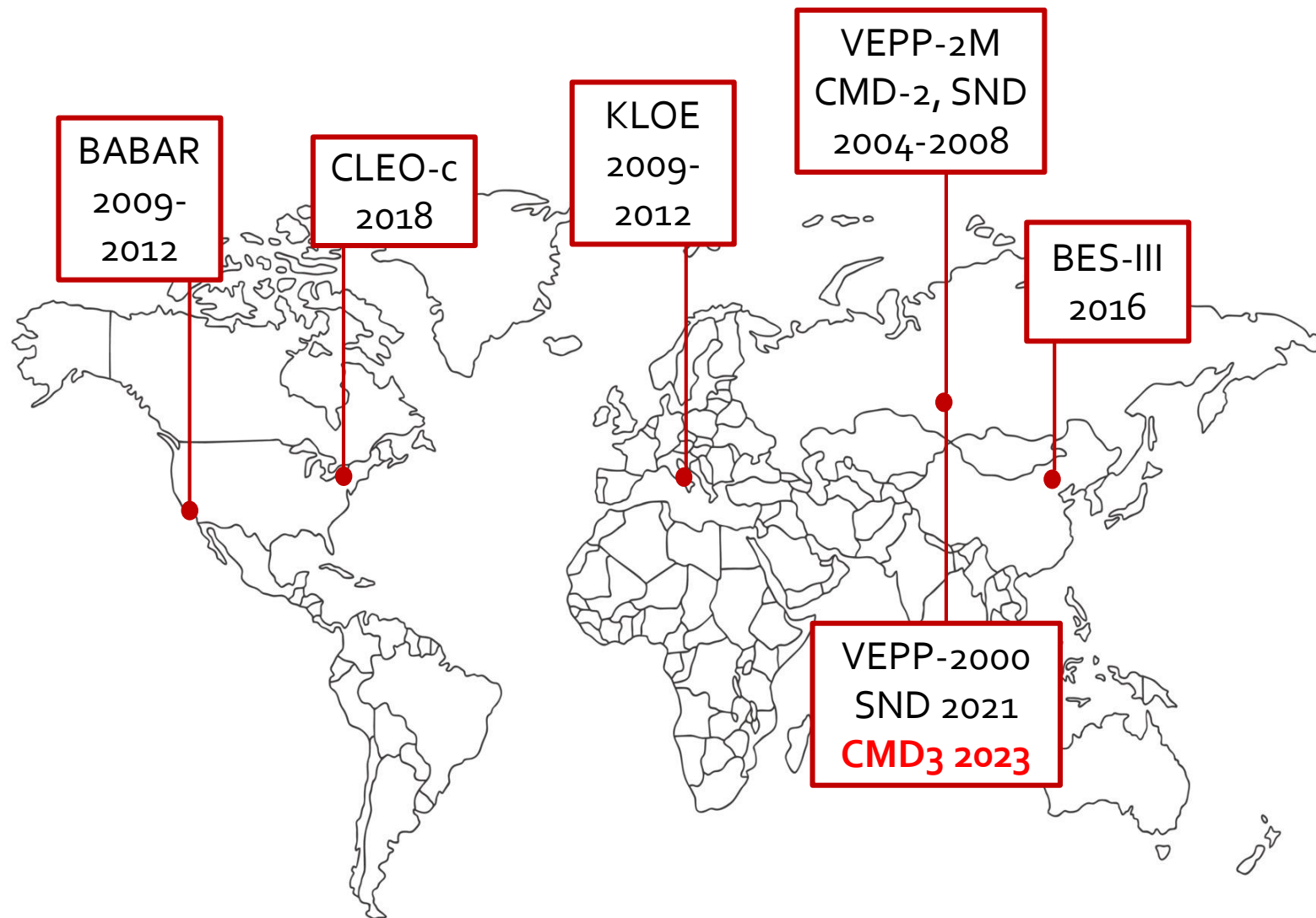
$$e^+e^- \rightarrow \mu^+\mu^-$$



$$e^+e^- \rightarrow e^+e^-$$

# Measurements of $e^+e^- \rightarrow \pi^+\pi^-$

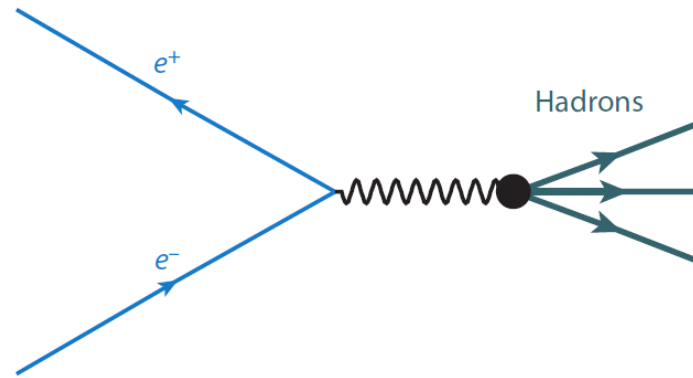
There are several measurements of  $\sigma(e^+e^- \rightarrow \pi^+\pi^-)$  with sub-percent systematic accuracy





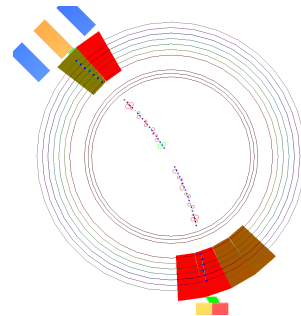
# Measurement techniques:

## Direct vs ISR

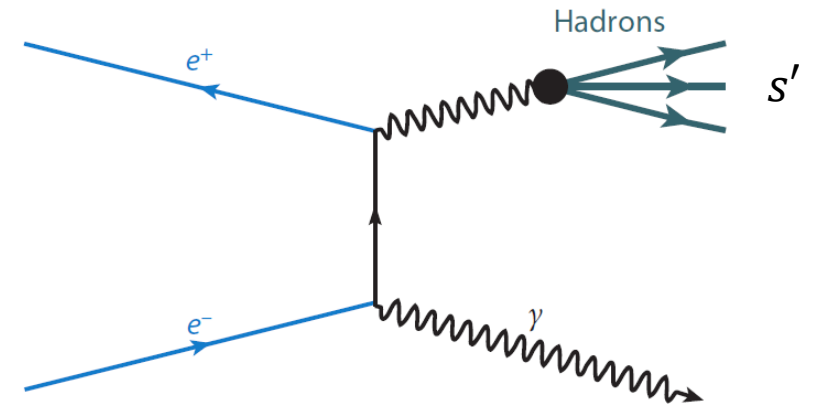


Direct measurement (Energy scan)

At fixed  $s$ :  $\sigma_{e^+e^- \rightarrow H}(s) \sim N_H/L$   
Data is taken at different  $s$

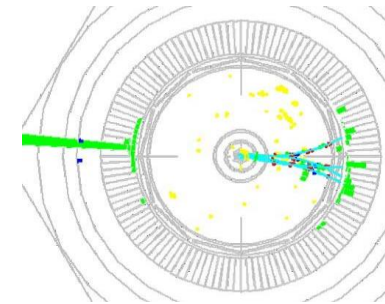


VEPP-2M: CMD-2, SND  
VEPP-2000: CMD-3, SND2k



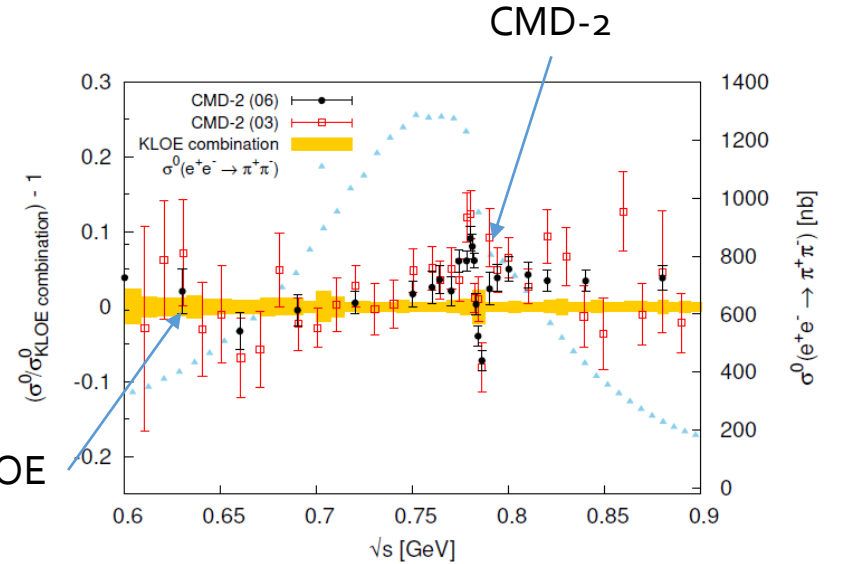
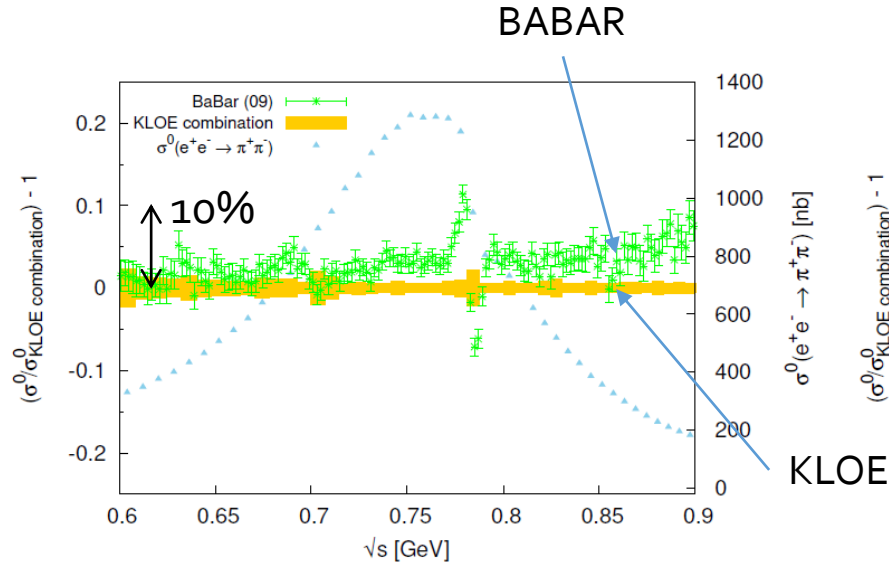
ISR (Initial State Radiation)

$\sigma_{e^+e^- \rightarrow H}(s') \sim \frac{dN_{H+\gamma}/ds'}{L \cdot dW/ds'}$   
Data is taken at fixed  $s > s'$



KLOE, BABAR, BES-III, CLEO

# Tensions in $e^+e^- \rightarrow \pi^+\pi^-$ data

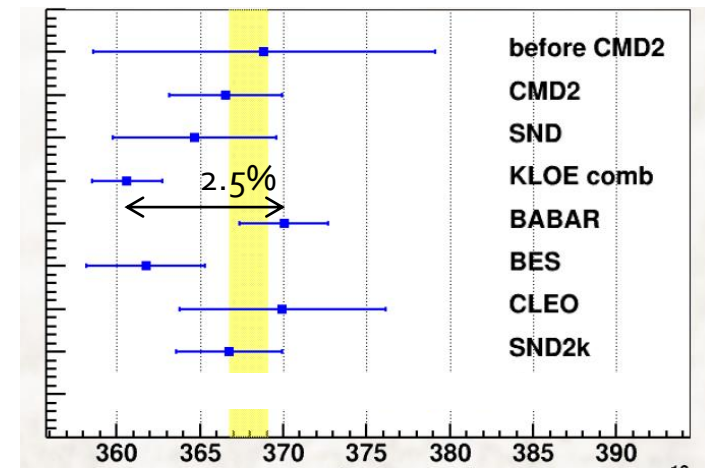


There are few-% discrepancies between various sub-% measurements of  $\sigma(e^+e^- \rightarrow \pi^+\pi^-)$   
*Unexplained*

WP2020: scale factor for  $\Delta a_\mu(Had; LO)$

**CMD-3 goal: new high statistics low systematics measurement of  $\sigma(e^+e^- \rightarrow \pi^+\pi^-)$  via energy scan**

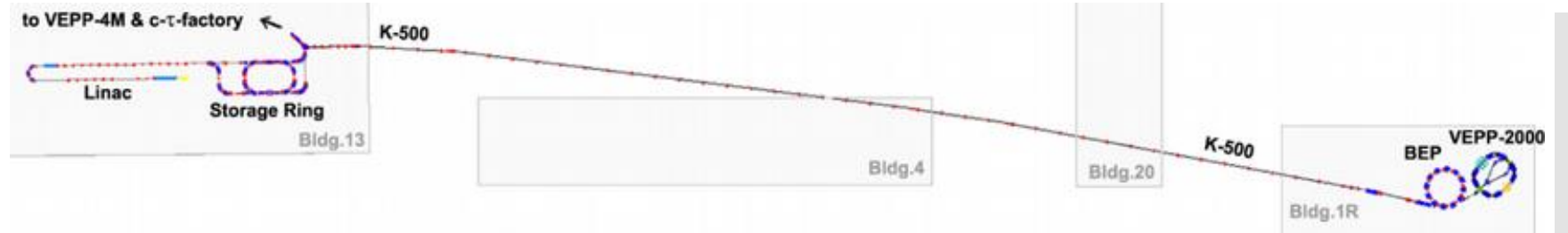
$$\alpha_\mu^{had}(LO; 2\pi, 0.6 < \sqrt{s} < 0.88 \text{ GeV})$$



$$\frac{1}{4\pi^3} \int_{0.6}^{0.88} \sigma^0(e^+e^- \rightarrow \pi^+\pi^-) K_\mu(s) ds$$

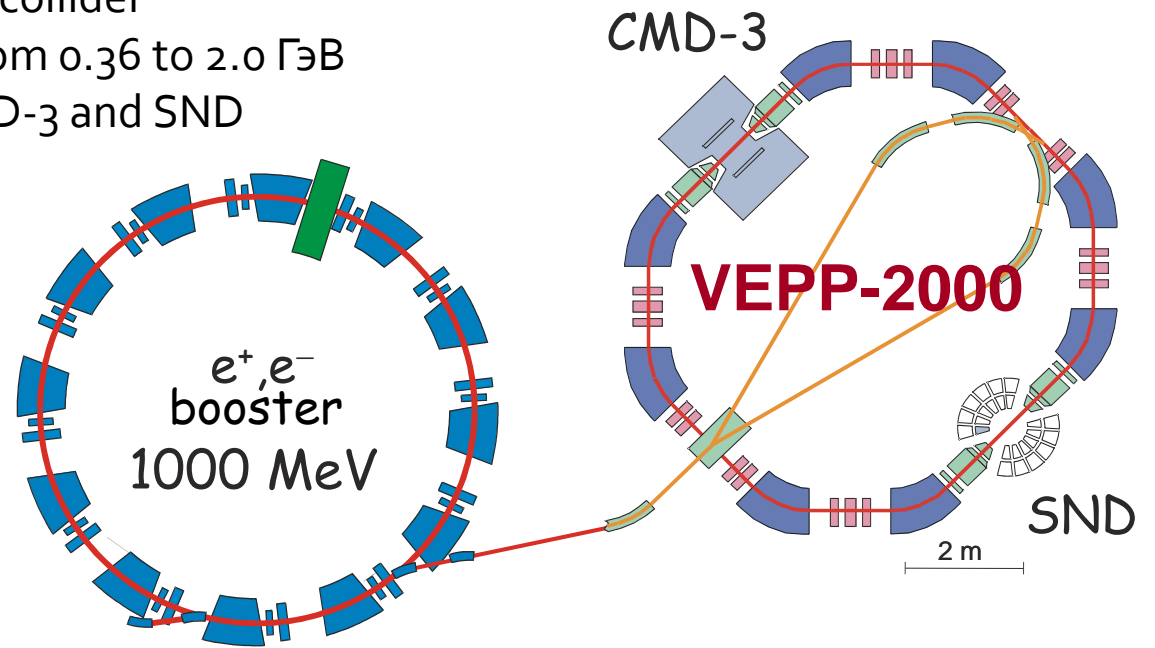
# CMD-3 measurement of $e^+e^- \rightarrow \pi^+\pi^-$ cross section

# VEPP-2000 collider



Electron-positron collider  
 Covers c.m. energy range from 0.36 to 2.0 ГэВ  
 Two experiments – CMD-3 and SND

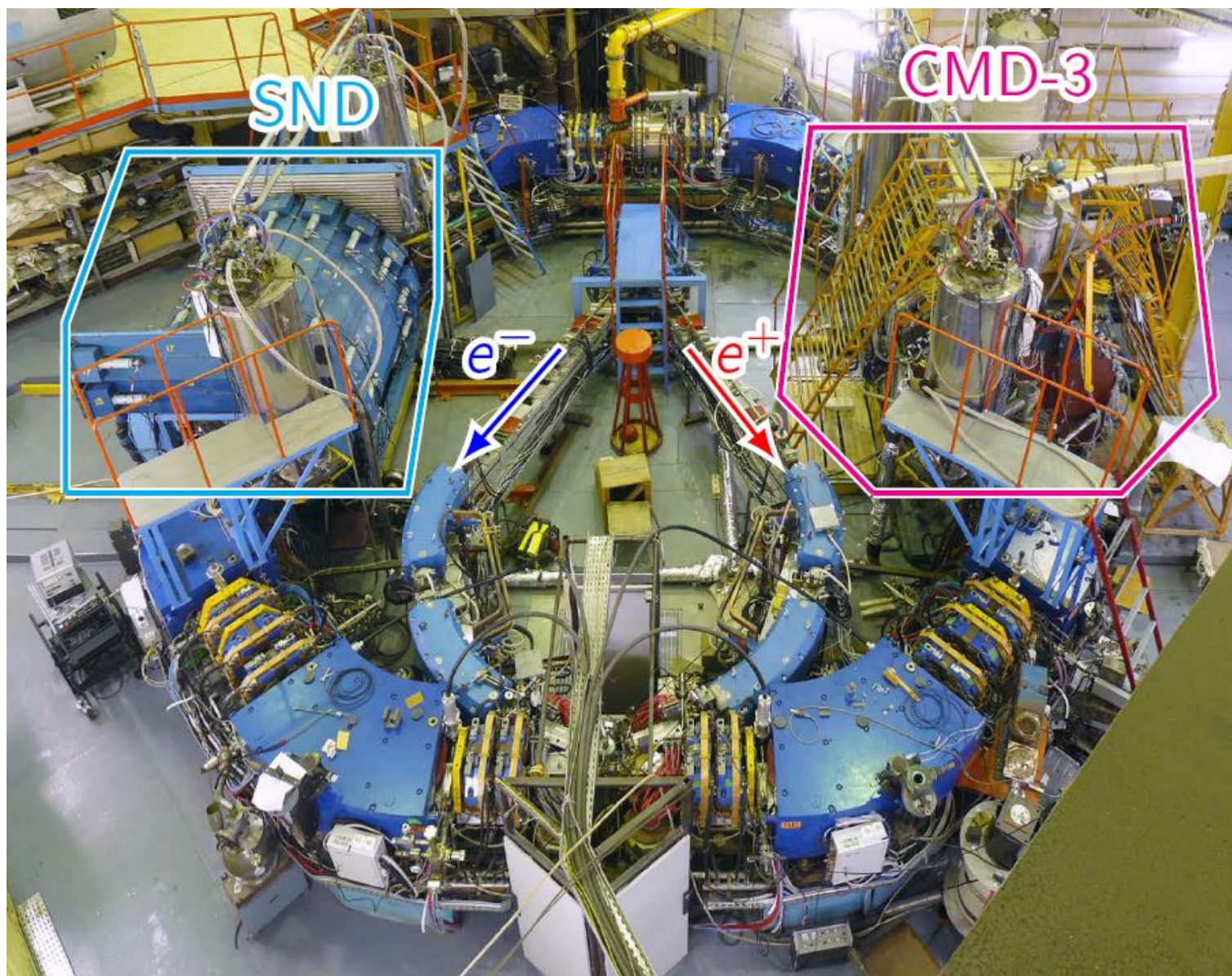
Design parameters @ 1 GeV	
Circumference	24.388 m
Beam energy	150 ÷ 1000 MeV
N of bunches	1×1
N of particles	1×10 <sup>11</sup>
Betatron tunes	4.14 / 2.14
Beta*	8.5 cm
BB parameter	0.1
Luminosity	1×10 <sup>32</sup> cm <sup>-2</sup> s <sup>-1</sup>



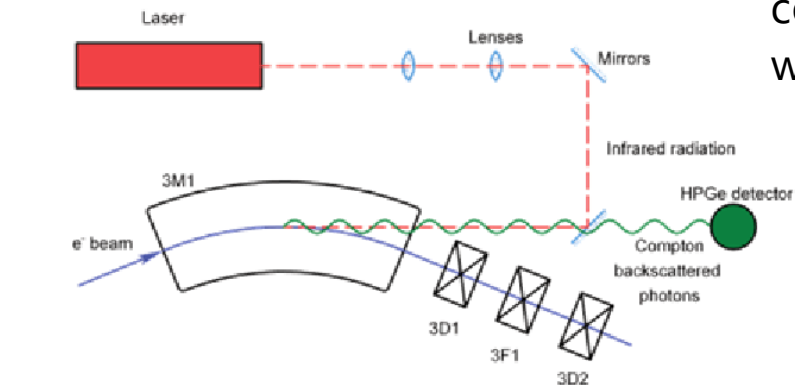
“Round beam” optics

Energy monitoring by Compton backscattering ( $\sigma_{\sqrt{s}} \approx 0.1$  MeV)

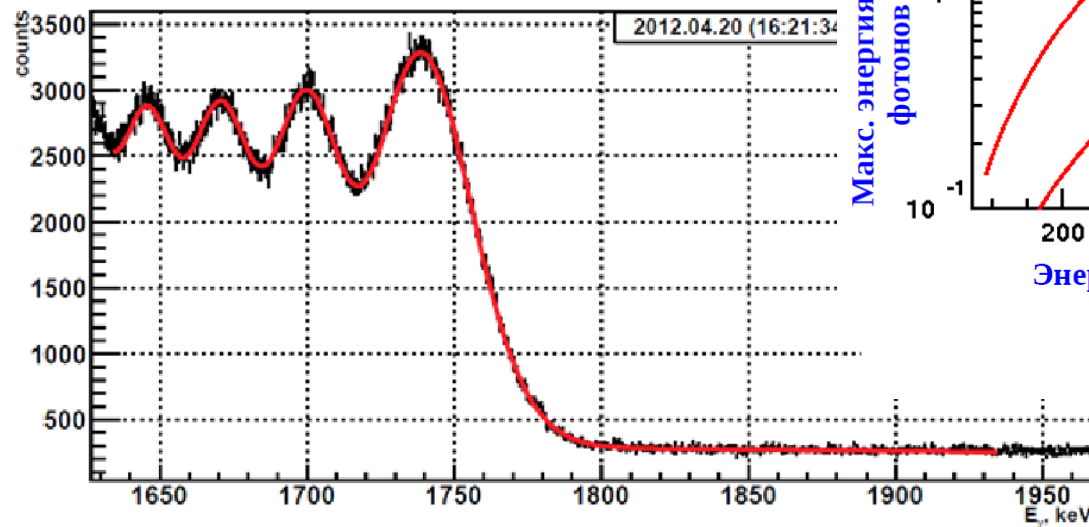
# VEPP-2000



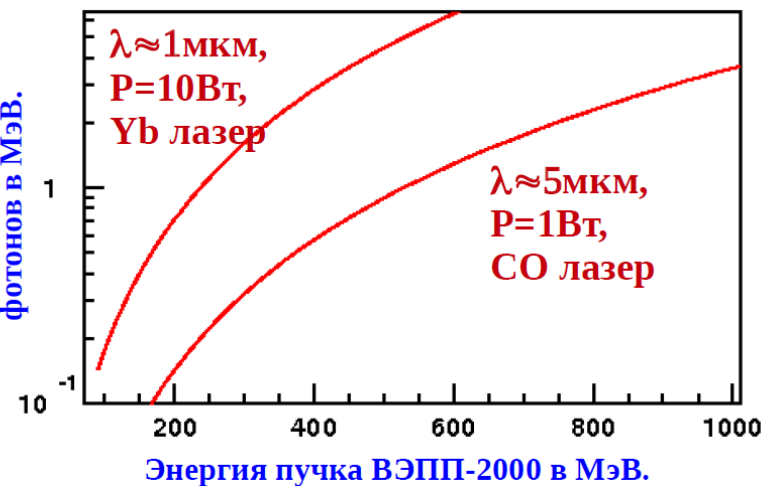
# Energy measurement



Starting from 2012, energy is monitored continuously using Compton backscattering, with  $\sim 30$  keV precision



Макс. энергия рассеянных фотонов в МэВ.

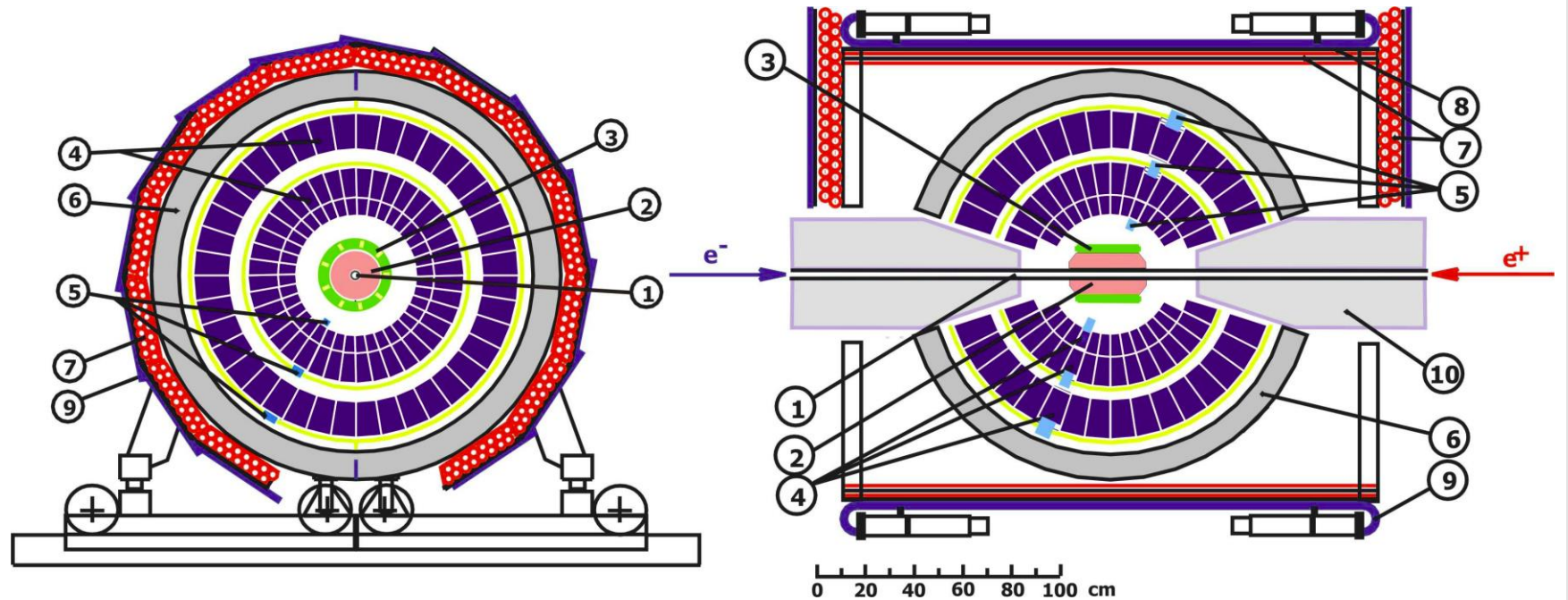


$$E = 993.662 \pm 0.016 \text{ МэВ}$$

MeV

M.N. Achasov et al. arXiv:1211.0103v1 [physics.acc-ph] 1 Nov 2012

# SND detector

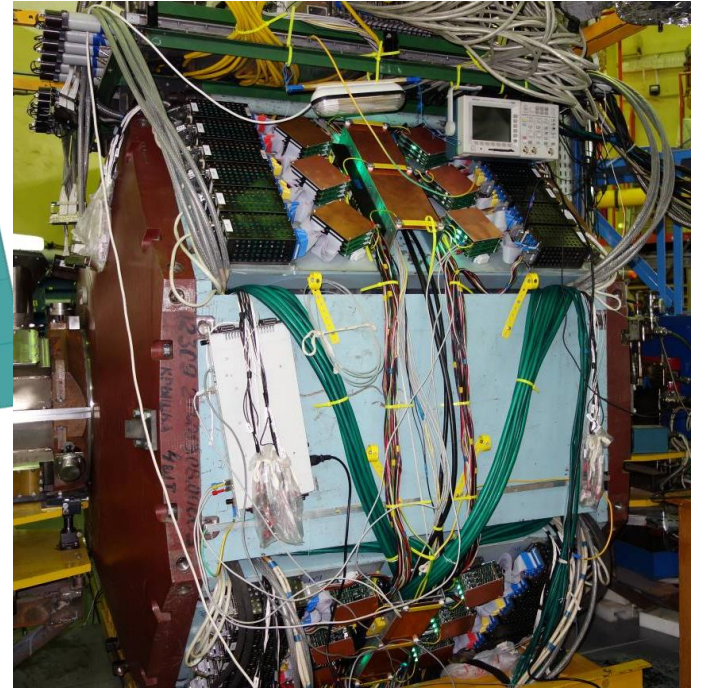
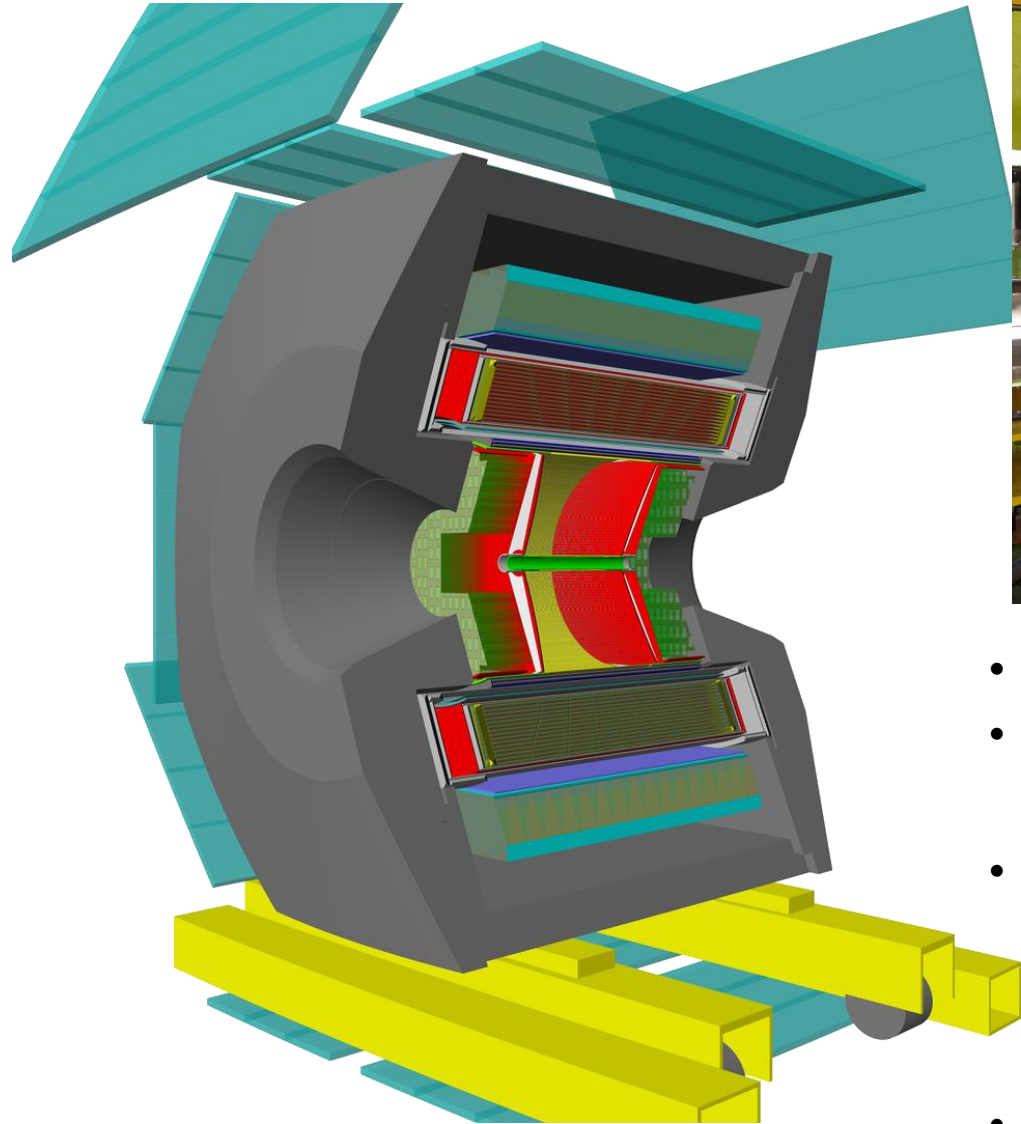


- 1 – beam pipe
- 2 – tracking system
- 3 – aerogel
- 4 – NaI(Tl) crystals

- 5 – phototriodes
- 6 – muon absorber
- 7–9 – muon detector
- 10 – focusing solenoid

# CMD-3 Detector

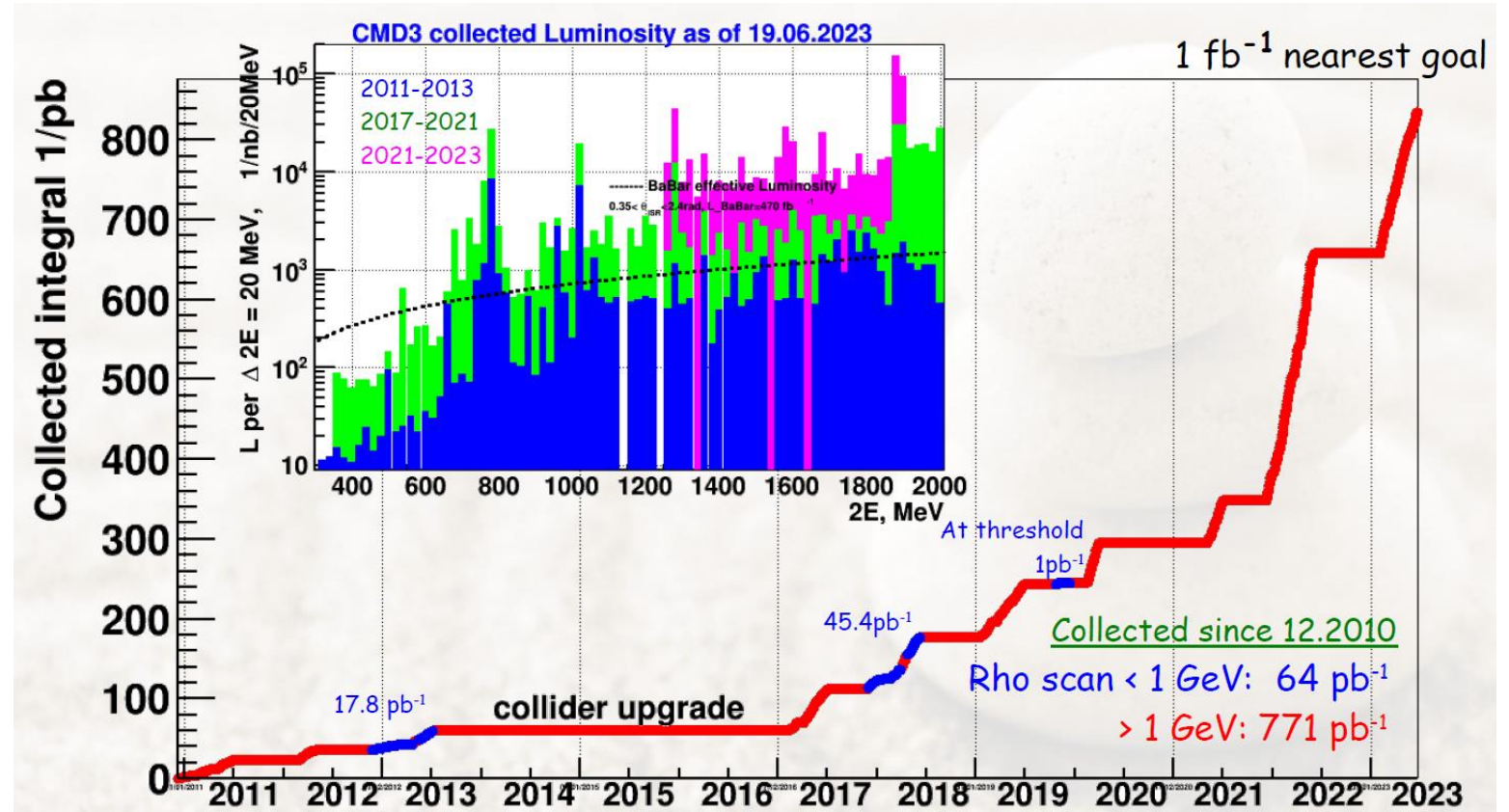
\*Cryogenic  
Magnetic Detector



- Magnetic field 1.0-1.3 T
- Drift chamber
  - $\sigma_{R\phi} \sim 100 \mu, \sigma_z \sim 2 - 3 \text{ mm}$
- EM calorimeter (LXE, CsI, BGO),  $13.5 X_0$ 
  - $\sigma_E/E \sim 3\% - 10\%$
  - $\sigma_\theta \sim 5 \text{ mrad}$
- TOF
- Muon counters

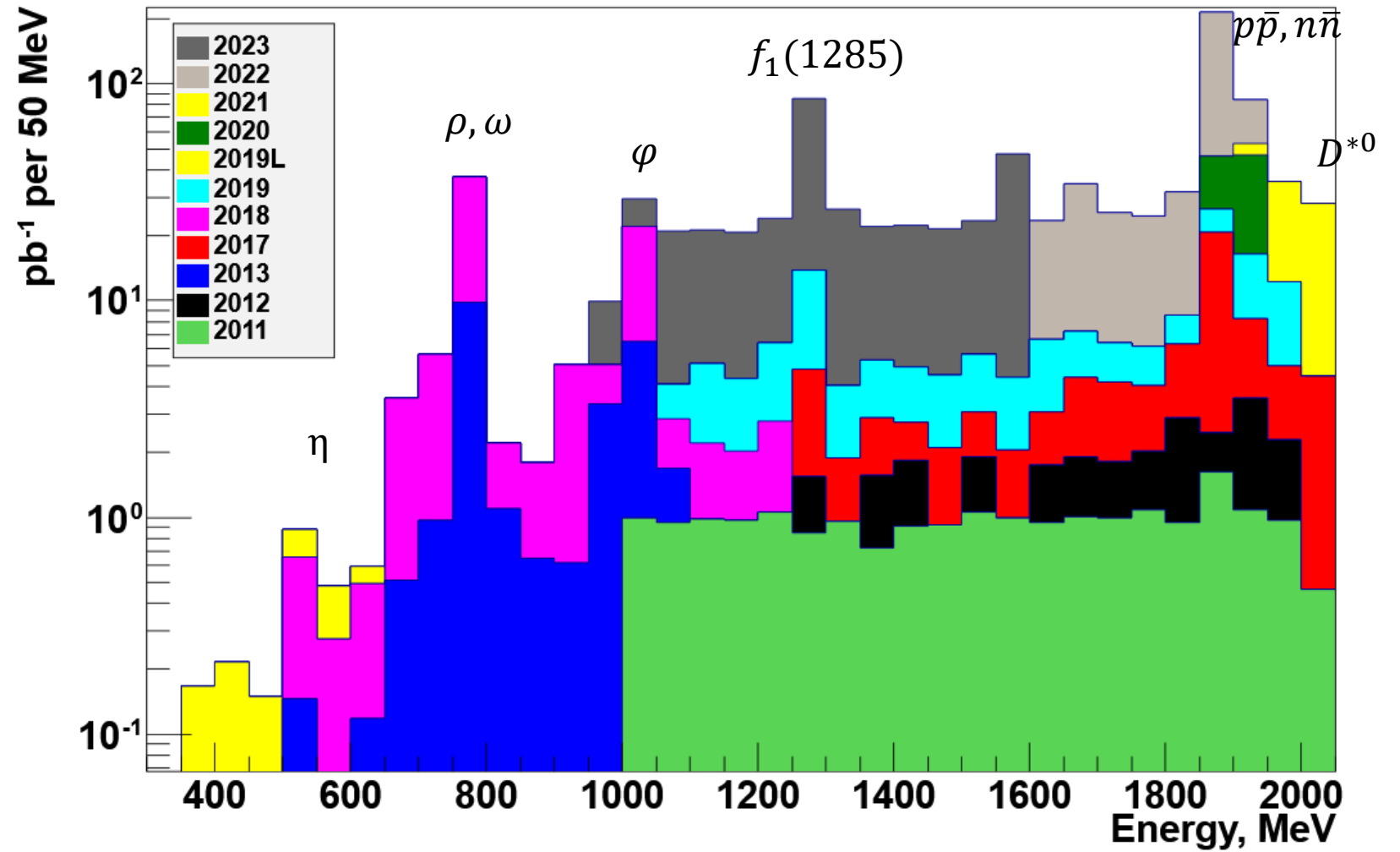


# Collected data



The  $e^+e^- \rightarrow \pi^+\pi^-$  result is based on 3 data taking seasons: 2013, 2018, 2020

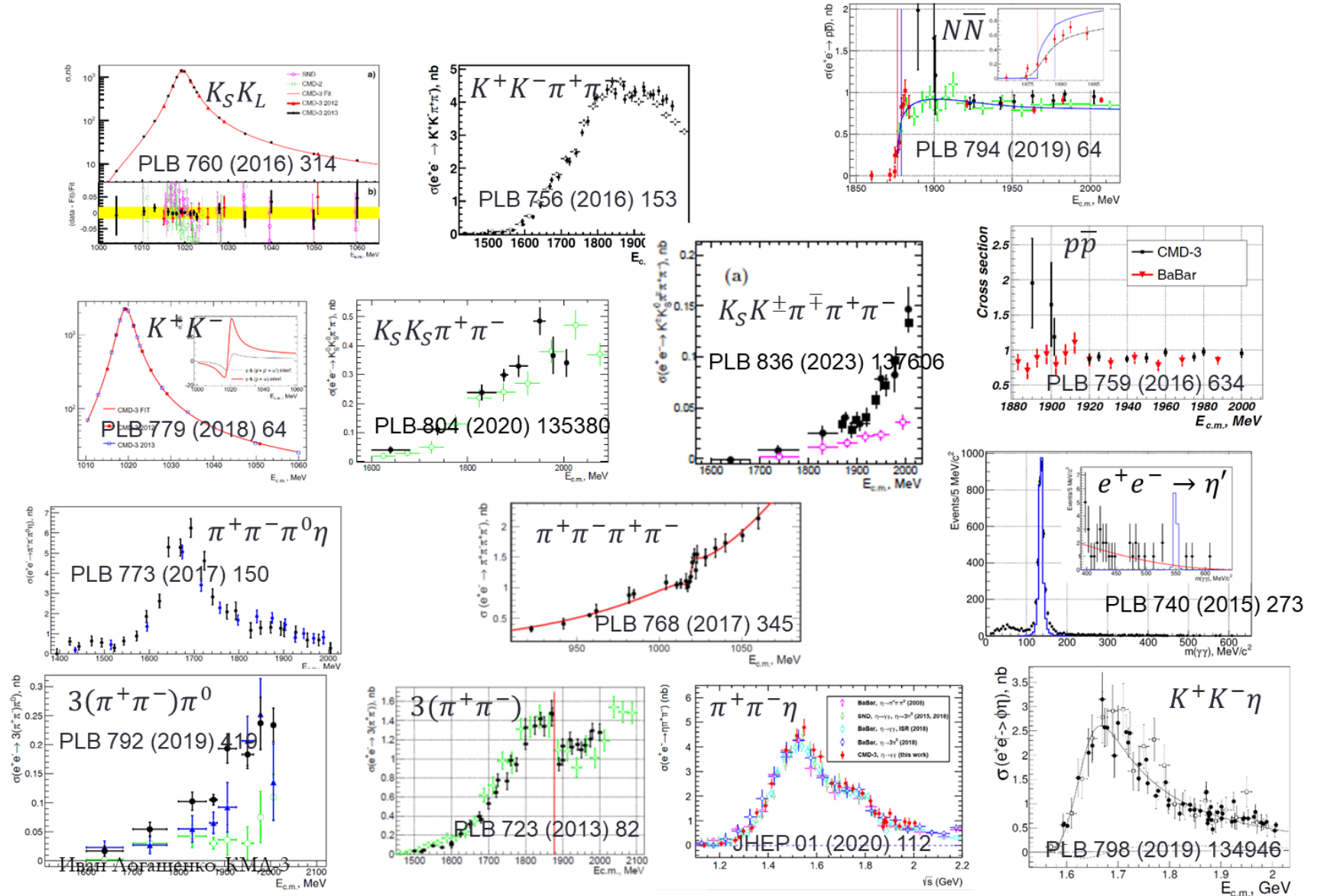
# Collected data



# Final states under analysis

Signature	Final states (preliminary, published)
2 charged	$\pi^+\pi^-$ , $K^+K^-$ , $K_S K_L$ , $p\bar{p}$
2 charged + $\gamma$ 's	$\pi^+\pi^-\gamma$ , $\pi^+\pi^-\pi^0$ , $\pi^+\pi^-2\pi^0$ , $\pi^+\pi^-3\pi^0$ , $\pi^+\pi^-4\pi^0$ , $\pi^+\pi^-\eta$ , $\pi^+\pi^-\pi^0\eta$ , $\pi^+\pi^-2\pi^0\eta$ , $K^+K^-\pi^0$ , $K^+K^-2\pi^0$ , $K^+K^-\eta$ , $K_S K_L \pi^0$ , $K_S K_L \eta$
4 charged	$2(\pi^+\pi^-)$ , $K^+K^-\pi^+\pi^-$ , $K_S K^\pm \pi^\mp$
4 charged + $\gamma$ 's	$2(\pi^+\pi^-)\pi^0$ , $2\pi^+2\pi^-2\pi^0$ , $\pi^+\pi^-\eta$ , $\pi^+\pi^-\omega$ , $2\pi^+2\pi^-\eta$ , $K^+K^-\omega$ , $K_S K^\pm \pi^\mp \pi^0$
6 charged	$3(\pi^+\pi^-)$ , $K_S K_S \pi^+\pi^-$
6 charged + $\gamma$ 's	$3(\pi^+\pi^-)\pi^0$
Neutral	$\pi^0\gamma$ , $2\pi^0\gamma$ , $3\pi^0\gamma$ , $\eta\gamma$ , $\pi^0\eta\gamma$ , $2\pi^0\eta\gamma$
Other	$n\bar{n}$ , $\pi^0 e^+ e^-$ , $\eta e^+ e^-$
Rare decays	$\eta'$ , $D^*(2007)^0$

# CMD-3 published results



$$e^+e^- \rightarrow \pi^+\pi^-$$

arXiv:2309.12910

Measurement of the pion formfactor with CMD-3 detector and its implication to the hadronic contribution to muon (g-2)

F.V. Ignatov,<sup>1,2</sup> R.R. Akhmetshin,<sup>1,2</sup> A.N. Amirkhanov,<sup>1,2</sup> A.V. Anisenkov,<sup>1,2</sup> V.M. Aulchenko,<sup>1,2</sup> N.S. Bashtovoy,<sup>1</sup> D.E. Berkaev,<sup>1,2</sup> A.E. Bondar,<sup>1,2</sup> A.V. Bragin,<sup>1</sup> S.I. Eidelman,<sup>1,2</sup> D.A. Epifanov,<sup>1,2</sup> L.B. Epshteyn,<sup>1,2,3</sup> A.L. Erofeev,<sup>1,2</sup> G.V. Fedotovitch,<sup>1,2</sup> A.O. Gorkovenko,<sup>1,3</sup> F.J. Grancagnolo,<sup>4</sup> A.A. Grebenuk,<sup>1,2</sup> S.S. Gribovan,<sup>1,2</sup> D.N. Grigoriev,<sup>1,2,3</sup> V.L. Ivanov,<sup>1,2</sup> S.V. Karpov,<sup>1</sup> A.S. Kasaev,<sup>1</sup> V.F. Kazanin,<sup>1,2</sup> B.I. Khazin,<sup>1</sup> A.N. Kirpotin,<sup>1</sup> I.A. Koop,<sup>1,2</sup> A.A. Korobov,<sup>1,2</sup> A.N. Kozyrev,<sup>1,2,3</sup> E.A. Kozyrev,<sup>1,2</sup> P.P. Krokovny,<sup>1,2</sup> A.E. Kuzmenko,<sup>1</sup> A.S. Kuzmin,<sup>1,2</sup> I.B. Logashenko,<sup>1,2</sup> P.A. Lukin,<sup>1,2</sup> A.P. Lysenko,<sup>1</sup> K.Yu. Mikhailov,<sup>1,2</sup> I.V. Obraztsov,<sup>1,2</sup> V.S. Okhapkin,<sup>1</sup> A.V. Otboev,<sup>1</sup> E.A. Perevedentsev,<sup>1,2</sup> Yu.N. Pestov,<sup>1</sup> A.S. Popov,<sup>1,2</sup> G.P. Razuvaev,<sup>1,2</sup> Yu.A. Rogovsky,<sup>1,2</sup> A.A. Ruban,<sup>1</sup> N.M. Ryskulov,<sup>1</sup> A.E. Ryzhenenkov,<sup>1,2</sup> A.V. Semenov,<sup>1,2</sup> A.I. Senchenko,<sup>1</sup> P.Yu. Shatunov,<sup>1</sup> Yu.M. Shatunov,<sup>1</sup> V.E. Shebalin,<sup>1,2</sup> D.N. Shemyakin,<sup>1,2</sup> B.A. Shwartz,<sup>1,2</sup> D.B. Shwartz,<sup>1,2</sup> A.L. Sibidanov,<sup>5</sup> E.P. Solodov,<sup>1,2</sup> A.A. Talyshev,<sup>1,2</sup> M.V. Timoshenko,<sup>1</sup> V.M. Titov,<sup>1</sup> S.S. Tolmachev,<sup>1,2</sup> A.I. Vorobiov,<sup>1</sup> Yu.V. Yudin,<sup>1,2</sup> I.M. Zemlyansky,<sup>1</sup> D.S. Zhadan,<sup>1</sup> Yu.M. Zharinov,<sup>1</sup> and A.S. Zubakin<sup>1</sup>

(CMD-3 Collaboration)

<sup>1</sup>Budker Institute of Nuclear Physics, SB RAS, Novosibirsk, 630090, Russia

<sup>2</sup>Novosibirsk State University, Novosibirsk, 630090, Russia

<sup>3</sup>Novosibirsk State Technical University, Novosibirsk, 630092, Russia

<sup>4</sup>Istituto Nazionale di Fisica Nucleare, Sezione di Lecce, Lecce, Italy

<sup>5</sup>University of Victoria, Victoria, BC, Canada V8W 3P6

(Dated: September 25, 2023)

The cross section of the process  $e^+e^- \rightarrow \pi^+\pi^-$  has been measured in the center of mass energy range from 0.32 to 1.2 GeV with the CMD-3 detector at the electron-positron collider VEPP-2000. The measurement is based on an integrated luminosity of about 88 pb<sup>-1</sup> out of which 62 pb<sup>-1</sup> constitutes a full dataset collected by CMD-3 at center-of-mass energies below 1 GeV. In the dominant region near  $\rho$ -resonance a systematic uncertainty of 0.7% has been reached. The impact of presented results on the evaluation of the hadronic contribution to the anomalous magnetic moment of muon is discussed.

Направлено в PRL

arXiv:2302.08834

Measurement of the  $e^+e^- \rightarrow \pi^+\pi^-$  cross section from threshold to 1.2 GeV with the CMD-3 detector

F.V. Ignatov<sup>a,b,1</sup>, R.R. Akhmetshin<sup>a,b</sup>, A.N. Amirkhanov<sup>a,b</sup>, A.V. Anisenkov<sup>a,b</sup>, V.M. Aulchenko<sup>a,b</sup>, N.S. Bashtovoy<sup>a</sup>, D.E. Berkaev<sup>a,b</sup>, A.E. Bondar<sup>a,b</sup>, A.V. Bragin<sup>a</sup>, S.I. Eidelman<sup>a,b</sup>, D.A. Epifanov<sup>a,b</sup>, L.B. Epshteyn<sup>a,b,c</sup>, A.L. Erofeev<sup>a,b</sup>, G.V. Fedotovitch<sup>a,b</sup>, A.O. Gorkovenko<sup>a,c</sup>, F.J. Grancagnolo<sup>e</sup>, A.A. Grebenuk<sup>a,b</sup>, S.S. Gribovan<sup>a,b</sup>, D.N. Grigoriev<sup>a,b,c</sup>, V.L. Ivanov<sup>a,b</sup>, S.V. Karpov<sup>a</sup>, A.S. Kasaev<sup>a</sup>, V.F. Kazanin<sup>a,b</sup>, B.I. Khazin<sup>b</sup>, A.N. Kirpotin<sup>a</sup>, I.A. Koop<sup>a,b</sup>, A.A. Korobov<sup>a,b</sup>, A.N. Kozyrev<sup>a,c</sup>, E.A. Kozyrev<sup>a,b</sup>, P.P. Krokovny<sup>a,b</sup>, A.E. Kuzmenko<sup>a</sup>, A.S. Kuzmin<sup>a,b</sup>, I.B. Logashenko<sup>a,b</sup>, P.A. Lukin<sup>a,b</sup>, A.P. Lysenko<sup>a</sup>, K.Yu. Mikhailov<sup>a,b</sup>, I.V. Obraztsov<sup>a,b</sup>, V.S. Okhapkin<sup>a</sup>, A.V. Otboev<sup>a</sup>, E.A. Perevedentsev<sup>a,b</sup>, Yu.N. Pestov<sup>a</sup>, A.S. Popov<sup>a,b</sup>, G.P. Razuvaev<sup>a,b</sup>, Yu.A. Rogovsky<sup>a,b</sup>, A.A. Ruban<sup>a</sup>, N.M. Ryskulov<sup>a</sup>, A.E. Ryzhenenkov<sup>a,b</sup>, A.V. Semenov<sup>a,b</sup>, A.I. Senchenko<sup>a</sup>, P.Yu. Shatunov<sup>a</sup>, Yu.M. Shatunov<sup>a</sup>, V.E. Shebalin<sup>a,b</sup>, D.N. Shemyakin<sup>a,b</sup>, B.A. Shwartz<sup>a,b</sup>, D.B. Shwartz<sup>a,b</sup>, A.L. Sibidanov<sup>a,d</sup>, E.P. Solodov<sup>a,b</sup>, A.A. Talyshev<sup>a,b</sup>, M.V. Timoshenko<sup>a</sup>, V.M. Titov<sup>a</sup>, S.S. Tolmachev<sup>a,b</sup>, A.I. Vorobiov<sup>a</sup>, I.M. Zemlyansky<sup>a</sup>, D.S. Zhadan<sup>a</sup>, Yu.M. Zharinov<sup>a</sup>, A.S. Zubakin<sup>a</sup>, Yu.V. Yudin<sup>a,b</sup>

<sup>a</sup>Budker Institute of Nuclear Physics, SB RAS, Novosibirsk, 630090, Russia

<sup>b</sup>Novosibirsk State University, Novosibirsk, 630090, Russia

<sup>c</sup>Novosibirsk State Technical University, Novosibirsk, 630092, Russia

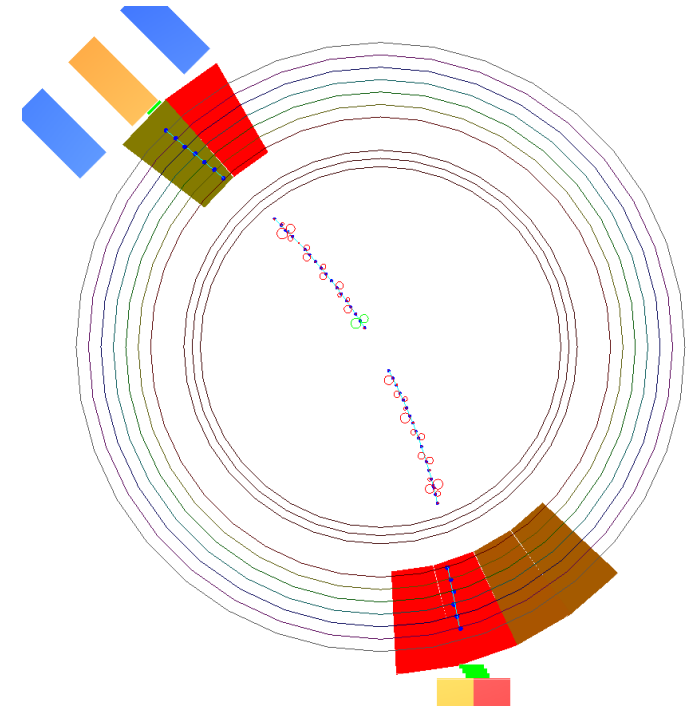
<sup>d</sup>University of Victoria, Victoria, BC, Canada V8W 3P6

<sup>e</sup>Istituto Nazionale di Fisica Nucleare, Sezione di Lecce, Lecce, Italy

Направлено в PRD

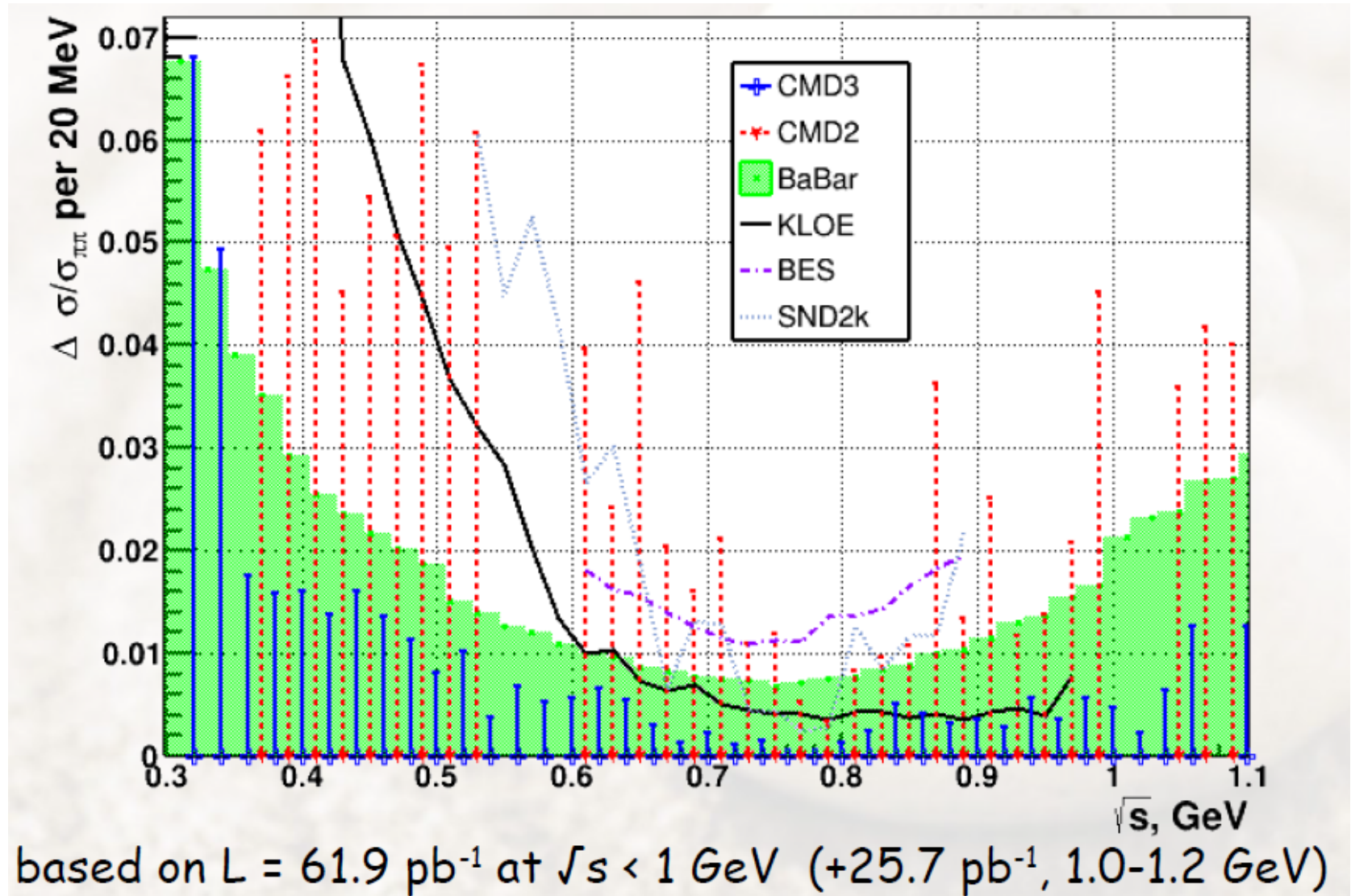
# Features of CMD-3 measurement

- World-largest statistics
  - 34 000 000  $e^+e^- \rightarrow \pi^+\pi^-$
  - 3 700 000  $e^+e^- \rightarrow \mu^+\mu^-$
  - 44 000 000  $e^+e^- \rightarrow e^+e^-$
- Many built-in cross checks
  - 3 methods for final states identification
  - 2 methods for angle measurement
  - Measurement of  $\sigma(e^+e^- \rightarrow \mu^+\mu^-)$
  - Measurement of charge asymmetry
- Very detailed study of potential systematics



Example of  $e^+e^- \rightarrow \pi^+\pi^-$  event

# Statistical precision of CMD-3 data



CMD-3

$e^+e^- \rightarrow \pi^+\pi^-$

analysis

Select events with 2 back-to-back tracks in the detector at large angle:

$e^+e^- \rightarrow e^+e^-, \mu^+\mu^-, \pi^+\pi^-$   
and cosmic background

Key pieces of analysis to reach high precision:

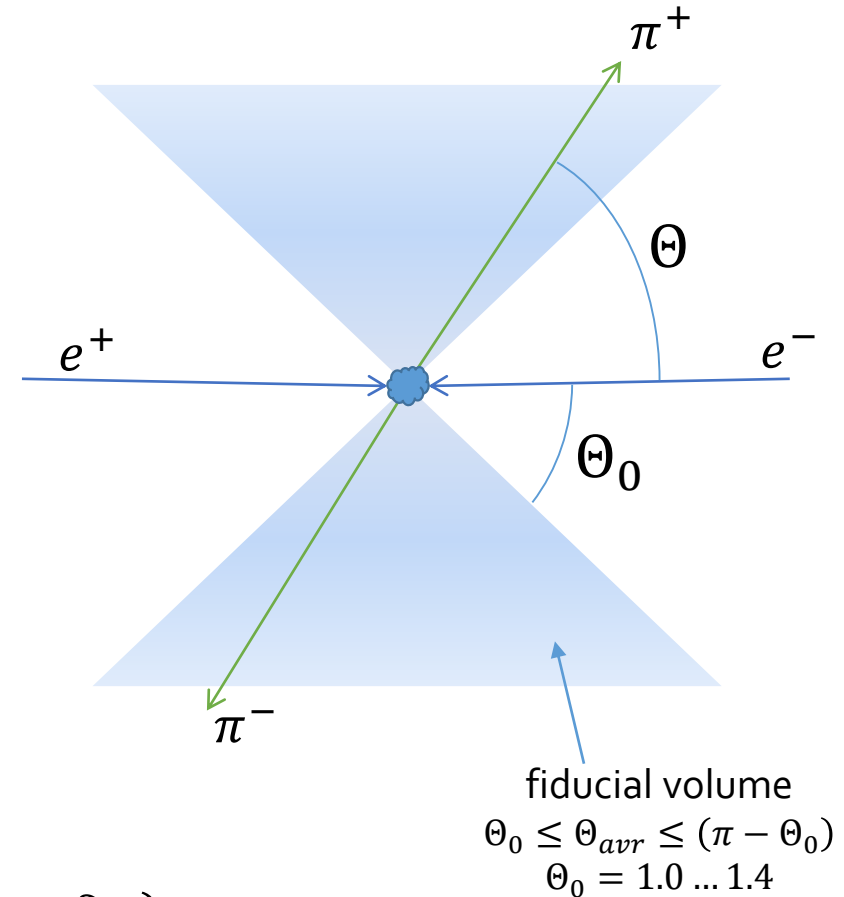
- $e/\mu/\pi$  separation
- radiative corrections
- fiducial volume
- detection efficiency corrections

$$\sigma(\pi^+\pi^-) = \frac{\pi\alpha^2}{3s} \beta_\pi^3 \cdot |F_\pi|^2$$

$$|F_\pi|^2 = \left( \frac{N_{\pi\pi}}{N_{ee}} - \Delta_{bg} \right) \cdot \frac{\sigma_{ee}^0 \cdot (1 + \delta_{ee}) \cdot \varepsilon_{ee}}{\sigma_{\pi\pi}^0 \cdot (1 + \delta_{\pi\pi}) \cdot \varepsilon_{\pi\pi}}$$

measured      Born cross-section      Detection efficiencies  
Radiative corrections

$e^+e^- \rightarrow e^+e^-, \mu^+\mu^-, \pi^+\pi^-$ ; cosmic bg





# Three methods of separation of $e^+e^-$ , $\mu^+\mu^-$ , $\pi^+\pi^-$

Separation (counting) of  $e^+e^-$ ,  $\mu^+\mu^-$ ,  $\pi^+\pi^-$  events is based on

- a) **momenta** of two particles
- b) or **energy deposition** in LXe calorimeter

$$-\ln L = -\sum_{bins} n_i \ln \left[ \sum_{a=ee,\mu\mu,\pi\pi,bg} N_a f_a(X^+, X^-) \right] + \sum_a N_a$$

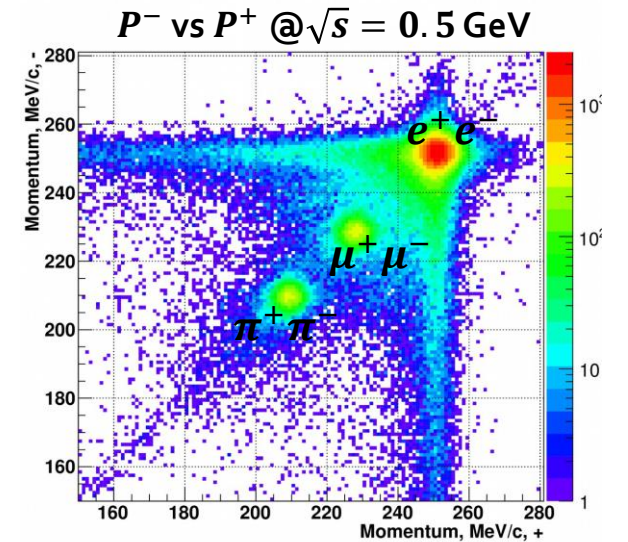
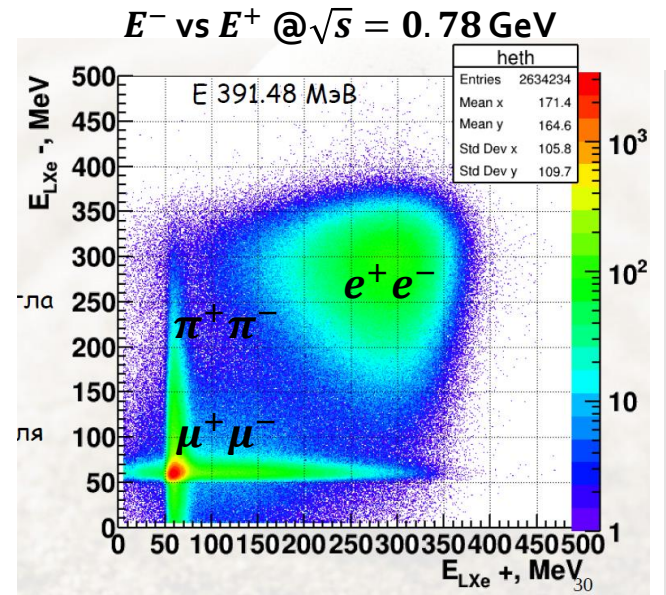
$X = P \text{ or } E$

$\pm$  sign reflects energy deposition and momentum of particle with corresponding charge

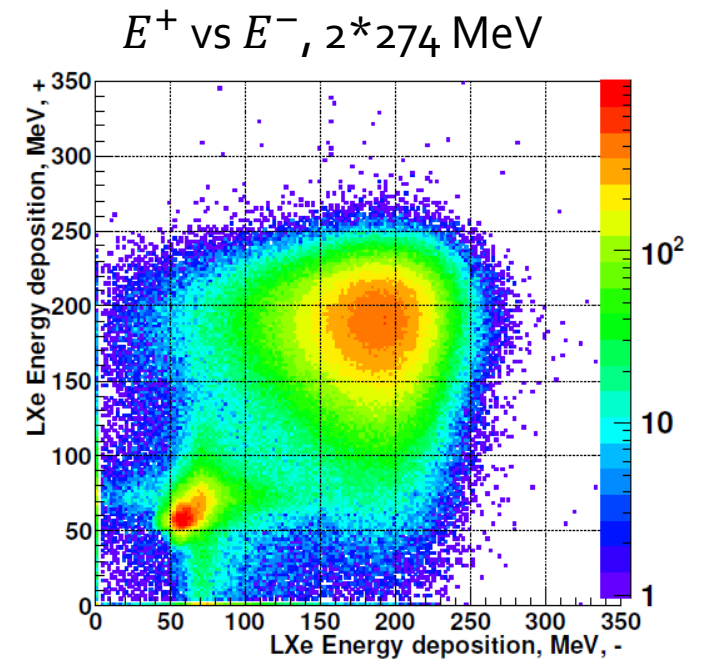
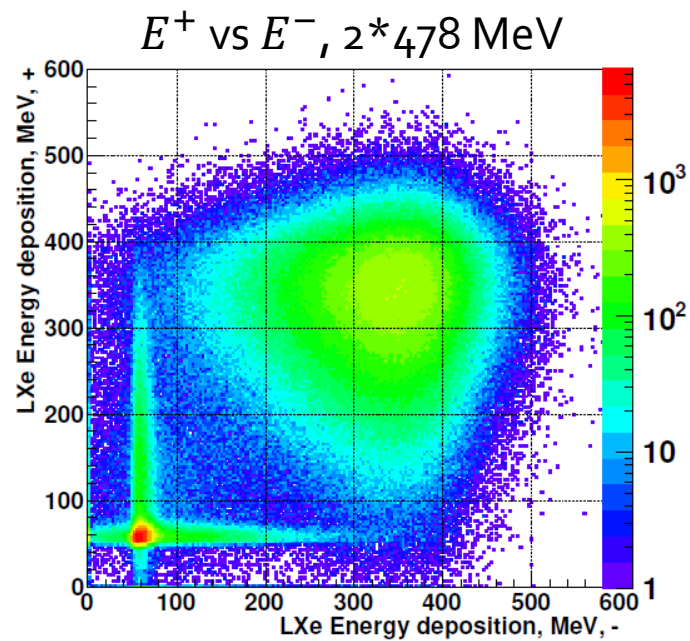
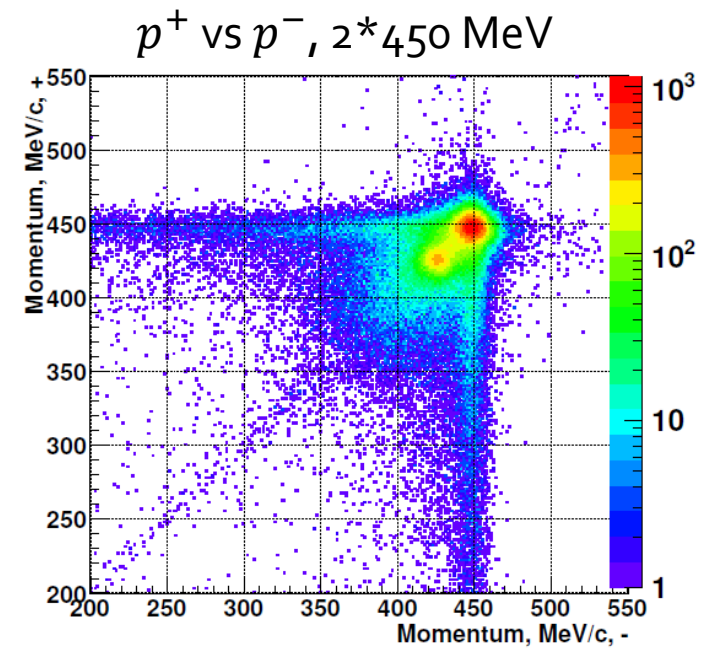
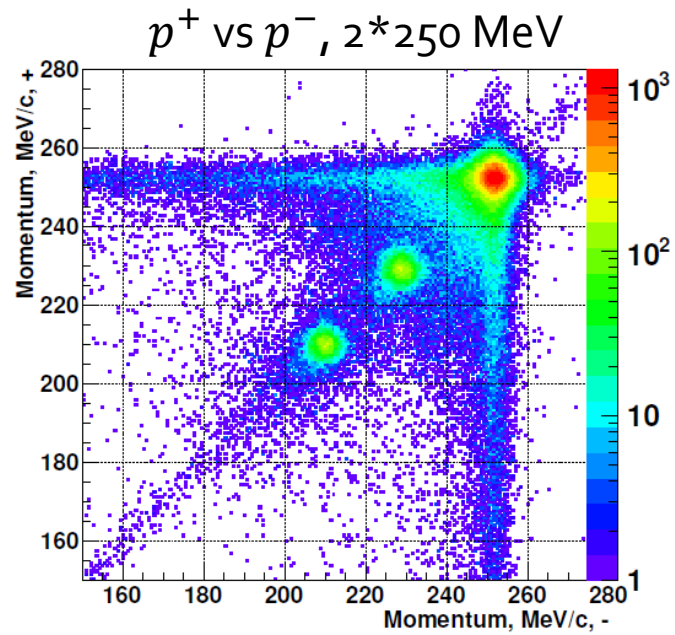
Independent check by **angular distribution**

For some fits ratio  $N_{\mu\mu}/N_{ee}$  is fixed to QED prediction, adjusted for RC and detector effects

Unique feature of CMD-3: three independent methods to measure  $N_{\pi\pi}/N_{ee}$ !



# E and P distributions



Where to get  
p.d.f.s  
 $f_X(p^+, p^-)$  and  
 $f_X(E^+, E^-)$ ?

## Separation by momentum

PDFs are based on MC

- “Ideal” p.d.f.s are generated using  $e^+e^- \rightarrow X^+X^-(\gamma)$  MC generator
- “Ideal” p.d.f.s are smeared with detector resolution function to get  $f_X(p^+, p^-)$

## Separation by energy deposition

PDFs are mostly empirical

- $f_X(E^+, E^-)$  are partly constructed using the data:
  - tagged electrons and positrons
  - cosmic muons

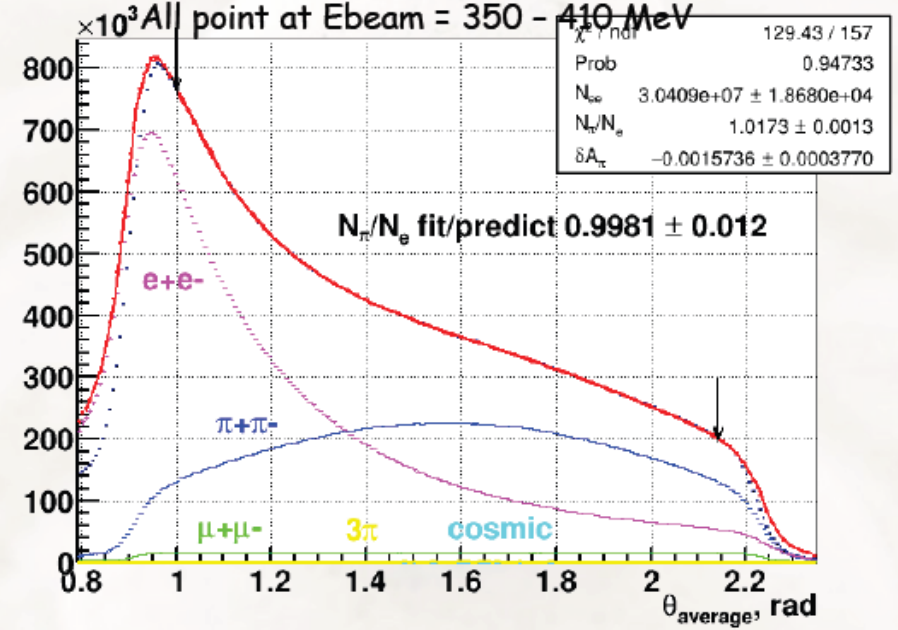
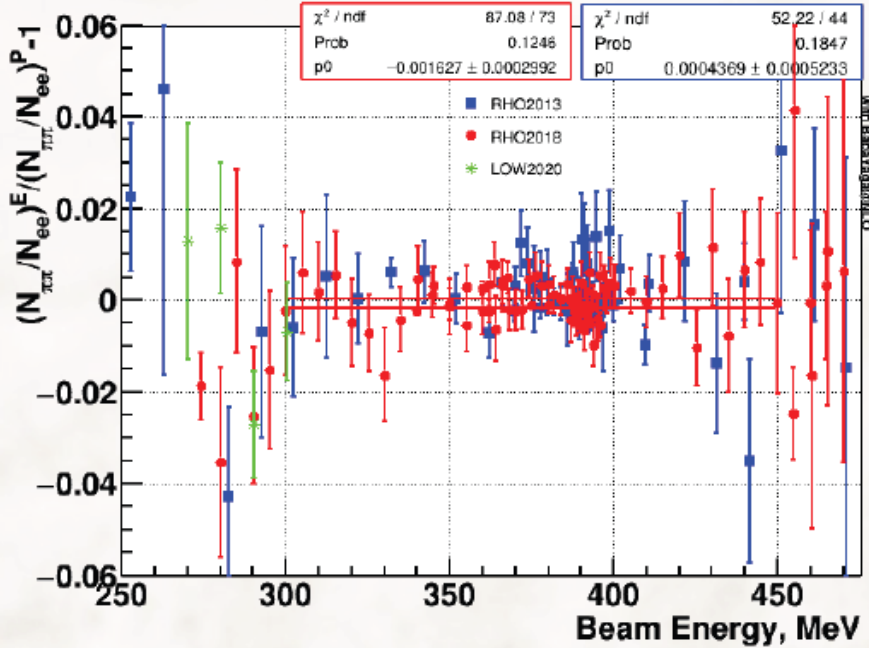
## Separation by angle distribution

1D fit of sum of  $f_X(\Theta_{avr})$

$f_X(\Theta_{avr})$  are taken from MC generator + efficiency corrections

Three methods agree to 0.2%!

E vs P separations



Fit by  $\theta$  distribution

For sum of  $\sqrt{s} = 0.7 - 0.82$  GeV points

by momenta in DCH:  $N_{\pi\pi} / N_{ee} = 1.0193 \pm 0.00030$

by energies in LXe  $\Delta N_{\pi\pi} / N_{ee} = -0.09 \pm 0.024\%$

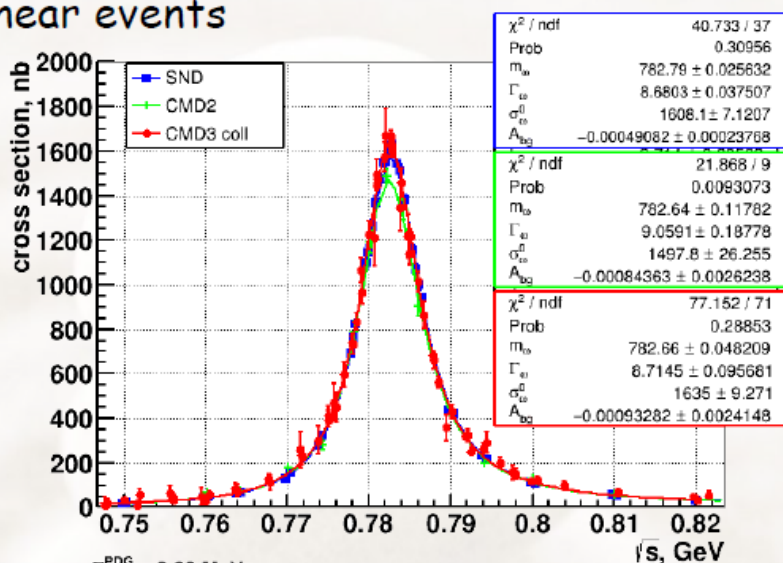
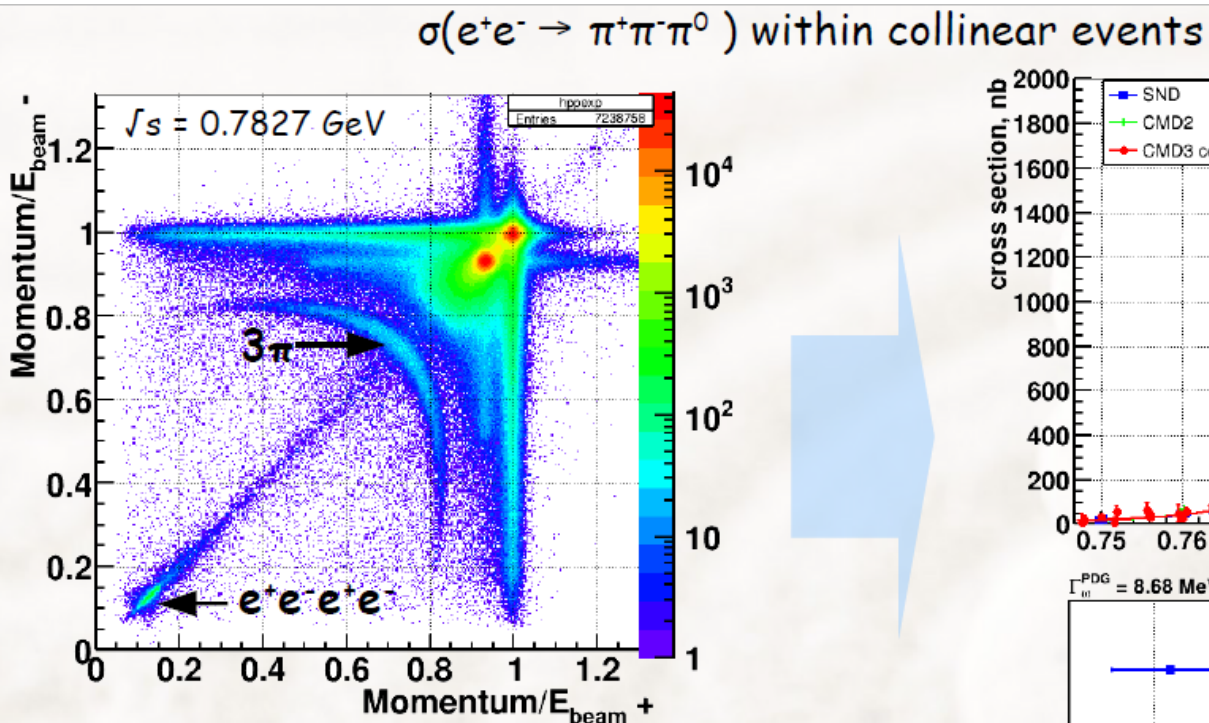
from theta with free  $\delta A$ :  $= -0.20 \pm 0.12\%$

with fixed  $\delta A=0$ :  $= +0.21 \pm 0.07\%$

Common stat from  
0.026%

# Background

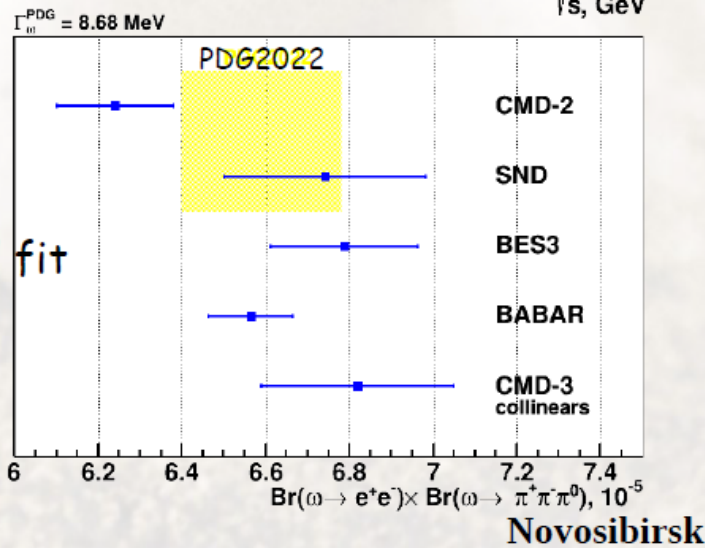
Collinear events are selected for  $2\pi$  analysis



$e^+e^- \rightarrow \pi^+\pi^-\pi^0$  is background for  $\pi^+\pi^-$  analysis (0.8% at  $\omega$ )  
 Number of  $3\pi$  events is additional parameter in likelihood fit  
 Main systematics (2.4%) inaccuracy of  $\rho\pi$  - model for efficiency determination, **total 3.3%**

$$B(\omega \rightarrow e^+e^-)B(\omega \rightarrow \pi^+\pi^-\pi^0) = (6.82 \pm 0.04 \pm 0.23) \times 10^{-5}$$

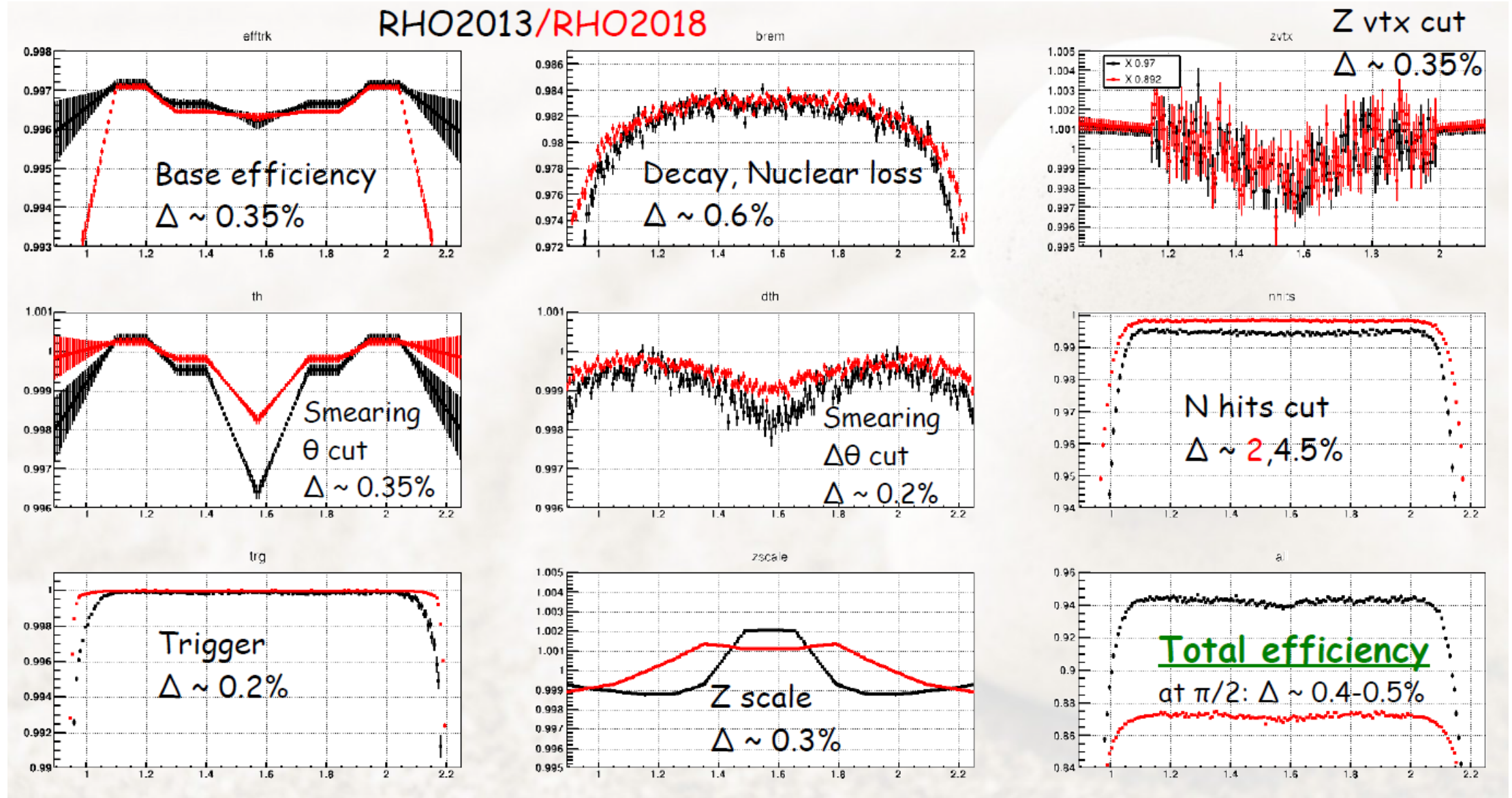
confirm SND@VEPP-2M result



February 2023

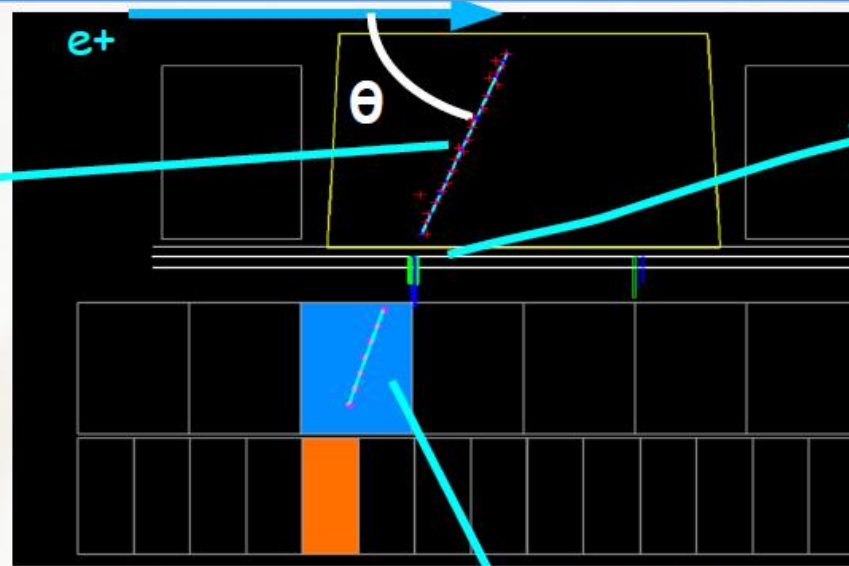
Novosibirsk

# Efficiency corrections



# Measurement of polar angle ( $Z$ )

Polar angle measured by **DC chamber** with help of charge division method ( $Z$  resolution  $\sim 2$ mm), **Unstable, depends on calibration and thermal stability of electronic** Calibration done relative to LXe (ZC)



## **ZC chamber**

(was in operation until mid 2017)  
multiwire chamber with 2 layers and with strip readout along  $Z$  coordinate

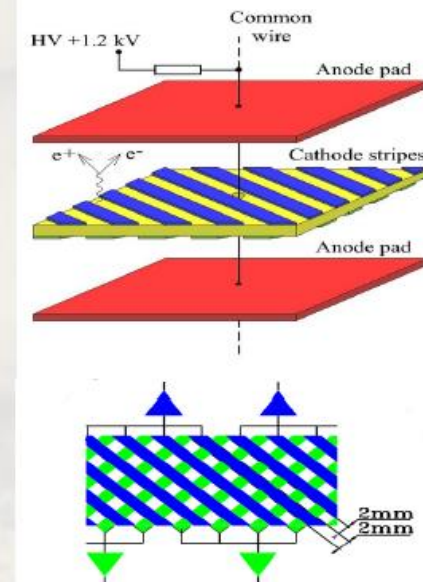
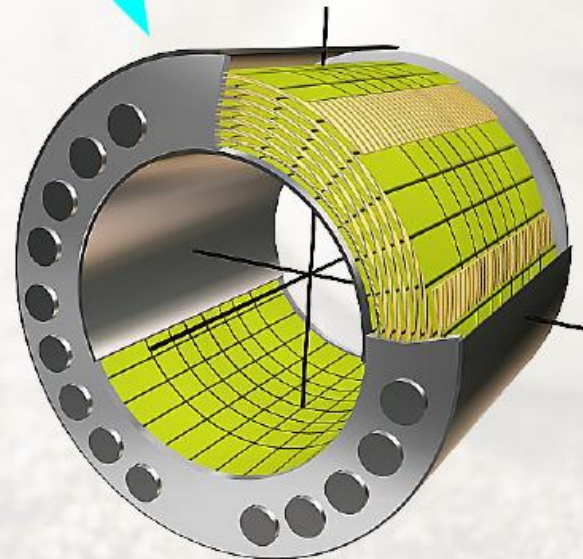
strip size: 6mm  
 $Z$  coordinate resolution  $\sim 0.7$  mm (for  $\theta_{\text{track}} \sim 1$  rad)

## **LXe calorimeter**

ionization collected in 7 layers with cathode strip readout,

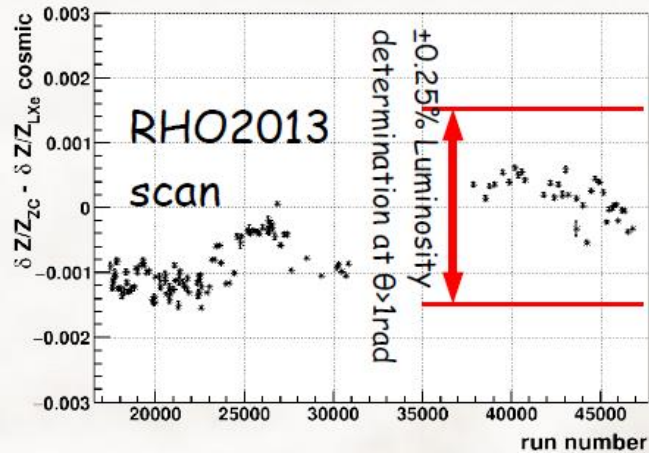
combined strip size: 10-15 mm  
Coordinate resolution  $\sim 2$ mm

strip precision, coordinate biases  $\sim 100$   $\mu\text{m}$   
should give  $\sim 0.1\%$  in Luminosity determination



# Cross-checks of polar angle (Z)

Monitoring of z-measurement between ZC vs LXe

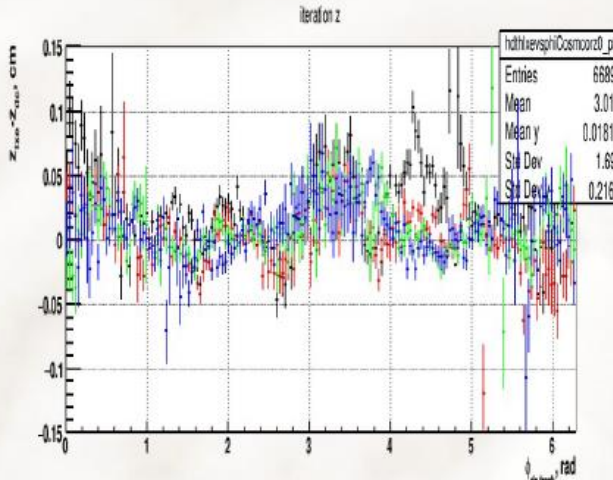


Variation because of DCh instability, different B field, ZC, LXe noise level

ZC/LXe comparison

0.25%

DC tracks vs LXe points



$\delta z \sim 0.5 \text{ mm}$  instability over regions at  $R=40 \text{ cm}$  (by  $\varphi$ , track direction, etc)

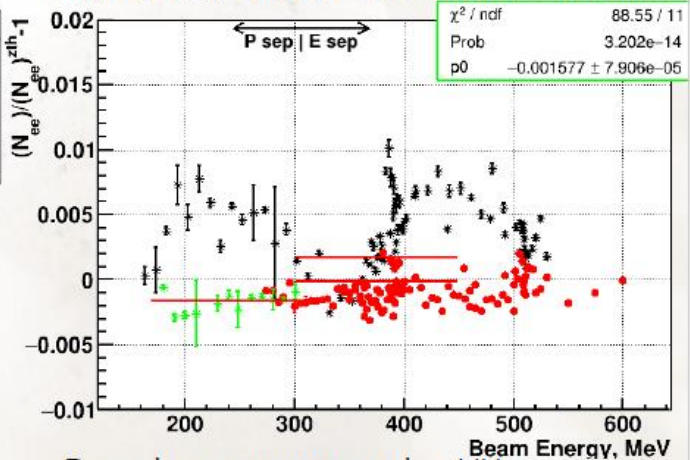
N.B. in average  $\langle \delta z \rangle$  should be better

LXe/ DC comparison

$\oplus$  0.3%  $\oplus$

= 0.8% (RHO2013) / 0.5% (RHO2018)

Inner DC radius effect:  $\theta$  - angle with Z vertex constrain / unconstrained case for 2 tracks



Inner layers operate at low HV  $\rightarrow$  Low resolution, higher systematics  
During RHO2013: 4 middle layers in DCH were switched off

$\rightarrow$  higher weights of inner layers

N.B.  $\theta$  - angle is defined with vertex constrain  $\rightarrow$  inner radius biases should be suppressed

Inner DC radius effect:

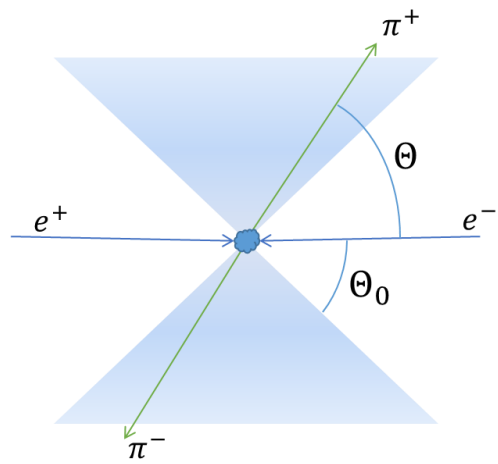
0.7% (RHO2013) / 0.3% (RHO2018)

February 2023

Novosibirsk



# Measurement of polar angle

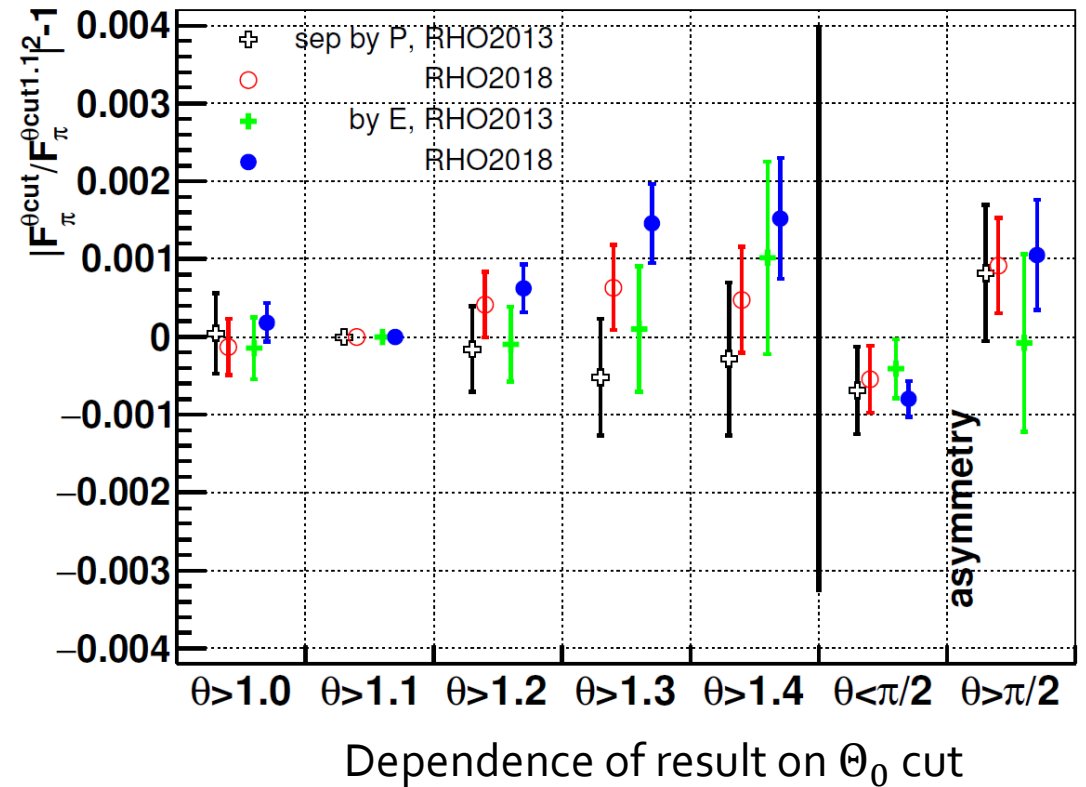


$\Theta$  angle is measured by drift chamber via charge division

Two detector systems with strips readout, LXe calorimeter and Z-chamber, are used for precise calibration and monitoring of DC

We need to precisely know the fiducial volume ( $\Theta_0$  cut).

$$|F_\pi|^2 = \left( \frac{N_{\pi\pi}}{N_{ee}} - \Delta_{bg} \right) \cdot \frac{\sigma_{ee}^0 \cdot (1 + \delta_{ee}) \cdot \varepsilon_{ee}}{\sigma_{\pi\pi}^0 \cdot (1 + \delta_{\pi\pi}) \cdot \varepsilon_{\pi\pi}}$$

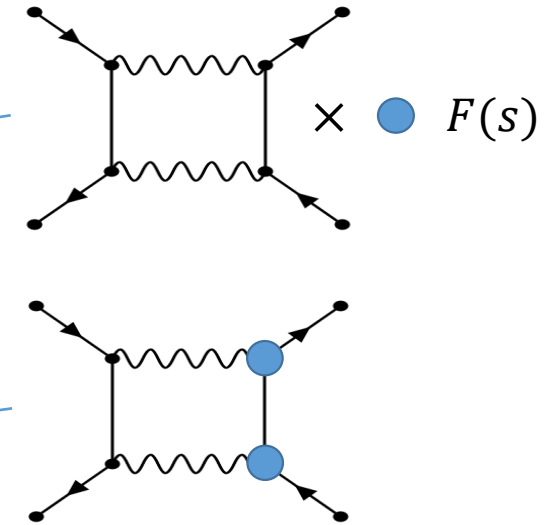
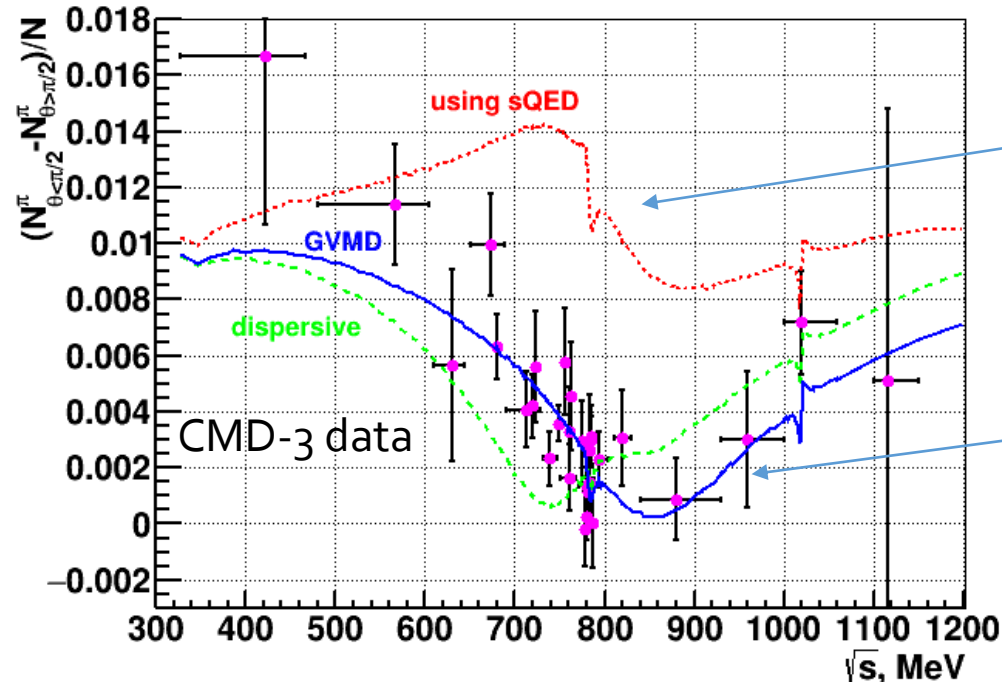
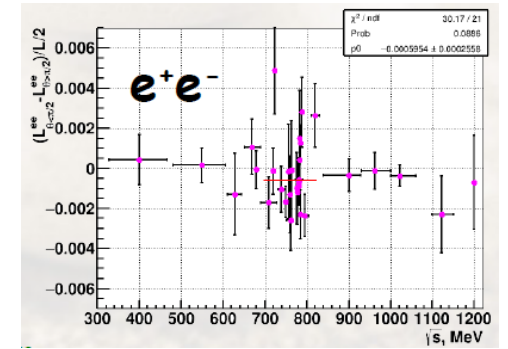


Factor 10 smaller compared to CMD-2, SND2k!

# Charge asymmetry in $e^+e^- \rightarrow \pi^+\pi^-$

Charge asymmetry in  $e^+e^- \rightarrow \pi^+\pi^-$  is due to interference between ISR/FSR and between one- and two-photon exchange

$$A = (N_{\Theta < \pi/2}^{\pi} - N_{\Theta > \pi/2}^{\pi})/N$$



The theoretical model by Lee, Ignatov, PLB 833 (2022) 137283 (GVDM) describes well the CMD-3 data  
 Recent calculation in dispersive formalism Colangelo et al., JHEP 08 (2022) 295 confirms the effect.

From  
measured  
cross section  
to input to  $a_\mu$   
calculation

“Visible” cross section  
 $\sigma(e^+e^-(\gamma) \rightarrow X(\gamma))$



Adjust for radiative  
corrections (ISR, FSR)  
 $\sigma(e^+e^- \rightarrow X)$



Adjust for vacuum polarization  
and return back FSR  
 $\sigma^0(e^+e^- \rightarrow X(\gamma))$

Here we correct for all  
detector effects

This one is used to get  
parameters of the  
resonances (mass, width,...)

This one is used in the  $a_\mu$   
integral

# MC generators for RC calculation

Two high precision MC generators is used

MCGPJ(0.2%,  $e^+e^-$ ,  $\mu^+\mu^-$ ,  $\pi^+\pi^-$ ) vs BabaYaga@NLO (0.1%,  $e^+e^-$ ,  $\mu^+\mu^-$ )

$e^+e^- \rightarrow e^+e^-(\gamma)$  : great consistency  $<0.1\%$  in the total cross section

$e^+e^- \rightarrow \mu^+\mu^-(\gamma)$  : It is missed mass term in FSR term in most of generators  
(effect 0.4% at  $\sqrt{s}=0.32$  GeV)

$e^+e^- \rightarrow \pi^+\pi^-(\gamma)$  : only MCGPJ available with 0.2% precision  
(for energy scan experiments)

Achieved precision in current analysis is sensitive  
for differential cross sections predictions

$e/\pi$  separation by momentum requires

$d\sigma/dP^+dP^-$  spectras as initial input

Asymmetry study requires  $d\sigma/d\theta$  spectras

# History: problem with “old” MCGPJ

Measurement of  $e^+e^- \rightarrow \pi^+\pi^-$  requires high precision calculation of radiative corrections.

Several MC generators available with 0.1-0.5% precision.

## CMD-3: MCGPJ generator

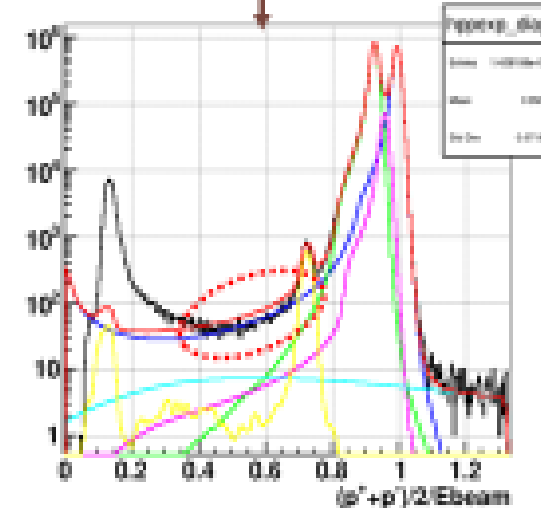
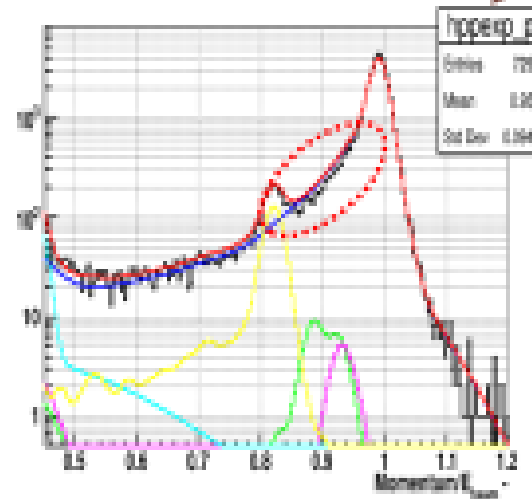
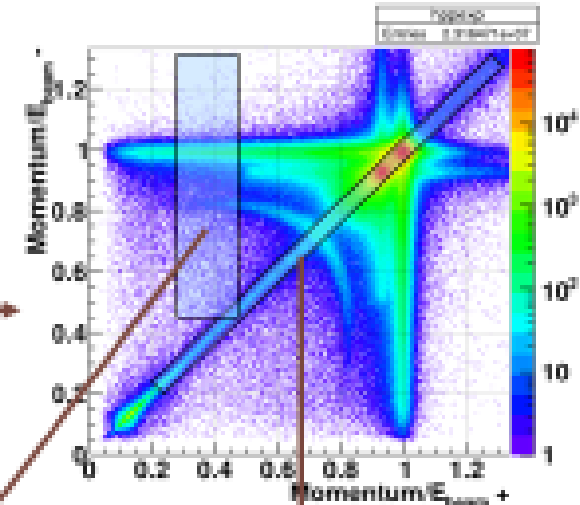
With high statistics we observed discrepancies in tails of  $e^+e^-$  experimental spectrum with theoretical prediction.

The corresponding changes in p.d.f.s  $f_{ee}(p^+, p^-)$  produce percent-level systematic shift of  $N(\pi^+\pi^-)$  for event separation by  $P$

- For the integral (radiative correction) the effect is negligible

$$\frac{p^-}{E_D} \text{ VS } \frac{p^+}{E_D}$$

All 2013 data  
 $2 \cdot 10^7$  events



MCGPJ was modified to improve the agreement: angular distribution for  $\gamma$  jets

# MC generators for RC calculation

**BaBaYaga@NLO shows better agreement with the data:**

1) Momentum spectras better describe data:  
gives consistent results in  $N_{\mu\mu}/QED$   
(effect on  $|F_{\pi}|^2 \sim 0.2\%$  at  $\sqrt{s}=0.78$  GeV, and rising to 1.5%  
at 0.9 GeV when using momentum-based separation)

2) Experimental asymmetry in  $e+e-$  data  
relative to BabaYaga@NLO:  
 $\delta A = -0.060 \pm 0.026 \%$   
relative to MCGPJ

$$\delta A = -0.140 \pm 0.026 \%$$

BabaYaga@NLO consistent with NNLO MCMule

$$\delta A = +0.006 \pm 0.003 \%$$
 at  $\sqrt{s}=0.76$  GeV

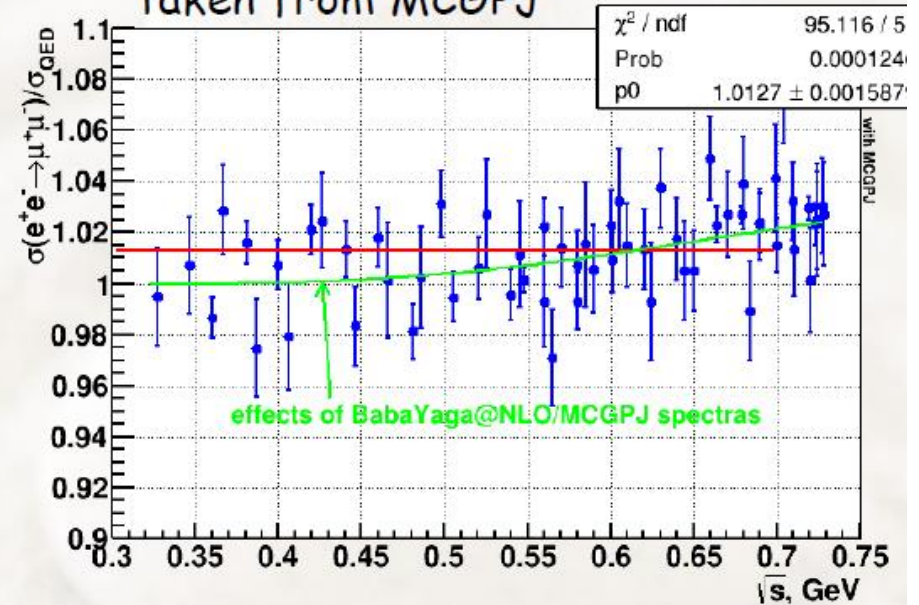
We adopted generators usage in this way:

$e+e-$  : BabaYaga@NLO

$\mu+\mu-$  : BabaYaga@NLO (differential cross section)  
MCGPJ (integral)

$\pi+\pi-$  : MCGPJ

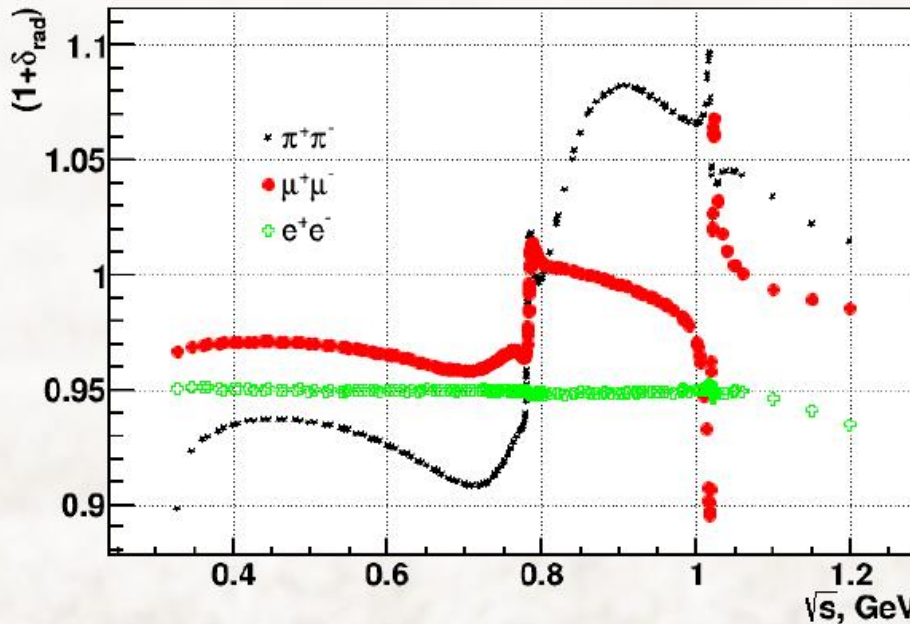
effect on  $N_{\mu\mu}/QED$   
with input  $d\sigma/dP^+dP^-$  spectra  
taken from MCGPJ



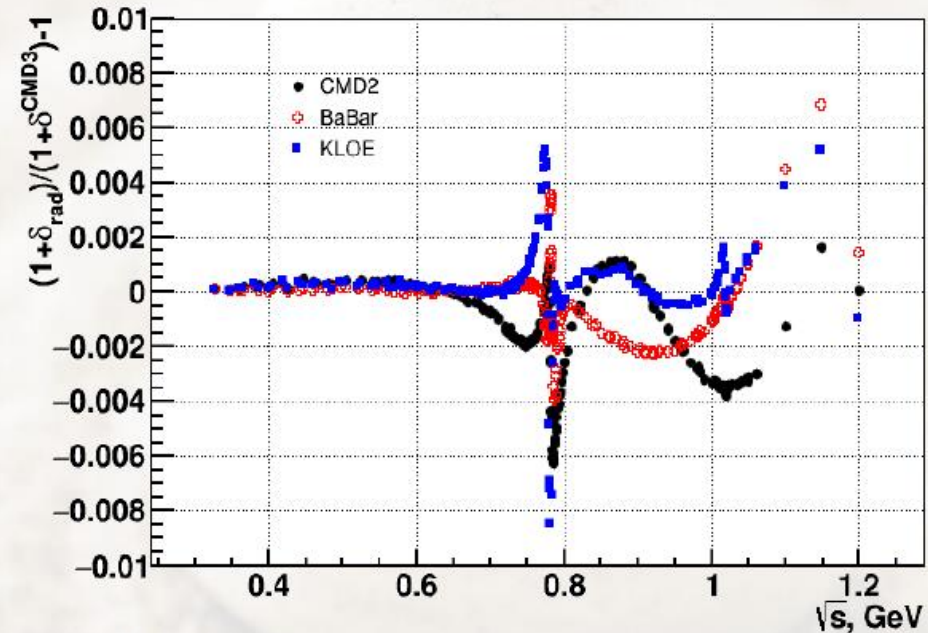
MCGPJ/BabaYaga@NLO difference gives systematics  
on  $|F_{\pi}|^2_{\pi}$  when using momentum-based separation  
**Better NNLO generators are needed for higher  
precision**

# MC generators for RC calculation

Radiative corrections within  
 $1. < (\pi + \theta^+ - \theta^-) / 2 < \pi - 1. \text{rad}$ ,  $|\Delta\phi| < 0.15$ ,  $|\Delta\theta| < 0.25$



Effect on  $2\pi$  radiative correction from  
different  $|F|^2_\pi$  parametrizations  
(over different datasets)



Systematic uncertainty

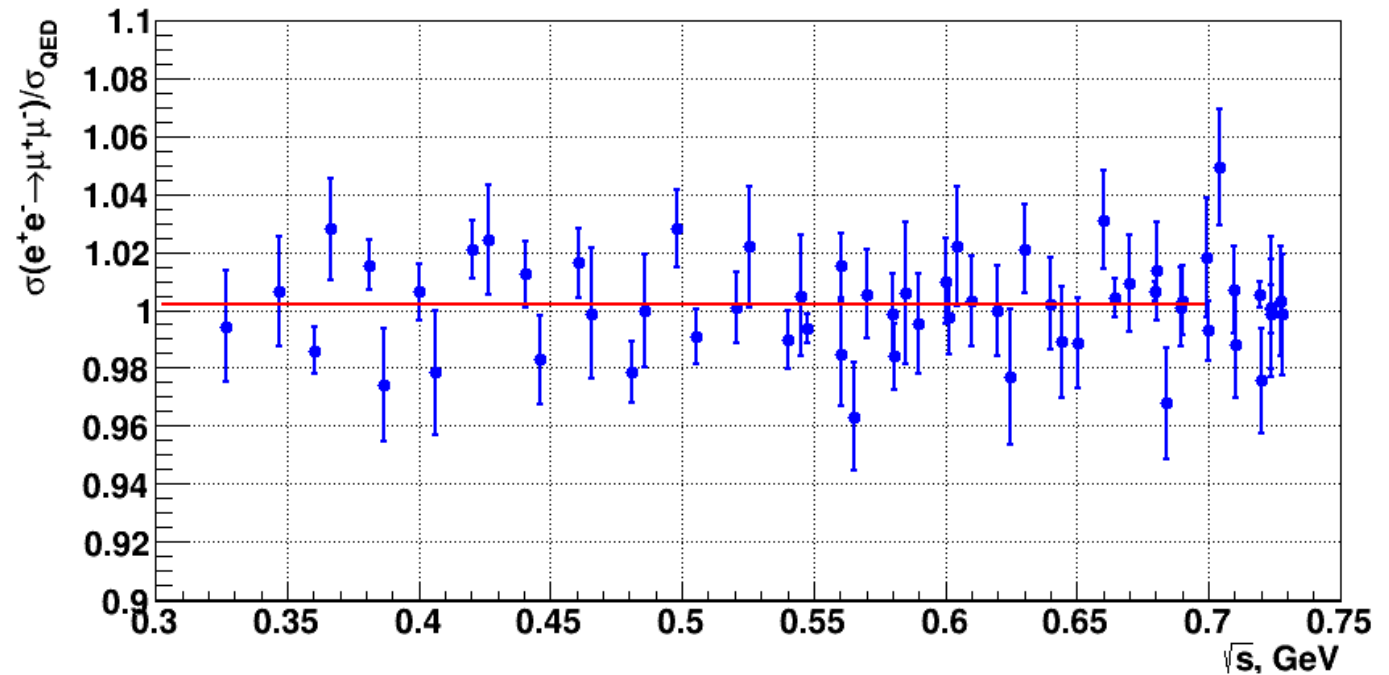
$$0.2\% (\pi + \pi^-) \oplus 0.2\% (F\pi, s > 0.74 \text{ GeV}) \oplus 0.1\% (e^+ e^-)$$

N.B. KLOE/BABAR difference in derivative 4%/0.4GeV,  
own CMD-3 is very possible as 1%/0.1 GeV  $\rightarrow$  same 0.2% estimation (from  $F\pi$  model)

# Measurement of $e^+e^- \rightarrow \mu^+\mu^-$

$e^+e^- \rightarrow \mu^+\mu^-$  events are identified as a by-product of analysis, which allows to measure  $\sigma(e^+e^- \rightarrow \mu^+\mu^-)$  and compare it to QED prediction

$$\sigma(e^+e^- \rightarrow \mu^+\mu^-)_{CMD3} / \sigma(e^+e^- \rightarrow \mu^+\mu^-)_{QED}$$



**+0.17 ± 0.16 %**

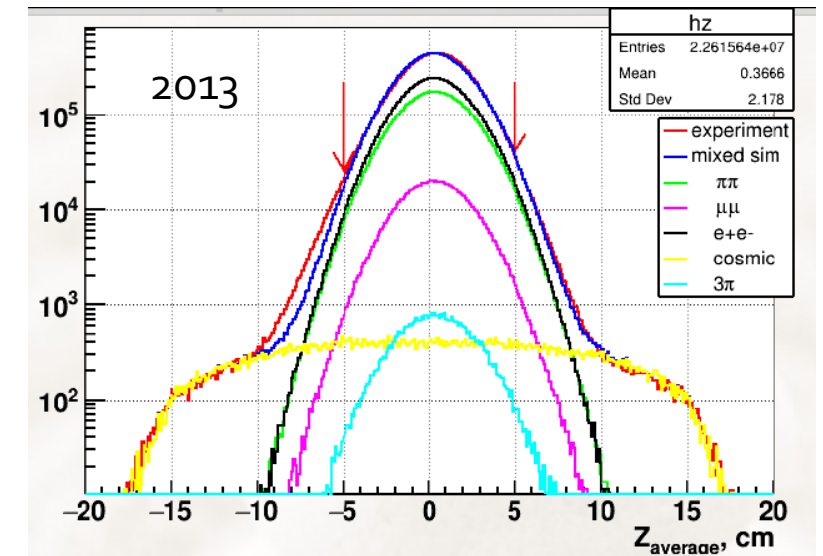
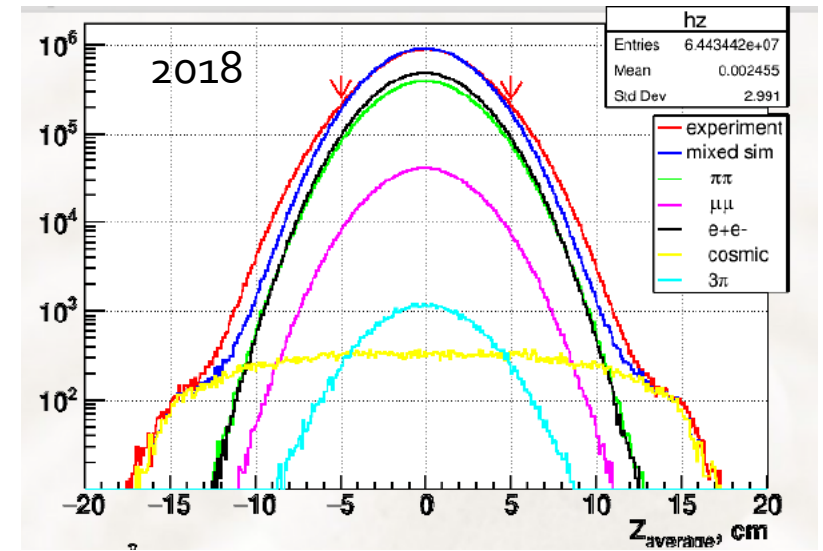
Powerful cross-check of  $\sigma(e^+e^- \rightarrow \pi^+\pi^-)$  measurement! All ingredients are tested: event separation, detection efficiencies, radiative corrections.



# Difference between 2013 and 2018 data

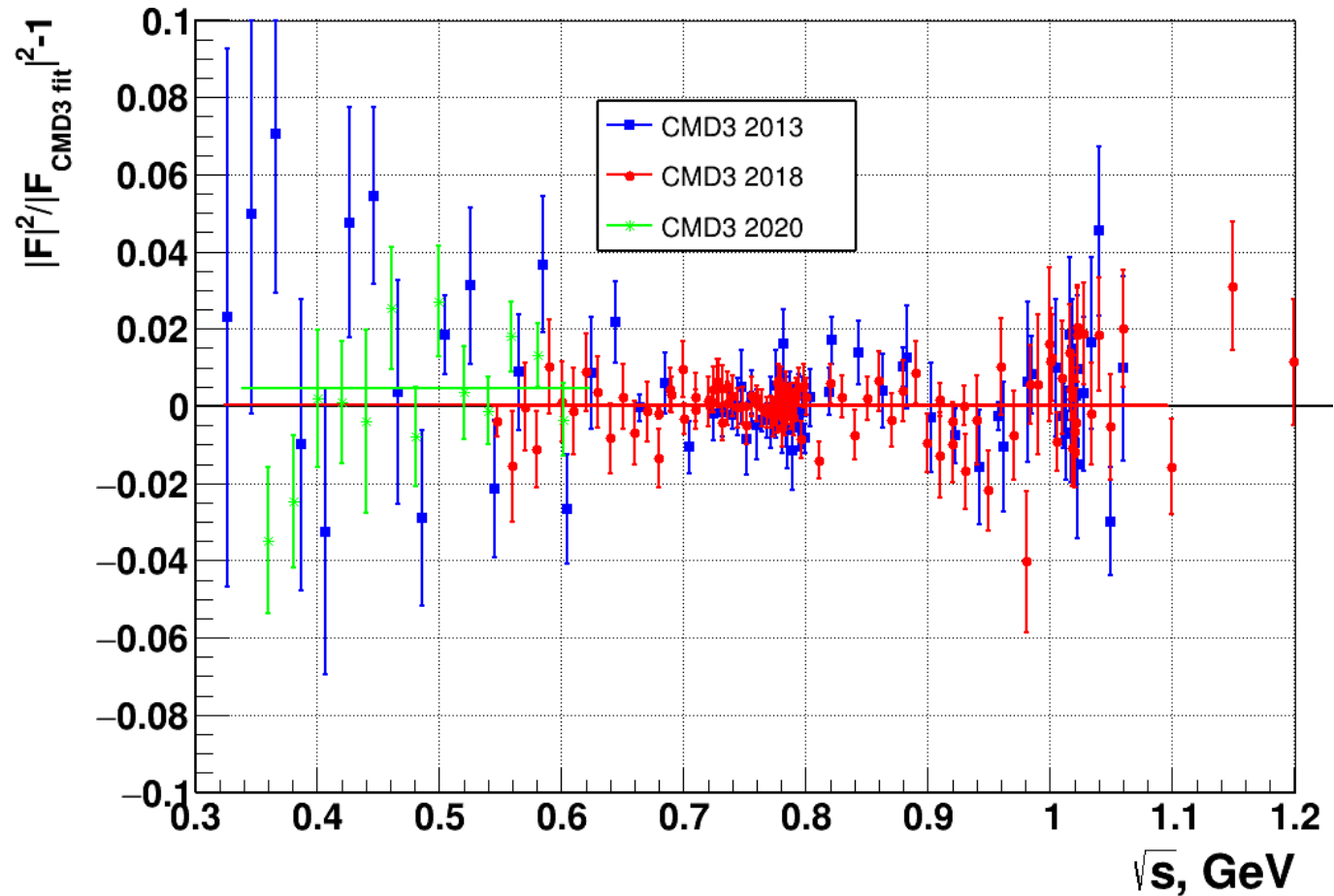
2013 and 2018 data were taken in the same energy range, but with significantly different detector conditions:

- luminosity integral in 2018 is factor 2-5 larger
- data rate (luminosity) in 2018 was factor 2-5 larger
- drift chamber in 2013 operated without 4 middle layers (out of 19)
- Z-chamber (important for precision determination of fiducial volume) broke before 2018 run
- Z beam size in 2018 was twice wider
- calorimeter electronics was significantly updated before 2018



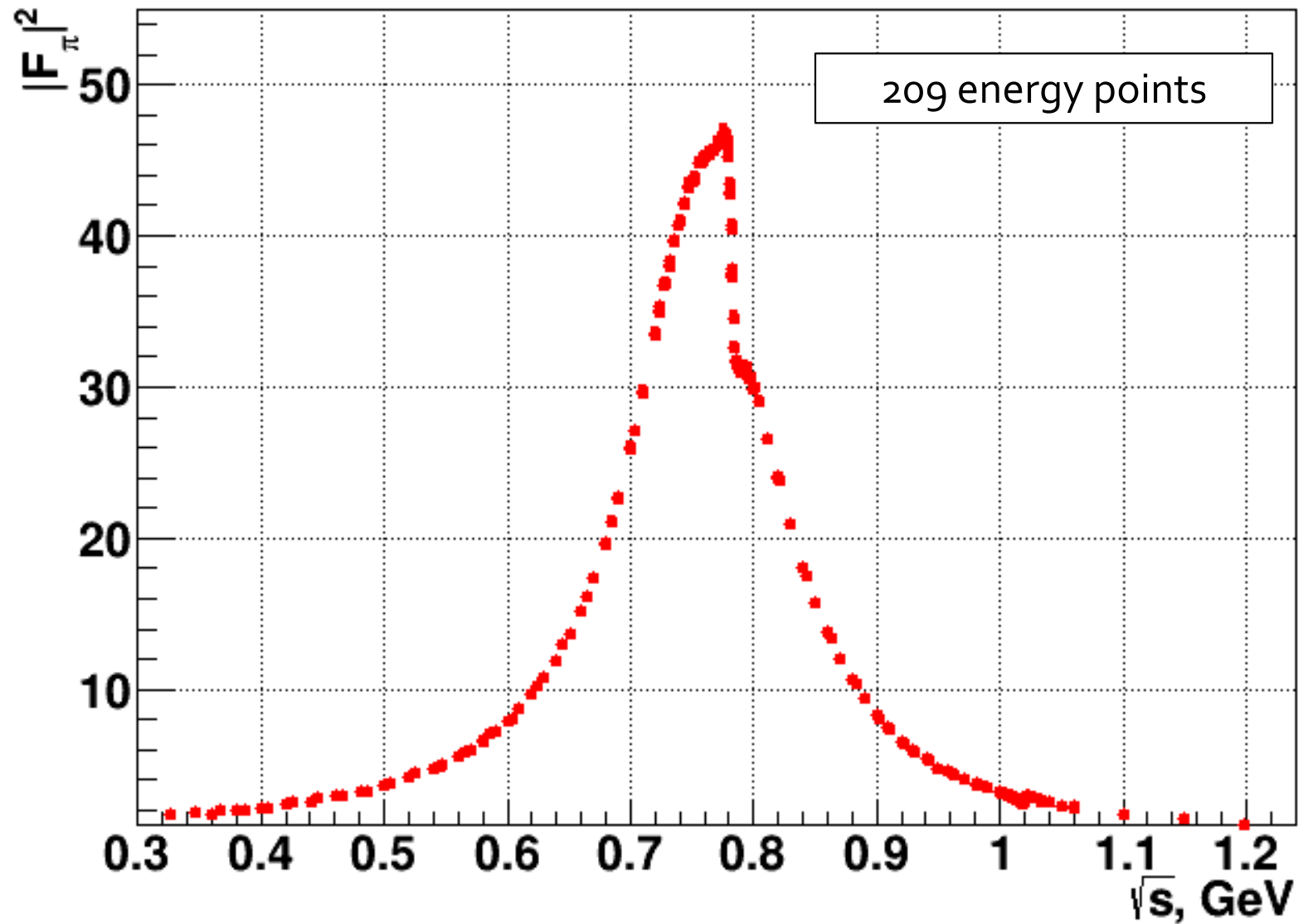
Z beam size

# Comparison of data taking seasons



Results based on 2013, 2018 and 2020 data only agree to  $\sim 0.1\%$ !  
The detector performance and run conditions were significantly different for these runs.

Measurement  
of  
 $e^+e^- \rightarrow \pi^+\pi^-$   
at CMD-3



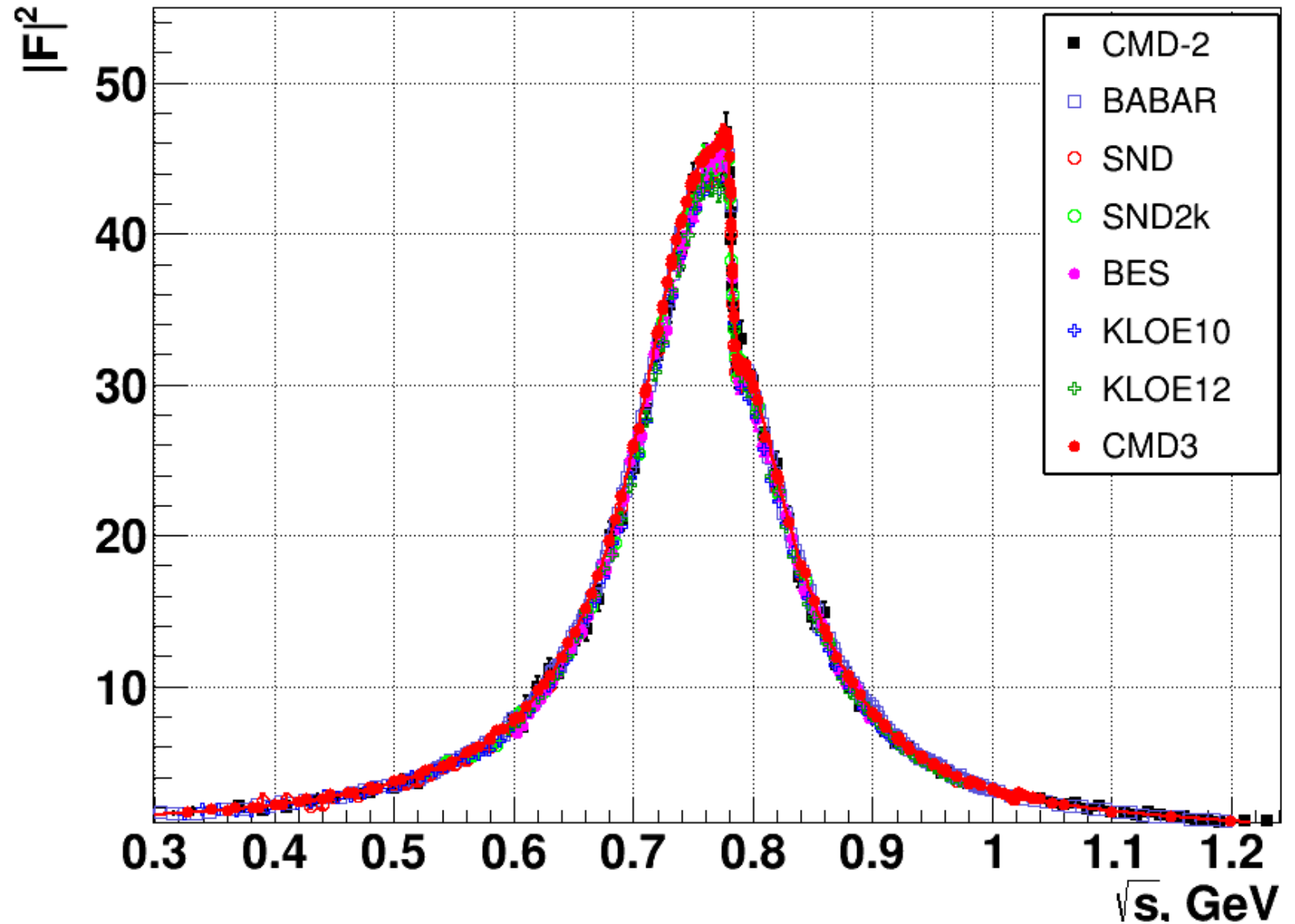
# Systematic errors

x Radiative corrections	0.2% ( $2\pi$ ) $\oplus$ 0.2% ( $F\pi$ ) $\oplus$ 0.1% ( $e+e^-$ )
x $e/\mu/\pi$ separation	0.5 (low) - 0.2 ( $\rho$ ) - 0.6 ( $\varphi$ ) %
x Fiducial volume	0.5% / 0.8% (RHO2013)
x Correlated inefficiency	0.1 ( $\rho$ ) - 0.15% ( $>1 \Gamma_{\pi B}$ )
x Trigger	0.05 ( $\rho$ ) - 0.3% ( $>1 \Gamma_{\pi B}$ )
x Beam Energy (by Compton $\sigma_{\epsilon} < 50$ keV)	0.1% (out of resonances), 0.5% (at $\omega, \varphi$ -peaks)
x Bremsstrahlung loss	0.05 %
x Pion specific loss	0.2% nuclear interaction
	0.2%(low) - 0.1% ( $\rho$ ) pion decay
<hr/>	
	CMD-3 $e^+ e^- \rightarrow \pi^+ \pi^-$ ana...
	0.8% (low) - 0.7% ( $\rho$ ) - 1.6% ( $\varphi$ )
	1.1% (low) - 0.9% ( $\rho$ ) - 2.0% ( $\varphi$ ) (RHO2013)

Conservative estimate

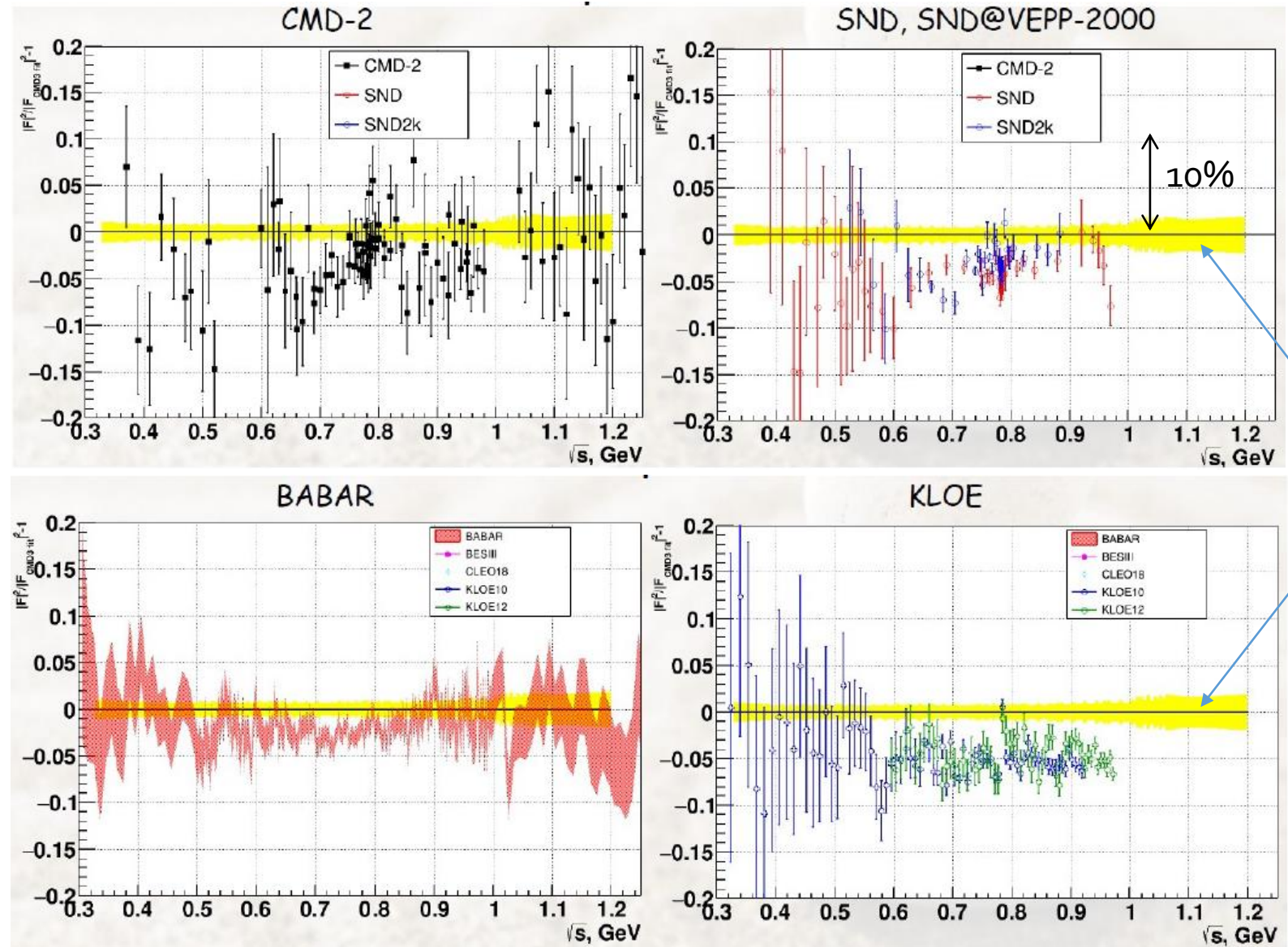
# Comparison to other measurements

At first glance, they look close to each other...



# Comparison to other measurements

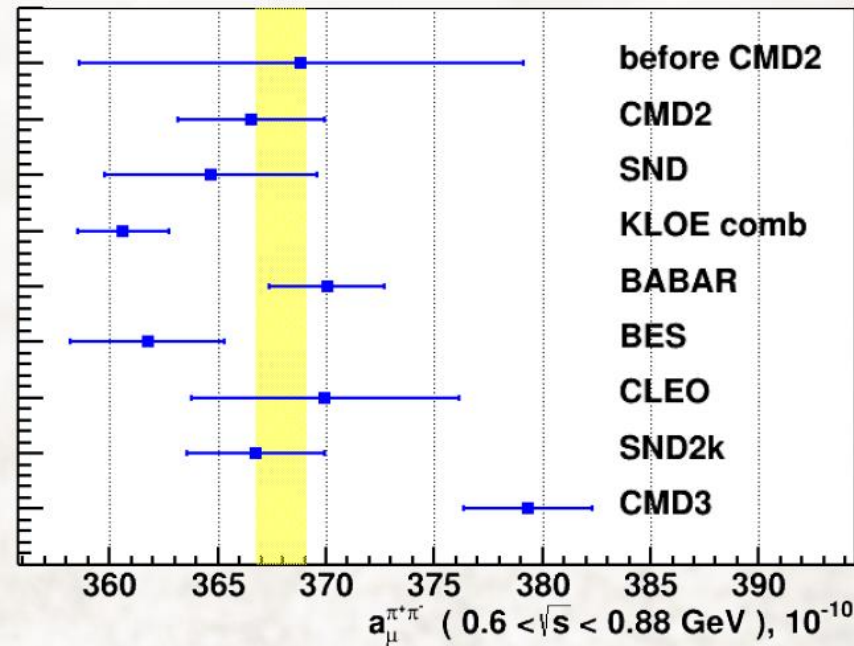
CMD-3 is systematically above previous measurements by ~2-5%



CMD-3

CMD-3  
 $e^+e^- \rightarrow$   
 $\pi^+\pi^-$ :  
 contribution to  
 $g-2$

$$a_{\mu}^{had,LO} = \frac{m_{\mu}^2}{12\pi^3} \int_{4m_{\pi}^2}^{\infty} \frac{\sigma_{e^+e^- \rightarrow \gamma^* \rightarrow hadrons}(s) K(s)}{s} ds$$



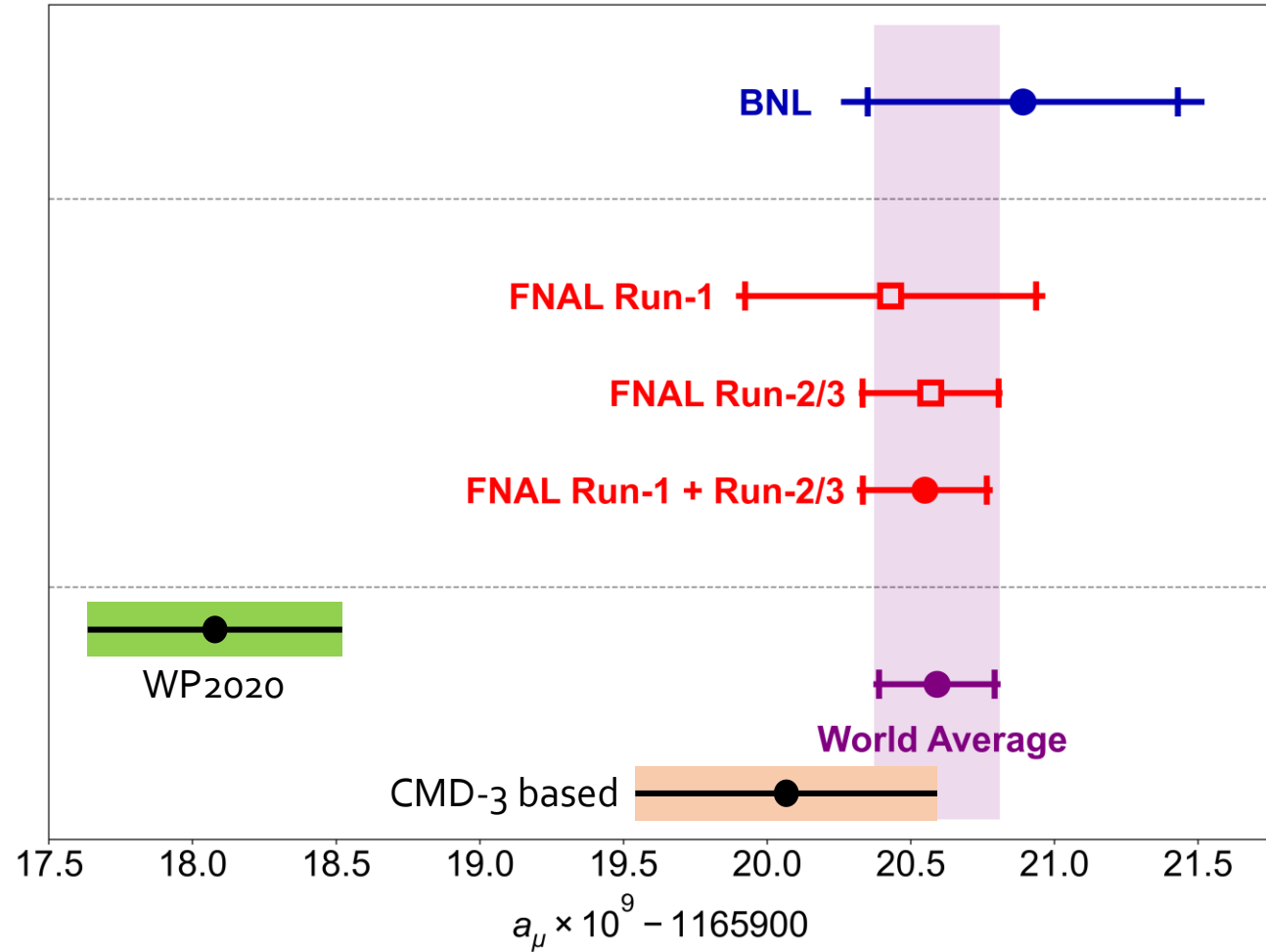
$0.6 < \sqrt{s} < 0.88 \text{ GeV}$

$a_{\mu}^{\pi\pi,LO}, 10^{-10}$

before CMD2	$368.8 \pm 10.3$
CMD2	$366.5 \pm 3.4$
SND	$364.7 \pm 4.9$
KLOE	$360.6 \pm 2.1$
BABAR	$370.1 \pm 2.7$
BES	$361.8 \pm 3.6$
CLEO	$370.0 \pm 6.2$
SND2k	$366.7 \pm 3.2$
CMD3	$379.3 \pm 3.0$
RHO2013	$380.06 \pm 0.61 \pm 3.64$
RHO2018	$379.30 \pm 0.33 \pm 2.62 \times 10^{-10}$
Sum	$379.35 \pm 0.30 \pm 2.95$

49

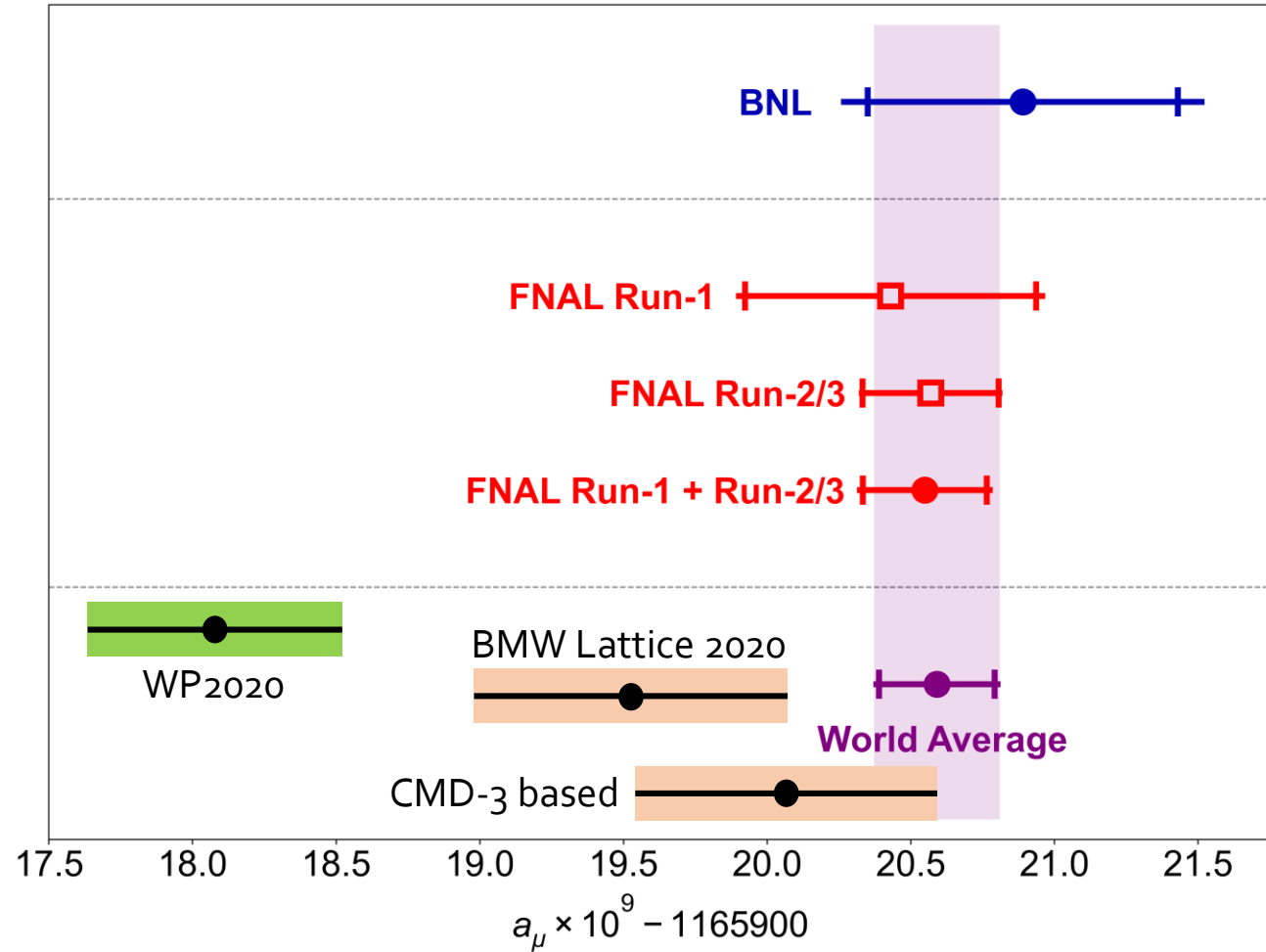
# Experiment vs SM prediction



At the moment, the SM prediction for  $a_\mu$  is unclear (due to hadronic contribution)



# Experiment vs SM prediction



At the moment, the SM prediction for  $a_\mu$  is unclear (due to hadronic contribution)

# What's next

# CMD-3: what we could do wrong?

CMD-3 measurement has many internal cross-checks which doesn't leave much space for unknowns.

- Is there problem with angle measurement (fiducial volume)?  
Unlikely: two systems are used; there is measurement of asymmetry; angle distribution agrees with simulation
- Is there problem with RC calculation?  
Unlikely as a source of discrepancy: CMD-2 and SND use the same code, and measurement of asymmetry agrees with RC MC generator. But there could be potential systematic shift in RC common for CMD-X/SND (e.g. for pions due to limitations of sQED).
- Is there problem with event separation?  
Unlikely: three methods agree (CMD-3 is the first measurement with several methods)
- Is there problem with trigger or detection efficiencies?  
Unlikely: should lead to shift of  $\sigma(\mu\mu)$ .
- Stupid mistake?  
Always possible, but we've done the whole analysis on MC data
- Unaccounted physical background which mimics  $e^+e^- \rightarrow \pi^+\pi^-$ ?  
Possible, but we accounted for all known backgrounds from  $e^+e^-$  annihilation. Something else? Beam/residual gas interactions?

# CMD-2 and CMD-3 are very different measurements

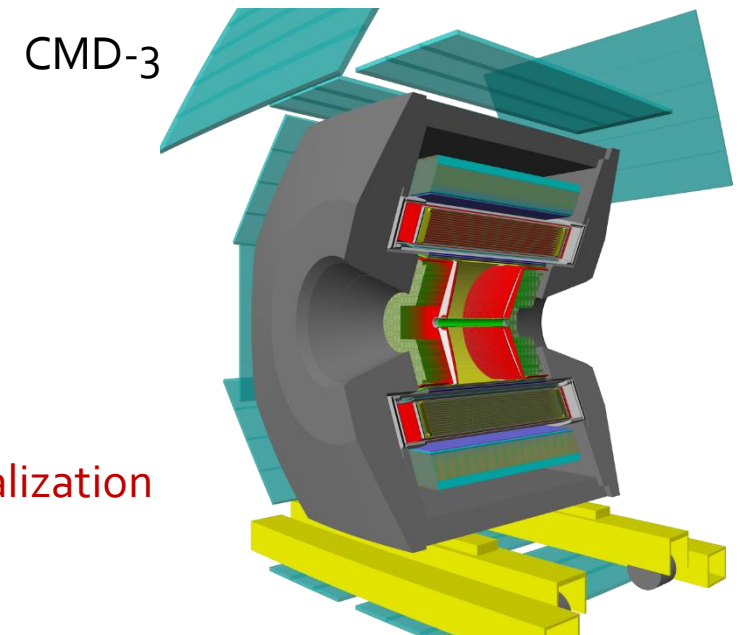
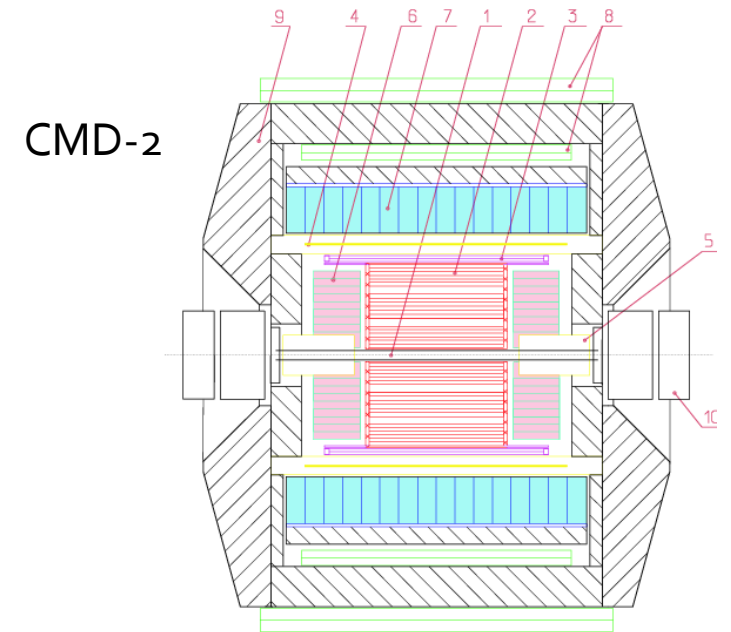
## Similarities:

- Two subsystems, endcap calorimeter (not used) and Z-chamber (only used in 2013 CMD-3 data)
- Analysis strategy

## Differences:

- Major detector systems (DC and calorimeter), electronics
- DC resolution
- Statistics (CMD-3 x30)
- Analysis implementation
- ...

**CMD-2 and CMD-3 are very different realization of the same-type measurement**



# Prospects for SM prediction

Discrepancies in  $e^+e^- \rightarrow H$  data make the SM prediction “blinded”

As of today, we don't have established estimate of  $a_\mu(SM)$

There are significant efforts to understand the discrepancies and to obtain additional new  $e^+e^- \rightarrow H$  data:

- SND has the same amount of data collected as CMD-3, analysis is in progress
- BABAR is making reanalysis of old data using new approach (angular analysis)
- KLOE-2 started analysis of collected data, not analyzed before
- BELLE-II plans to do ISR measurement of  $e^+e^- \rightarrow H$  cross sections

There is dedicated experiment, Muone, being prepared at CERN to measure hadronic contribution via  $e\mu$  scattering

There is fast progress in lattice calculations

There are good chances to improve precision of SM prediction in coming years

# Измерение адронных сечений для $(g - 2)_\mu$

FNAL expected precision of 140 ppb corresponds to  $0.25\% \cdot \alpha_\mu^{had,LO}$

Вклад сильных взаимодействий:  $a_\mu(had) = \int \sigma_{e^+e^- \rightarrow \text{адроны}}(s) K(s) ds$

Чтобы точность теории «догнала» эксперимент, необходимо измерить адронные сечения с точностью  $\sim 0.2\%$  (КМД-3:  $\sim 0.8\%$ )

Канал	Вклад, $\cdot 10^{10}$ (KNT19)	Отн.точность: надо (есть)
$\pi^+\pi^-$	504.23(1.90) (0.4%) ха-ха	0.23% (0.8%)
$\pi^+\pi^-\pi^0$	46.63(94) (2.0%)	1.1% (1.5-3%)
$\pi^+\pi^-\pi^+\pi^-$	13.99(19) (1.4%)	0.8% (2-3%)
$\pi^+\pi^-\pi^0\pi^0$	18.15(74) (4.0%)	2.3% (5%)
$K^+K^-$	23.00(22) (1.0%)	0.6% (2%)
$K_S K_L$	13.04(19) (1.5%)	0.7% (2%)
<b><math>a_\mu(had; LO)</math></b>	<b>692.8(2.4) (0.35%)</b>	<b>0.2%</b>

Сценарий «равномерного» улучшения

# CMD-3 plans

## Short-term (~1 year)

Collect additional data dedicated to systematic checks of the measurement (with different detector and running conditions).

## Long term (~5-10 years)

The CMD-3 measurement is systematically limited – detector upgrade.

Detector upgrades under discussions: new drift chamber, new Z-chamber at inner and outer radii (probably, integrated with DC), *dedicated PID/TOF?,...*

The goal is to reach ~0.2-0.3% in  $\sigma(e^+e^- \rightarrow \pi^+\pi^-)$

The precision critically depends on development on new generation of MC generators for radiative corrections

# Источники систематических ошибок $e^+e^- \rightarrow \pi^+\pi^-$

## Систематические ошибки КМД-3

		Планы КМД-3	Надо
x Radiative corrections	0.2% (2π) ⊕ 0.2% (Fπ) ⊕ 0.1% (e+e-)	0.1%	0.1%
x e/μ/π separation	0.5 (low) - 0.2 (ρ) - 0.6 (φ) %	0.2%	0.1%
x Fiducial volume	0.5% / 0.8% (RHO2013)	0.2%	0.1%
x Correlated inefficiency	0.1 (ρ) - 0.15%(>1 ГэВ)	0.1%	
x Trigger	0.05 (ρ) - 0.3% (>1 ГэВ)		
x Beam Energy (by Compton $\sigma_E < 50$ keV)	0.1% (out of resonances), 0.5% (at ω, φ -peaks)	0.2%	0.1%
x Bremsstrahlung loss	0.05 %		
x Pion specific loss	0.2% nuclear interaction 0.2%(low) - 0.1% (ρ) pion decay		0.1%
<small>CMD-3 <math>e^+e^- \rightarrow \pi^+\pi^-</math> ana...</small>			
	0.8% (low) - 0.7% (ρ) - 1.6% (φ)		
	1.1% (low) - 0.9% (ρ) - 2.0% (φ) (RHO2013)		

Ключевые требуемые улучшения:

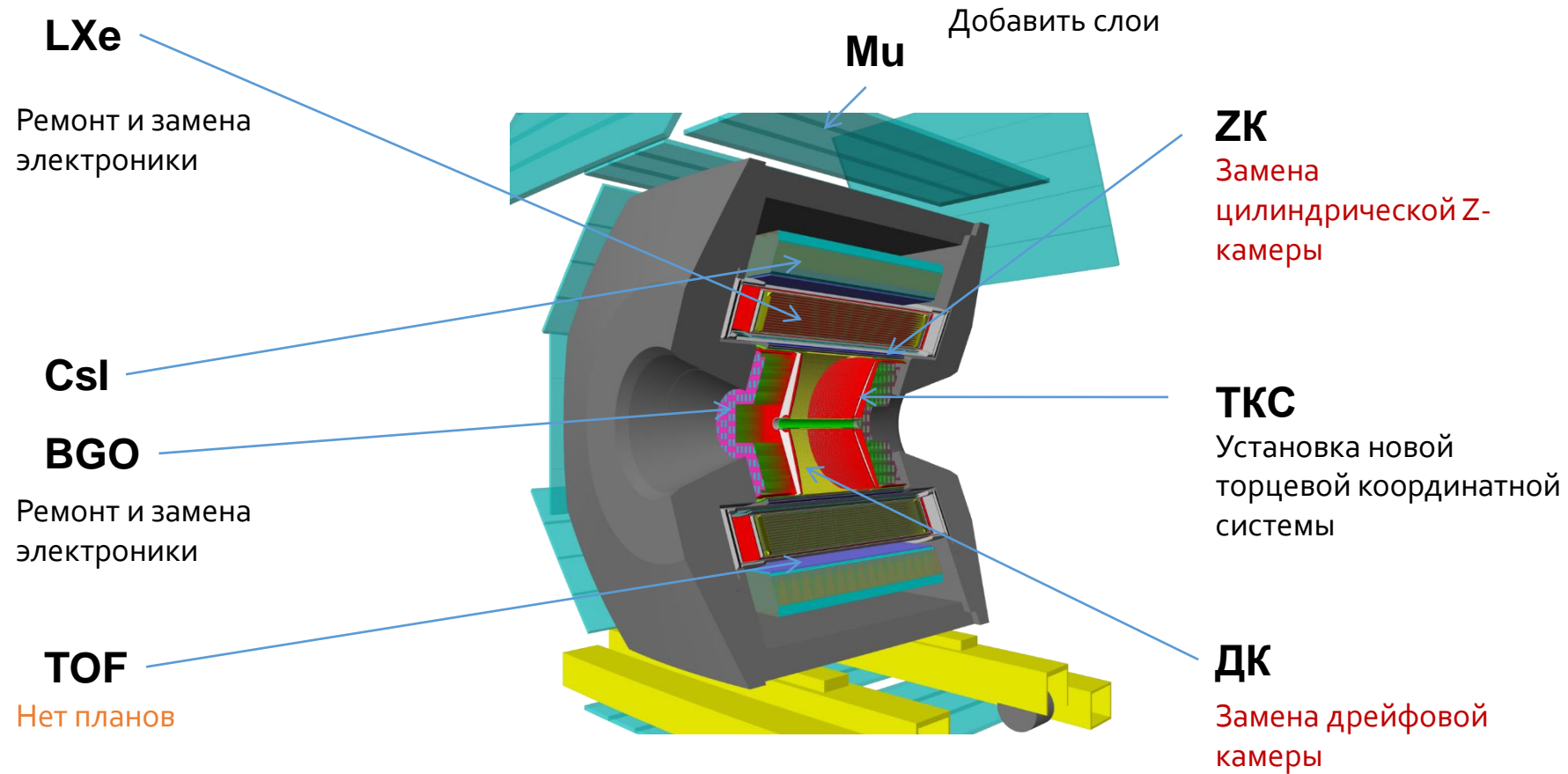
- Идентификация (разделение)
- Телесный угол
- Ядерные взаимодействия (вакуумная труба)

и параллельное развитие расчетов радиационных поправок...

**Статистика КМД-3: ~0.08%, 7 месяцев**



# Возможные пути модернизации КМД-3



# Разработка НОВОЙ дрейфовой камеры

- Идет моделирование разных вариантов
- Идут подготовительные R&D, общие для всех вариантов  
Проволока, пины, конструкционные материалы, электроника
- К концу 2024 года – понимание конструкции

Стоимость: O(10 млн.руб.) на материалы и комплектующие

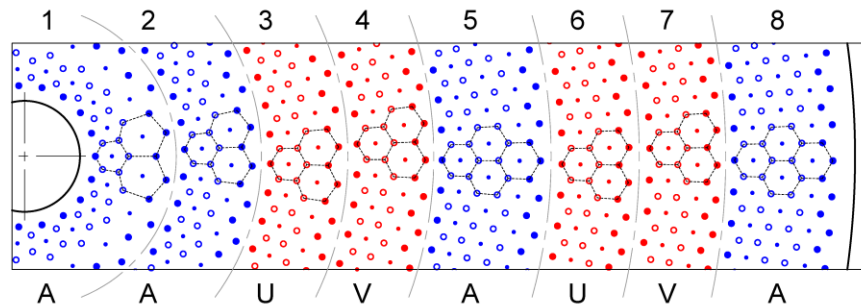
SUPERLAYER NUMBER	NUMBER OF LAYERS	NUMBER OF CELLS IN LAYER	NUMBER OF CELLS IN SUPERLAYER	STEREO ANGLE, mrad	CELL SIZE $r \pm \Delta r$ , mm		RADIUS OF ANODE WIRE LAYER, mm
1	2	19	38	0	6.000	0.175	31.543
					8.642	0.038	43.185
2	2	37	74	0	6.279	0.094	64.106
					7.516	0.019	74.762
3	2	53	106	-45	6.529	0.068	95.422
					7.391	0.014	106.078
4	2	69	138	-48	6.667	0.054	126.848
					7.330	0.011	137.512
5	3	87	261	0	6.662	0.042	157.404
					7.072	0.008	167.757
					7.534	0.001	178.827
6	2	109	218	-99	6.683	0.034	200.831
					7.093	0.007	211.266
7	2	125	250	-101	6.750	0.030	232.613
					7.109	0.006	243.097
					6.772	0.027	263.236
8	3	141	423	0	7.091	0.005	273.713
					7.370	0.001	284.629
TOTAL	18		1508				

The CMD new drift chamber geometry

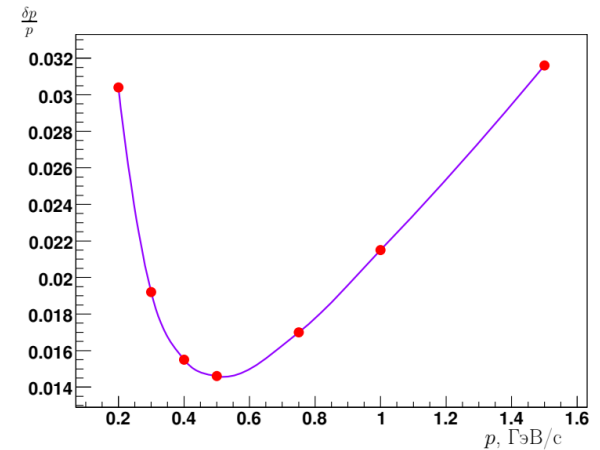
INNER DIAMETER, mm	40
OUTER DIAMETER, mm	600
WIRE LENGTH, mm	440
ENDPLATE THICKNESS, mm	7
NUMBER OF WIRES:	5 804
● SIGNAL 25 $\mu$ m	1 508
● FIELD 100 $\mu$ m	1 920
○ FIELD 125 $\mu$ m	2 376
TOTAL TENSION LOAD, kg	882
ENDPLATE FLEXURE (MAX) <sup>*</sup> , mm	3.1

<sup>\*</sup>ENDPLATE MATERIAL:  
NIKAM M55J quasi-isotropic carbon fiber with  
Young's modulus  $E = 168$  GPa

A – axial  
U, V – stereo



Вариант со стерео-слоями

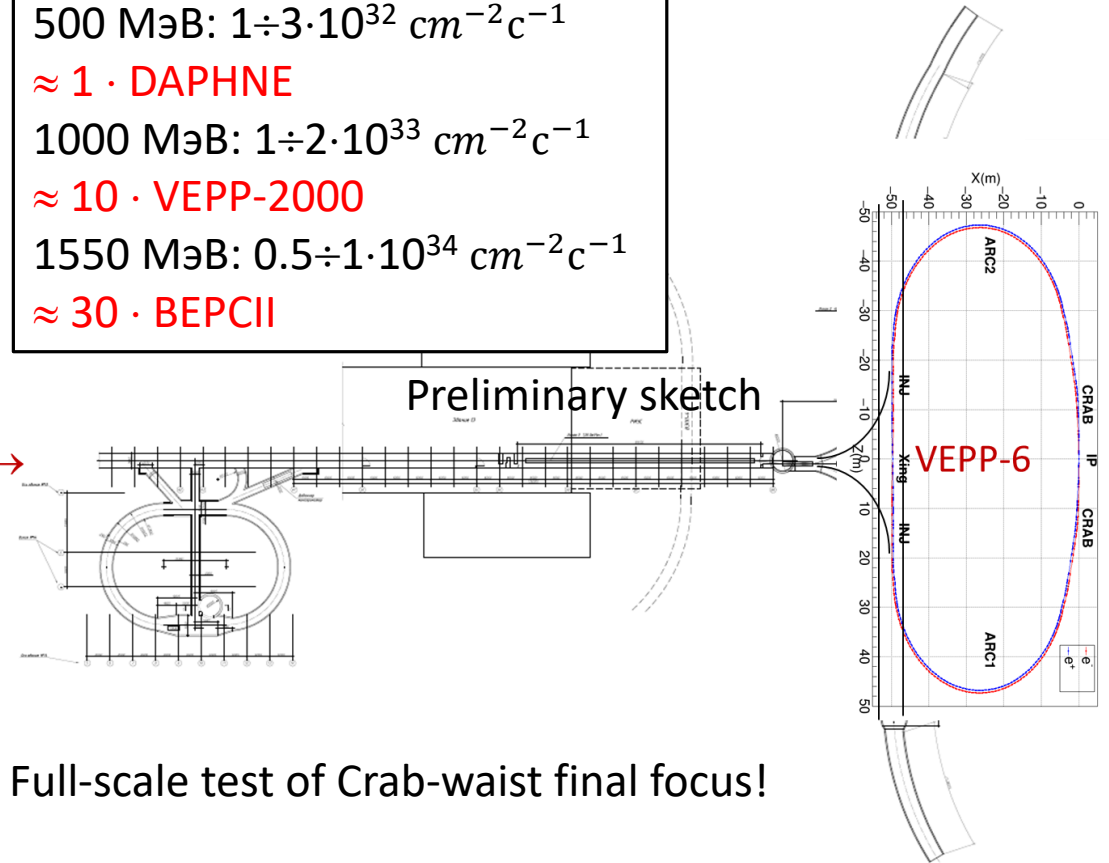


# Under consideration: VEPP-6

- $e^+e^-$  collider
  - Beam energy from <0.5 to 1.6 GeV ( $J/\psi$ ) (2.0 GeV)
  - Luminosity  $\mathcal{L} \approx 10^{34} \text{ cm}^{-2} \text{ c}^{-1}$  @ 1.6 GeV
- General purpose detector
  - Tracking
  - Calorimetry
  - Particle ID
- Physics
  - $J/\psi$  decays
  - Baryon thresholds
  - Measurement of R
  - ... **Complementary to Super charm-tau factory**

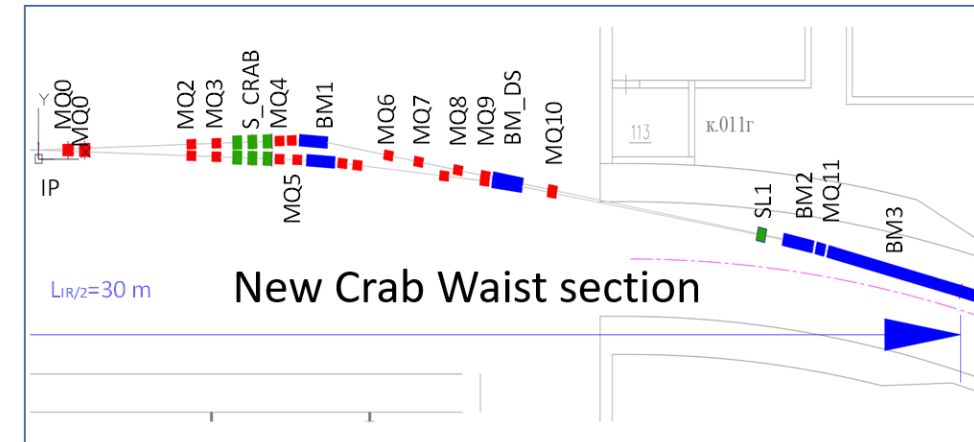
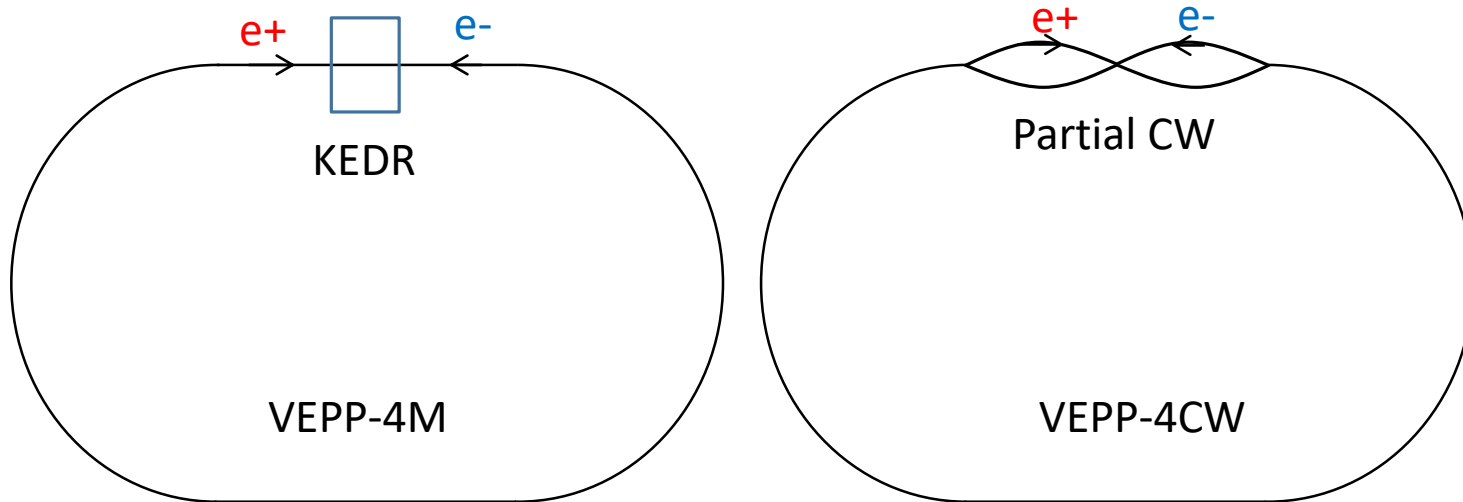
500 MэB:  $1 \div 3 \cdot 10^{32} \text{ cm}^{-2} \text{ c}^{-1}$   
 $\approx 1 \cdot \text{DAPHNE}$   
 1000 MэB:  $1 \div 2 \cdot 10^{33} \text{ cm}^{-2} \text{ c}^{-1}$   
 $\approx 10 \cdot \text{VEPP-2000}$   
 1550 MэB:  $0.5 \div 1 \cdot 10^{34} \text{ cm}^{-2} \text{ c}^{-1}$   
 $\approx 30 \cdot \text{BEPCII}$

$e^+e^-$  from existing injector →



Full-scale test of Crab-waist final focus!

# Under consideration: CW at VEPP-4M



There is proposal to make a test of CW at VEPP-4M

What can be tested: final focus elements, nonlinear beam dynamics, beam-beam effects, backgrounds,...

VEPP-4M straight section is modified.  
Electrostatic separation of colliding beams.

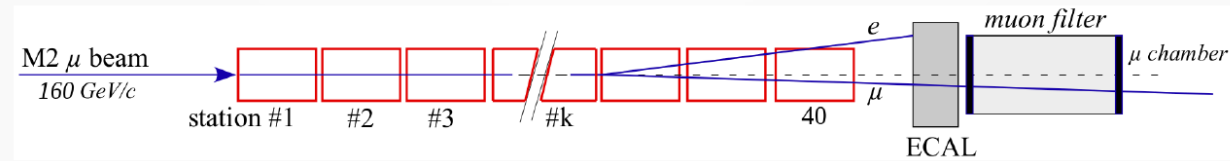
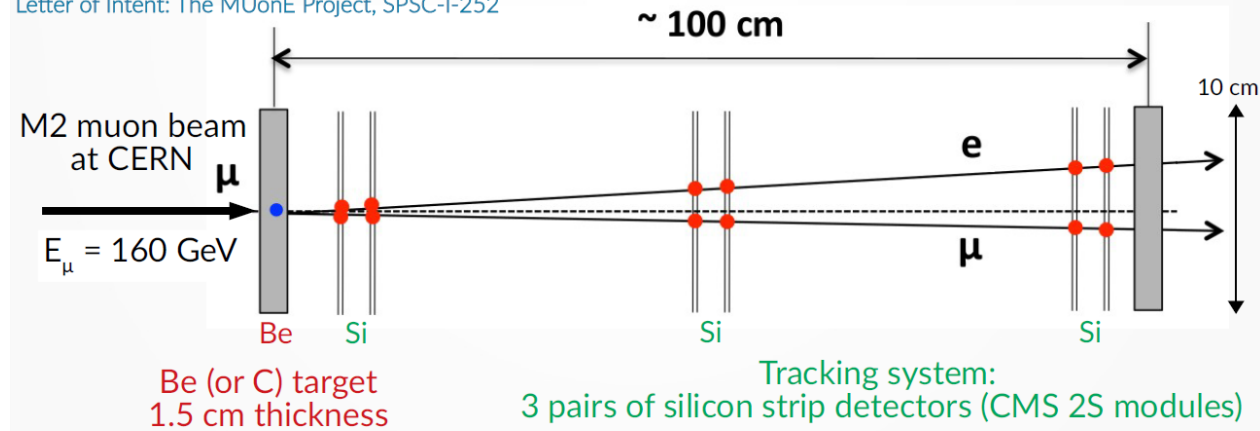
Beneficial for all future collider projects

Dedicated experiment to measure hadronic contribution in t-channel.

$$\alpha_{\mu}^{HLO} = \frac{\alpha_0}{\pi} \int_0^1 dx (1-x) \Delta\alpha_{had}[t(x)]$$

Lautrup, Peterman, De Rafael, Phys. Rep. C3 (1972), 193

Letter of Intent: The MUonE Project, SPSC-I-252



Measured: angular distribution of  $\mu e$  scattering;  $4 \cdot 10^{12}$  events!

Now: proof-of-concept data taking; final result after LHC LS3 (2029-)

# Conclusion

- CMD-3 performed a new measurement of  $\sigma(e^+e^- \rightarrow \pi^+\pi^-)$  at energies  $\sqrt{s} < 1.2$  GeV
  - The best statistical precision in the world
  - Up to 0.7% systematic accuracy – on a par with previous measurement
- The measurement is supported by accompanying measurements of  $\sigma(e^+e^- \rightarrow \mu^+\mu^-)$  and charge asymmetry of  $e^+e^- \rightarrow \pi^+\pi^-$
- The CMD-3 result is systematically larger than previous measurements
- The SM prediction of muon  $(g-2)$ , based on CMD-3 result, is in agreement with recent muon  $(g-2)$  measurement at FNAL
- The status of SM prediction is unclear; with amount of world-wide dedicated efforts, expect improvement in theory in coming years

**Ultimate goal: Hadron data = Lattice = MUONE**